EGAS MONIZ SCHOOL of HEALTH & SCIENCE | INSTITUTO UNIVERSITÁRIO EGAS MONIZ

INSTITUTO UNIVERSITÁRIO EGAS MONIZ

MESTRADO EM TECNOLOGIAS LABORATORIAIS EM CIÊNCIAS FORENSES

SURVIVAL, DEVELOPMENT AND BIOACCUMULATION RATE OF *CALLIPHORA VICINA* LARVAE (DIPTERA: CALLIPHORIDAE) TO INCREASING CONCENTRATIONS OF METALS

Trabalho submetido por

Ana Catarina Montanha Fialho

para a obtenção do grau de Mestre em Tecnologias Laboratoriais em Ciências Forenses

setembro de 2024

EGAS MONIZ SCHOOL of HEALTH & SCIENCE | INSTITUTO UNIVERSITÁRIO EGAS MONIZ

INSTITUTO UNIVERSITÁRIO EGAS MONIZ

MESTRADO EM TECNOLOGIAS LABORATORIAIS EM CIÊNCIAS FORENSES

SURVIVAL, DEVELOPMENT AND BIOACCUMULATION RATE OF *CALLIPHORA VICINA* LARVAE (DIPTERA: CALLIPHORIDAE) TO INCREASING CONCENTRATIONS OF METALS

Trabalho submetido por

Ana Catarina Montanha Fialho

para a obtenção do grau de **Mestre** em Tecnologias Laboratoriais em Ciências Forenses

Trabalho orientado por

Prof. Doutor Carlos Família

e coorientado por

Prof. Doutor José Brito e Mestre Paulo Mascarenhas

setembro de 2024

Agradecimentos

Primeiramente, agradecer aos meus pais por me apoiarem sempre em todas as decisões e me permitirem seguir os meus sonhos, por financiarem este mestrado e sempre acreditarem em mim.

Ao orientador deste projeto, Professor Carlos Família, pelo acompanhamento e interesse ao longo deste último ano e por ter permitido a realização deste trabalho.

Um especial agradecimento ao meu coorientador, Professor José Brito, pela paciência e ajuda na etapa mais crítica deste projeto. Este trabalho não teria sido possível sem a sua ajuda.

Um grande agradecimento ao verdadeiro orientador deste trabalho, o Professor Paulo Mascarenhas, pela ideia do projeto, por sempre acreditar e encorajar o meu trabalho. Não podia pedir por melhor orientador! Espero continuar a trabalhar consigo e continuar a investigação nesta área tão interessante.

Um agradecimento também à Professora Luísa Gonçalves pela ajuda na parte química. E também agradecer ao Professor Alexandre Quintas, por mostrar sempre interesse em qualquer projeto e apoiar sempre os seus alunos, em qualquer circunstância.

Agradecer ao Instituto Universitário Egas Moniz por me acolher, por permitir a realização deste trabalho, e pela disponibilidade do espaço dentro das melhores condições.

Agradecer aos meus colegas de curso por me acolherem e acompanharem nesta jornada, por permitirem a realização deste curso da melhor maneira possível e por terem feito este mestrado mais divertido. Um agradecimento especial à Rafaela por todos os trabalhos de grupo feitos e pelo apoio e amizade que partilhamos. E um grande agradecimento ao Alfredo, por ter acompanhado o meu trabalho e por ser o meu maior apoio emocional quando mais precisava, e me dar a força e motivação quando pensava em desistir do trabalho, e por todas as fofocas, risadas e desesperos que partilhamos.

Finalmente, agradecer aos meus amigos pelo apoio emocional durantes estes 2 anos, por estarem sempre ao meu lado quando mais preciso, para desabafar ou esquecer os problemas.

Declaração de Honra

Código | IMP-EM-EI-111_00

Declaro, por minha honra, que o presente trabalho académico é original e foi elaborado por mim própria, não se tendo recorrido a quaisquer outras fontes, para além das indicadas, usadas, adotadas literalmente ou adaptados a partir dos seus originais (em fontes impressas, não impressas ou na internet) e encontram-se adequados, identificados e citados, com observância das convenções do trabalho académico em vigor.

Mais declaro que esta Dissertação/Tese "Survival, development and bioaccumulation rate of *Calliphora vicina* larvae (Diptera: Calliphoridae) to increasing concentrations of metals" não foi apresentada, para efeitos de avaliação, a qualquer outra entidade ou instituição, para além da(s) diretamente envolvida(s) na sua elaboração, e que os conteúdos das versões impressa e eletrónica são inteiramente coincidentes.

Declaro, igualmente, encontrar-me ciente de que a inclusão, neste texto, de qualquer falsa declaração terá consequências legais.

Data: 30/09/2024

Declaração Conflito de Interesses (DCI)

Código | IMP-EM-EI-110_00

Eu Ana Catarina Montanha Fialho, referente a Dissertação/Tese "Survival, development and bioaccumulation rate of *Calliphora vicina* larvae (Diptera: Calliphoridae) to increasing concentrations of metals" declaro que não possuo conflitos de interesse de ordem pessoal, comercial, académica, político ou financeiro.

Data: 30/09/2024

Declaração de Financiamento

Código | IMP-EM-EI-113_00

Eu Ana Catarina Montanha Fialho, referente a Dissertação/Tese "Survival, development and bioaccumulation rate of *Calliphora vicina* larvae (Diptera: Calliphoridae) to increasing concentrations of metals" declaro que o meu trabalho não se encontra financiado.

Resumo

Os metais pesados são uma ameaça séria à saúde humana, uma vez que podem ser tóxicos mesmo em baixas concentrações, e inclusivamente levar à morte. No entanto, a análise de metais pesados em cadáveres em decomposição pode ser desafiante, devido à interferência da decomposição da matriz ou à ausência de amostras biológicas tradicionais. Neste sentido, a entomologia forense pode ser uma ferramenta útil, onde o recurso a insetos necrófagos que consigam bioacumular estas substâncias pode facilitar a sua análise e quantificação. As moscas varejeiras, como a *Calliphora vicina* (*C. vicina*), são normalmente as primeiras a colonizar os cadáveres e, por isso, as mais elegíveis a serem utilizadas como evidência entomológica. No entanto, estas substâncias podem afetar a taxa de crescimento e a sobrevivência das larvas necrófagas destes insetos, comprometendo a sua utilidade como marcadores toxicológicos para metais pesados, bem como o seu valor na determinação dos intervalos pós-morte (PMI).

Neste projeto, foram estudadas a taxa de sobrevivência, o desenvolvimento e a bioacumulação de larvas de *C. vicina* em relação aos metais pesados mais associados ao envenenamento humano – Arsénio (As), Mercúrio (Hg), Chumbo (Pb) e Cádmio (Cd). Para tal, as larvas de *C. vicina* foram expostas a concentrações crescentes de cada um desses metais pesados durante um período de seis dias. O comprimento e o peso das larvas foram medidos, e as concentrações dos metais foram determinados por Espectrometria por Fluorescência de Raios-X Dispersiva em Comprimento de Onda (WDXRF), Espectrometria de Emissão Ótica com Plasma Indutivamente Acoplado (ICP-OES) e Espectrometria de Absorção Atómica (AAS).

Todos os metais pesados em estudo induziram um aumento na taxa de mortalidade, sendo o As o mais tóxico para esta espécie. Concentrações elevadas de cada metal pesado limitaram o desenvolvimento das larvas, resultando em peso e comprimento reduzidos, com tamanhos semelhantes aos dos primeiros instares. Estes resultados indicam que concentrações elevadas de metais pesados podem enviesar as estimativas do PMI baseadas em evidências entomológicas. Todos os metais foram detetados com sucesso nas larvas e no substrato; no entanto, não foi observada bioacumulação de As, Hg ou Pb nas larvas de *C. vicina*. A bioacumulação foi verificada apenas para o Cd, com concentrações 3 a 4 vezes superiores nas larvas em comparação com o substrato.

Palavras-chave: entomologia forense, metais pesados, WDXRF, AAS, ICP-OES.

Abstract

Heavy metal poisoning is a serious threat to human health, as heavy metals are highly toxic in low concentrations. Exposure to these substances has the potential to result in chronic or acute poisoning, which can have adverse effects on human health and, in some cases, may ultimately lead to death. The analysis of heavy metals on decaying corpses can be challenging due to the interference of matrix decomposition or the absence of traditional biological samples. In such cases, forensic entomology can be a useful tool, as necrophagous insects may facilitate the detection of these substances. For example, the blowfly *Calliphora vicina* (*C. vicina*) is a common early colonizer of decomposing corpses, and thus may be a suitable candidate for use as entomological evidence. Nevertheless, these toxic substances have the potential to impact insect growth and survival rates, which may, in certain circumstances, restrict their use as toxicological markers and for *post-mortem* interval (PMI) estimations.

The present study sought to ascertain the impact of the most prevalent heavy metals responsible for human poisoning – Arsenic (As), Mercury (Hg), Lead (Pb), and Cadmium (Cd) – on the survival, development, and bioaccumulation rate of *C. vicina* larvae. To this end, *C. vicina* larvae were reared in increasing concentrations of each heavy metal for a six-day period. The length and weight of the larvae were measured, and the concentrations were analysed using Wavelength Dispersive X-Ray Fluorescence Spectrometry (WDXRF), Inductively Coupled Plasma Optical Emission Spectroscopy (ICP-OES), and Atomic Absorption Spectroscopy (AAS).

Each heavy metal resulted in elevated mortality rates in a dose-dependent manner, with As being the most toxic for this species. The development of *C. vicina* larvae was found to be limited by high concentrations of all heavy metals, resulting in a reduction in weight and length, with sizes comparable to that observed in the first and second instars. The findings demonstrate that elevated concentrations of heavy metals can potentially introduce bias in PMI estimations based on entomological evidence. All metals were successfully detected on the larvae and rearing substrate. However, no evidence was established for the bioaccumulation of As, Hg, or Pb from *C. vicina* larvae. Verification of bioaccumulation was limited to Cd, with larvae concentrations 3 to 4 times higher than those observed in the substrate.

Key-words: forensic entomology, heavy metals, WDXRF, AAS, ICP-OES.

Table of contents

List of Figures

List of Tables

List of abbreviations

δ-ALA: δ-Aminolevulinic Acid

δ-ALAD: δ-Aminolevulinic Acid Dehydratase

AAS: Atomic Absorption Spectroscopy

As(III): Arsenite

As(V): Arsenate

As: Arsenic

AsH_3: Arsine

ATP: Adenosine Triphosphate

Ba: Barium

BAF: Bioaccumulation Factor

BBB: Blood-Brain Barrier

Cd: Cadmium

Cu: Copper

CVAAS: Cold Vapor Atomic Absorption Spectrometry

DMA-III: Dimethylarsonous Acid

DMA-V: Dimethylarsinic Acid

DNA: Deoxyribonucleic Acid

GSH: Glutathione

GSR: Gunshot Residue

GSSG: Glutathione Disulfide

Hg: Mercury

Hg0: Elemental Mercury

Hg^{1+}: Mercurous Mercury

Hg^{2+}: Mercuric Mercury

ICP-MS: Inductively Coupled Plasma Mass Spectroscopy

IPC-OES: Inductively Coupled Plasma Optical Emission Spectroscopy

LD: Limit of Detection

LD50: Lethal Dose 50

MeHg: Methylmercury

MMA-III: Monomethylarsonous Acid

MMA-V: Methylarsonic Acid

mPMI: Minimum *Post-Mortem* Interval

MT: Metallothionein

NADPH: Nicotinamide Adenine Dinucleotide Phosphate Hydrogen

OES: Optical Emission Spectroscopy

Pb: Lead

PMI: *Post-Mortem* Interval

PMT: Photomultiplier Tube

R^2: Coefficient of Determination

Rh: Rhodium

RNS: Reactive Nitrogen Species

ROS: Reactive Oxygen Species

Sb: Antimony

TEL: Tetraethyllead

Tl: Thallium

WDXRF: Wavelength-Dispersive X-ray Fluorescence

XRF: X-Ray fluorescence

Zn: Zinc

1. Introduction

1.1. Heavy metals

"Heavy metal" is a term that defines metallic elements that have a high atomic weight and a density at least five times higher than water. Given the connection between heaviness and toxicity, the term "heavy metals" also embraces metalloids, since they induce toxicity at low levels of exposure (Flora, 2009; Tchounwou et al., 2012).

These metals naturally occur in the environment and are distributed throughout ecosystems by the geological and biological cycles (Flora, 2009; Tchounwou et al., 2012). Their distribution can result from a number of different processes, including atmospheric deposition, erosion of natural deposits, the re-suspension of sediment, volcanic eruptions, and the evaporation of metals into soil and groundwater. However, the majority of their presence in the environment and subsequent human exposure can be attributed to industrial and anthropogenic activities, including mining and smelting operations, the industrial production of plastics, textiles, and microelectronics, nuclear power stations, and the agricultural use of metals (Caito & Aschner, 2015; Tchounwou et al., 2012).

Human exposure generally occurs in occupational settings, commercial products, traditional medicines, intentional exposure, and contaminated water and food sources (Sharma et al., 2014). In fact, contamination of water, air, and food by toxic metals puts hundreds of millions of people at risk every day, especially those in developing countries (Rehman et al., 2018).

The spectrum of exposure to these substances can range from chronic, low-level exposure to acute, high-dose exposure, depending on various factors related to exposure, such as dose, route of entry, duration, and frequency. The primary routes of human exposure to metals include oral ingestion, inhalation, and dermal contact (Baldwin & Marshall, 1999; Ufelle & Barchowsky, 2021). Acute heavy metal poisoning is a consequence of a sudden and significant intake of a toxic dose of a metal. Although uncommon, acute exposure typically arises from industrial accidents, inadvertent contamination of water or food supplies, and suicidal and homicidal poisonings (Caito & Aschner, 2015; Flora, 2009). Chronic toxicity is a consequence of prolonged exposure to lower doses of toxic substances, which frequently occurs in occupational settings and in residential areas situated in the proximity of contaminated environments. Chronic toxicity may have a deleterious effect on human health due to the distribution and accumulation of metals in

tissues over time (Caito & Aschner, 2015). Additionally, the person's age, sex, and capacity for biotransformation could impact metal toxicity (Ufelle & Barchowsky, 2021).

The most common heavy metals responsible for human poisoning are Arsenic (As), Mercury (Hg), Lead (Pb) and Cadmium (Cd) (Balali-Mood et al., 2021). These heavy metals are regarded as non-essential because they lack any discernible biological functions. These substances present a significant risk to human health, as they have been demonstrated to induce damage to multiple organs even at low levels of exposure. This damage can affect various vital organs, including the liver, brain, and kidneys (Tchounwou et al., 2012). In addition, the human body cannot transform nor destroy these metals, which leads to their accumulation, emphasising their toxic properties (Ufelle & Barchowsky, 2021). As such, heavy metal poisoning can result in gastrointestinal and kidney dysfunction, nervous system disorders, skin lesions, vascular damage, immune system dysfunction, cancer and eventually death (Balali-Mood et al., 2021).

Heavy metals exert their toxicity through a variety of mechanisms. The primary mechanism of toxicity is the induction of oxidative stress by generating reactive oxygen species (ROS) (Figure 1). These ROS can cause lipid peroxidation, DNA damage, depletion of proteins, activation of apoptotic pathways, and overwhelm cellular antioxidant defences (Sharma et al., 2014; Ufelle & Barchowsky, 2021). Besides, heavy metals have variable oxidation states, which allows them to interfere with standard biological mechanisms by losing one or more electrons to form cations, which have an affinity to the nucleophilic sites of essential macromolecules (Balali-Mood et al., 2021; Ufelle & Barchowsky, 2021). Another mechanism of toxicity is mimicry and competition with essential metals, displacing them, which leads to the disruption of metabolic functions. In addition, most of these heavy metals have a high affinity to sulfhydryl groups, affecting the correct activity of essential proteins and consequently producing more ROS (Ufelle & Barchowsky, 2021).

Most of these toxic metals are considered carcinogenic as they can bind to the DNA structure, inducing aberrant gene expression and promoting ineffective DNA repair. Besides, some heavy metals can induce epigenetic changes, such as DNA methylation (Balali-Mood et al., 2021; Ufelle & Barchowsky, 2021).

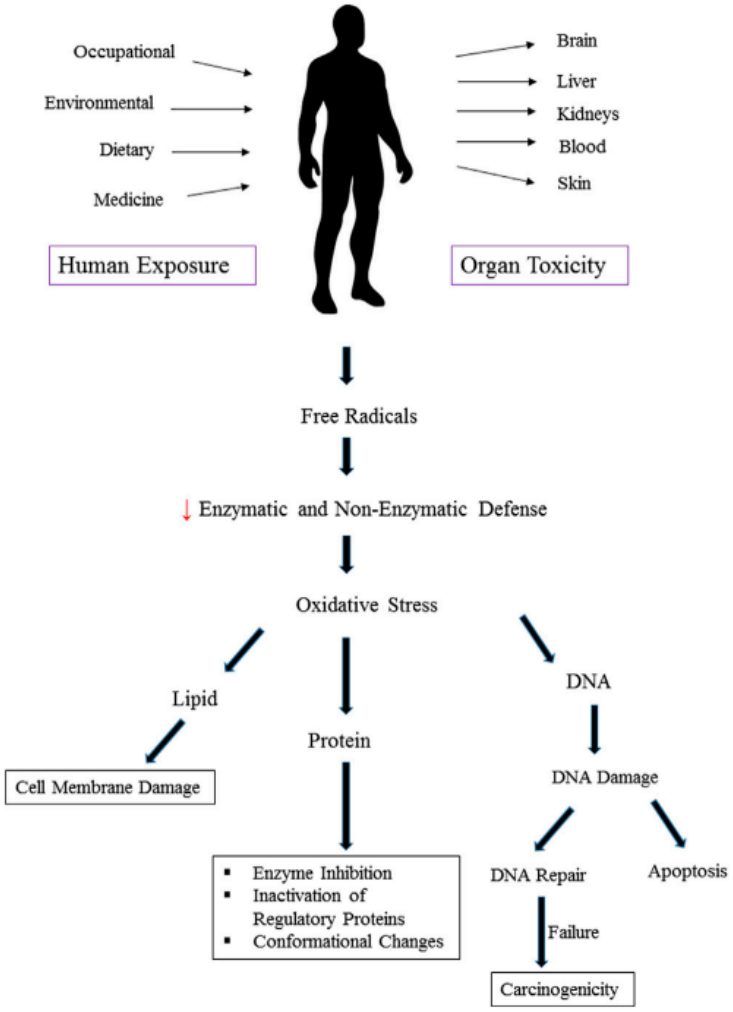

Figure 1: Oxidative stress and organ toxicity due to heavy metal exposure. From Balali-Mood et al. (2021).

1.1.1. Arsenic

Arsenic (As) is a toxic metalloid that occurs in the earth's crust, often together with other metals and sulphur. It exists in the inorganic – trivalent arsenite (As(III)) and pentavalent arsenate (As(V)) –, organic, arsine (AsH_3), and elemental forms. Its toxicity is dependent on its chemical form. Elemental and organic forms are considered to be non-toxic, whereas inorganic arsenic and arsenic gas (arsine) are highly toxic (Balali-Mood et al., 2021; Nurchi et al., 2020).

Exposure to As primarily occurs by ingestion, but inhalation and absorption through the skin are possible. Sources of As exposure are mainly contaminated food and water or occupational exposure. Occupational exposure to As usually occurs from arsenic fumes in the smelting industry, manufacture of pesticides and herbicides, production of electronic semiconductors, and wood preservation products. Fortunately, As compounds in commercial and agricultural products have been banned in Western countries due to

the increasing evidence of As toxicity (Nurchi et al., 2020; Ufelle & Barchowsky, 2021). Also, As and other heavy metals have been found in unsafe concentrations in traditional Chinese and Indian medicines (Hardin et al., 2023; Nurchi et al., 2020). Food, particularly rice and seafood, is the primary source of As exposure for many individuals. The concentrations of As in rice and other plants are due to contamination of water or soil, which contains inorganic As. Seafood primarily contains organic forms of As, which are less toxic, although some species can also accumulate inorganic As (Nurchi et al., 2020; Ufelle & Barchowsky, 2021). Environmental exposure to As is mainly caused by As-contaminated drinking water. In fact, the World Health Organization estimates that between 94 and 220 million people are exposed to As-contaminated drinking water above the recommended threshold of 10 μg/L (Podgorski & Berg, 2020), mostly in developing countries. For example, in Bangladesh, 57.5% of the studied population had skin lesions caused by As poisoning (Flora, 2009).

Arsenic trioxide has been approved as an anticancer treatment of acute promyelocytic leukemia as a last resource treatment, due to its cytotoxicity and ability to induct apoptosis in leukemic cells (Nurchi et al., 2020; Tchounwou et al., 2012).

As is historically associated with homicidal poisonings, being known as the “king of poisons” and “poison of kings”, being the poison of choice of European royalty from the 15th to the 19th century and used as a chemical weapon during World War I (Caito & Aschner, 2015). Nowadays, acute As poisoning is rare, but there are still episodes being reported. The majority of them are cases of self-poisoning, many of them life-threatening. These suicide attempts often involve the ingestion or injection of As, which can be found readily available online or in many workspaces at the industry (Tournel et al., 2011; Vantroyen et al., 2004; Yilmaz et al., 2009). Homicide cases using As are less common, nonetheless they still happen. For example, in 2003, a case of mass acute As poisoning in a church community in the United States of America was reported after a member of the church deliberately contaminated the coffee (Mills et al., 2013). In 2011, a strange case of sudden death was investigated after the deceased raised the possibility of being poisoned. After analysis, a high concentration of As and other metals was discovered (Duncan et al., 2015). Interestingly, Sikary (2019) discovered that As is still one of the most used drugs in homicidal poisonings in India.

After ingestion, inorganic As is well absorbed (80% to 90%) from the gastrointestinal tract. Inorganic As rapidly binds to haemoglobin in erythrocytes and is distributed to the

liver, kidneys, heart, lungs, and neural tissues within 24 hours. Arsenite As(III) usually enters the cells via a simple diffusion mechanism. Arsenate As(V), however, can cross the cell membrane via a phosphate transport system (Munday & Ford, 2011), uppon which about 50 to 70% is immediately reduced to trivalent arsenic As(III). As(III) is then methylated to methylarsonic acid (MMA-V) and dimethylarsinic acid (DMA-V), with the production of intermediary metabolites, in particular, monomethylarsonous acid (MMA-III) and dimethylarsonous acid (DMA-III). The production of methylated trivalent compounds corresponds to bioactivation and contributes to As toxicity, while the formation of methylated pentavalent As can be considered a detoxification process, given that trivalent As was shown to be more toxic than the pentavalent form (Munday & Ford, 2011; Nurchi et al., 2020). In humans, the bioavailability of inorganic As is 60% to 87%, and inorganic As and its metabolites are mainly excreted in urine and bile (Mochizuki, 2019).

Most of the toxicity of As results from its ability to interact with sulfhydryl groups and to substitute phosphorous in multiple biochemical reactions (Tchounwou et al., 2012). Indeed, trivalent As compounds possess a high affinity for sulfhydryl groups, which enables As to alter protein structure and inhibit a range of enzymes. The disruption of normal protein function has deleterious consequences for the organism, particularly concerning those involved in cellular energy metabolism and the synthesis and repair of DNA (Mochizuki, 2019; Ufelle & Barchowsky, 2021). Pentavalent arsenate and methylated arsenic mimic phosphorous, and can inhibit phosphotransfer reactions such as mitochondrial oxidative phosphorylation (Sharma et al., 2014; Ufelle & Barchowsky, 2021).

As is unable to generate ROS directly. Alternatively, As and its metabolites interact with essential cysteines in protein receptors and enzymes, stimulating NADPH oxidases to generate ROS (Ufelle & Barchowsky, 2021). The accumulation of ROS is harmful to the organism since it leads to a chain of reactions, such as activating inflammatory pathways, disruption of cell signalling pathways, and DNA and mitochondrial damage. For example, the accumulation of ROS is responsible for lipid bi-layer damage, which causes mitochondrial swelling. Trivalent As also inhibits the pyruvate dehydrogenase, which blocks the Krebs cycle and inhibits oxidative phosphorylation, decreasing ATP production and resulting in cell damage (Balali-Mood et al., 2021).

Besides, trivalent As reacts with reduced glutathione (GSH) and cysteine and decreases their bioavailability, therefore causing a depletion of the antioxidant system (Flora, 2009). In addition to ROS, As exposure can also initiate the generation of reactive nitrogen species (RNS) (Jomova et al., 2011).

As can exert its carcinogenic effects through several mechanisms, including inhibition of DNA repair, induction of chromosomal aberrations and DNA breakage, modulation of DNA synthesis and gene expression, and interference with cell signaling pathways, particularly the p53 signaling pathway, which plays a role in a number of cellular functions, such as apoptosis and differentiation. Additionally, As can promote tumour progression by causing epigenetic changes, such as histone modification and DNA methylation, which lead to aberrant gene expression (Nurchi et al., 2020; Tchounwou et al., 2012).

These metabolic interferences may lead to multi-organ failure. Therefore, As has been associated with various types of cancer, cardiovascular disease, diabetes, neurological disorders, and skin lesions (Jomova et al., 2011).

1.1.2. Mercury

Mercury (Hg) is a naturally occurring element in the air, water, and soil. It exists in three distinct forms: elemental mercury (Hg0), inorganic mercury – in mercurous (Hg^{1+}) or mercuric (Hg^{2+}) form – and organic mercury, with each having its profile of toxicity. The toxicity related of Hg increases as follows: Hg0 < inorganic (Hg^{2+} and Hg^{1+}) < organic Hg (Balali-Mood et al., 2021; Ufelle & Barchowsky, 2021). Mercury poisoning can result from ingestion, inhalation, injection, or dermal absorption of Hg compounds, with most human exposure to Hg originating from dental amalgam, ingestion of contaminated fish, or occupational exposure (Bernhoft, 2012; Graeme & Pollack, 1998).

At room temperature, elemental Hg (Hg0) exists in liquid form with high vapour pressure, being released into the environment as Hg0 vapour. Hg0 vapour is much more hazardous than liquid Hg. Hg0 is rarely found in its pure state but is extracted from cinnabar, corderoite, or livingstonite ores. Atmospheric Hg0 is derived from natural sources, such as volcanic eruptions and evaporation from oceans and soils. Anthropogenic sources also contribute to atmospheric Hg concentrations. These sources include emissions from metal mining and smelting, coal combustion, and industrial waste. Once in the atmosphere, Hg0 vapour is oxidized to a water-soluble inorganic form (Hg^{2+}) and returns to the earth's surface in rainwater. In water environments, Hg suffers a process of biotransformation,

where it is methylated by microorganisms, forming methylmercury (MeHg). MeHg is a bioaccumulative and biomagnifying substance that accumulates with ease in the food chain of aquatic environments, beginning with plankton and progressing to fish, sea mammals, and ultimately, humans (Caito & Aschner, 2015; Ufelle & Barchowsky, 2021). This is termed the Hg cycle, as presented in Figure 2. Thus, Hg is ubiquitous in the environment, and human exposure to some form of Hg is inevitable.

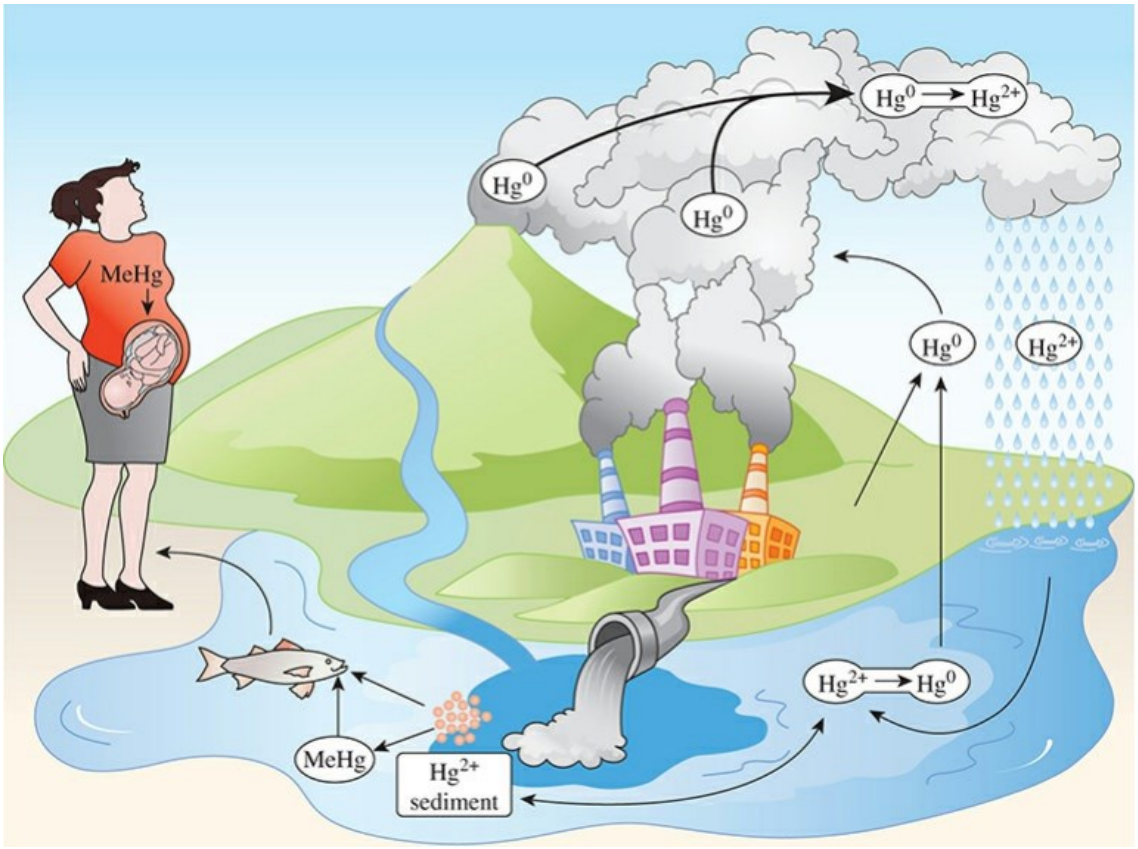

Figure 2: Mercury cycle. From Ufelle & Barchowsky (2021).

The human utilization of elemental Hg has been on decline. However, it persists in a number of sectors, including the chlor-alkali industry, the electronic industry, dental amalgams, and the production of fluorescent lamps. Inorganic Hg compounds have previously been utilized in the production of medical and cosmetic products, including antiseptics, teething powders, and skin-lightening creams. Phenylmercury compounds have been employed as preservatives in a variety of medicinal products, including thimerosal, antiseptics, and disinfectants. Additionally, alkylmercury compounds have been used as insecticides and fungicides. However, in response to heightened concerns about Hg toxicity, most Hg products have been prohibited and replaced with safer alternatives (Caito & Aschner, 2015; Tchounwou et al., 2012). Other important but occasional causes of Hg exposure include ethnic remedies and cosmetics, which are

banned in the European Community but available in other parts of the world (Baldwin & Marshall, 1999). Acute Hg exposure is uncommon and usually due to industrial accidents or suicidal ingestions.

Hg is linked to the Minamata disease, which occurred in Japan in the 1950s, killing more than 1,000 people over the years (Harada, 1995). From the 1920s to the 1960s, a Japanese chemical factory was using Hg as a catalyst in the production of acetaldehyde and vinyl chloride. Methylmercury chloride was being released into the Minamata Bay from the factory's effluent. Here, MeHg was sequestered by microorganisms and bioaccumulated throughout the food chain. Nearly 150 tons of MeHg were discharged into Minamata Bay for four decades. Only in August 1956, Hg poisoning was identified as the cause for the Minamata disease. In the following years, symptoms like chronic brain damage, mental retardation, developmental disturbances, liver disease, hypertension, and poor metabolism were observed in the children of mothers exposed to contaminated fish (Graeme & Pollack, 1998).

The use of Hg for self-poisoning purposes is still frequently described in literature. Many cases involve the injection of Hg salts (Dias et al., 2016; Michielan et al., 2018; Wang et al., 2007), or elemental Hg injection (Da Broi et al., 2017; Sukheeja et al., 2014; Yudelowitz, 2017). Many of these cases have deadly outcomes, as the diagnosis can be difficult with non-specific symptoms. Also, the involvement of Hg in homicidal cases is rare, but there are still a few reported cases in recent years. In 2012, a case was reported of a woman who was discovered deceased at her residence after five months of illness. Toxicological analysis revealed the presence of elevated levels of Hg in multiple tissues. It was found that her husband had been injecting her with Hg (Yan et al., 2012). Lu et al. (2017) reported a case of a 34-year-old male who was poisoned by his girlfriend, also by injecting Hg. The Hg used in these situations is found in obsolete medical devices like thermometers or bought online.

Liquid elemental Hg is poorly absorbed by ingestion and skin contact and does not appear to be toxic. Its toxicity derives from its potential to release Hg0 vapour (Balali-Mood et al., 2021; Sharma et al., 2014). Hg0 vapour is rapidly absorbed (about 80%) in the lungs, and, because of its high lipid solubility, it quickly diffuses into the blood and is distributed to all tissues. After absorption, Hg0 vapour is oxidized to divalent inorganic Hg (Hg^{2+}), a process likely mediated by catalases (Sharma et al., 2014; Ufelle & Barchowsky, 2021). A significant portion of Hg0 vapour crosses the blood-brain barrier (BBB) and placenta

freely before being oxidized. In the brain, it is oxidized to Hg^{2+}, and excreted very slowly, increasing its neurotoxicity. About 10% of Hg0 vapour is exhaled within a week of exposure, and the converted Hg^{2+} is excreted in urine and feces, with a half-life of 1 to 2 months (Baldwin & Marshall, 1999; Ufelle & Barchowsky, 2021).

Inorganic Hg is poorly absorbed from the gastrointestinal tract (only 7% to 15% of the ingested dose) and is mainly concentrated in the kidneys (Campbell, 1999; Ufelle & Barchowsky, 2021). Renal uptake of inorganic Hg occurs through reabsorption from proximal tubules in the form of cysteine S-conjugates (Cys-S-Hg-S-Cys) or from the basolateral membrane through organic anion transporters. Inorganic Hg salts, which are mainly excreted in urine and feces, do not easily pass the BBB or placenta (Balali-Mood et al., 2021; Ufelle & Barchowsky, 2021). Hg^{2+} salts are usually more toxic than Hg^{1+} because of their greater solubility in water and quicker absorption by the gastrointestinal tract (Sharma et al., 2014).

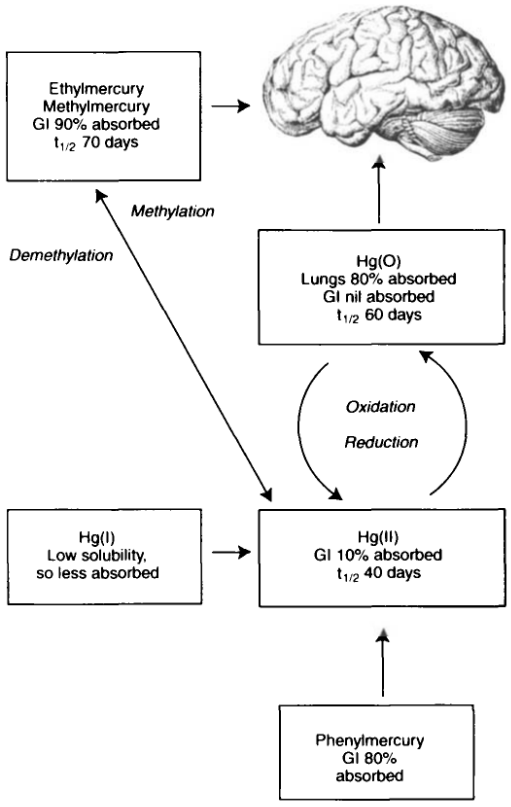

Figure 3: Mercury metabolism. Adapted from Baldwin & Marshall (1999).

Organic Hg compounds are well absorbed from the gastrointestinal tract (80 to 90%) and distributed throughout the body within 30 hours. Phenylmercury can also be absorbed through the skin. MeHg is bound to thiol-containing molecules such as cysteine (CH_3-

Hg-Cys), which mimics methionine, and so it crosses the BBB and placenta through the neutral amino acid carrier (Baldwin & Marshall, 1999; Ufelle & Barchowsky, 2021). About 90% of the MeHg is eliminated in the feces, with a half-life of 45 to 70 days. Organic Hg compounds are demethylated by bacteria to Hg^{2+} in the lower intestine. The explained metabolism of Hg is represented in Figure 3.

All forms of Hg are toxic, causing gastrointestinal toxicity, neurotoxicity, and nephrotoxicity.

Both inorganic and organic Hg have a high affinity to sulfhydryl groups of cellular proteins. This mechanism is responsible for producing nonspecific cell injury or even cell death. Consequently, Hg can potentially impair multi-organ function (Caito & Aschner, 2015; Ufelle & Barchowsky, 2021). These thiol groups are important functional moieties in antioxidant molecules; therefore, Hg causes a depletion of the antioxidant system (Bernhoft, 2012). Besides, Hg disrupts intracellular calcium homeostasis (Ufelle & Barchowsky, 2021).

Hg increases the production of ROS through the inhibition of glutathione peroxidases and the electron transport chain of mitochondria. This results in lipid peroxidation, protein oxidation, and DNA oxidation (Bernhoft, 2012; Tchounwou et al., 2012). ROS play a major role in mediating Hg-induced carcinogenesis, as ROS are known to cause DNA damage. These free radicals directly act on nucleic acids and may generate genetic mutations. Besides, they may induce conformational changes in proteins responsible for DNA repair, mitotic spindle, and chromosomal segregation (Crespo-López et al., 2009; Tchounwou et al., 2012).

Li et al. (2006) discovered that Hg can directly interact with DNA, with organic Hg compounds exhibiting a much higher affinity for DNA than inorganic forms. Each Hg species shows a preference for different DNA bases. Specifically, there is a predominance of guanine and cytosine binding with MeHg, adenine and cytosine binding with ethylmercury, and thymine binding with inorganic Hg. Phenylmercury, however, does not display any selectivity for binding to any of the four DNA bases. Instead, these interactions affect the secondary structure of DNA.

1.1.3. Cadmium

Cadmium (Cd) is an environmental pollutant that also occurs naturally on earth, in soil and minerals. Human activities, mainly industrial and agricultural, have increased the

human exposure to this metal. Cd is frequently used in industrial activities, such as the production of nickel-cadmium batteries, colour pigments, and several alloys, as a barrier to control nuclear fission, as a plastic stabilizer, and in phosphate fertilizers (Rehman et al., 2018; Sharma et al., 2014; Ufelle & Barchowsky, 2021). The global Cd production is estimated to be approximately 13,000 tons annually. However, since 1970, the use of Cd has decreased due to the growing recognition of its toxicity (Campbell, 1999; Flora, 2009).

The most dangerous characteristic of Cd is that it accumulates in the body, primarily on the liver and kidneys, due to its long biological half-life of 17 to 30 years.

Food is the primary source of exposure to Cd for the general population, while inhalation of Cd-containing fumes is the dominant route of exposure in occupational settings. Tobacco smoking is another major source of exposure to Cd, as tobacco plants tend to accumulate relatively high Cd concentrations (Balali-Mood et al., 2021; Ufelle & Barchowsky, 2021). Drinking Cd-contaminated water is another common source of exposure to this toxic metal. For example, in Saudi Arabia, water samples from private wells were contaminated with Cd, with 1-26 μg/L concentrations, and, in Sweden, water sampled from wells showed Cd concentrations up to 5 μg/L. Safe Cd concentration in water is considered of less than 3 μg/L. (Rehman et al., 2018).

Cases of Cd self-poisonings are extremely rare. However, a case of an attempted suicide with Cd has been documented, involving the ingestion of an industrial solution containing both Cd and barium concentrations, obtained from the person's local workspace (Hung & Chung, 2004).

Moreover, Cd was responsible for the *itai-itai* disease in Japan in the 1960s due to a mass Cd contamination of rice and water supplies. The patients suffered from painful degenerative bone disease, kidney failure, and gastrointestinal and lung diseases, which caused high mortality rates (Balali-Mood et al., 2021; Nishijo et al., 2017).

Cd is poorly absorbed upon oral exposure. Only about 5% is absorbed in the gastrointestinal tract. However, it may be increased to 20% by dietary iron deficiencies (Campbell, 1999; Ufelle & Barchowsky, 2021). When exposure occurs through inhalation, absorption is generally more extensive, up to 60%. Derman absorption is very minimal (0.2-0.8%). Following absorption, Cd is transported in the blood by binding to albumin, facilitating its rapid redistribution to the liver and kidneys. In the liver, Cd leads

to the production of metallothionein (MT), to which it binds. Subsequently, the complex is transported to the kidney for excretion. In this process, the Cd-bound MT is reabsorbed and degraded in the lysosomes of the renal tubules, resulting in the release of Cd atoms. These atoms can either recombine with MT or cause renal toxicity. Cd is excreted poorly through the urine and feces (Baldwin & Marshall, 1999; Ufelle & Barchowsky, 2021).

Similar to other heavy metals, oxidative stress is considered the principal mechanism of Cd toxicity. Cd indirectly induces the formation of ROS through several processes. These include decreasing intracellular glutathione levels and binding to thiol groups of enzymes involved in antioxidant defences, thereby inhibiting their activities. Cd also forms cadmium-selenium complexes in the active center of glutathione peroxidase, an antioxidant enzyme, inhibiting their function (Sharma et al., 2014).

Cd competes with essential metals such as zinc, iron, selenium, copper, and calcium, disrupting various cellular processes, including metal membrane transport and energy metabolism. This competition leads to the dysregulation of metal homeostasis. Cd inhibits complex III of the mitochondrial electron transport chain, increasing ROS production, which can damage the mitochondrial membrane and trigger apoptosis. Endoplasmic reticulum stress and the resultant cell apoptosis is another proposed pathway of Cd toxicity (Balali-Mood et al., 2021; Sharma et al., 2014).

The oxidative stress caused by Cd leads to DNA damage and mutations by promoting cellular proliferation, inhibiting apoptotic and DNA repair mechanisms, causing DNA breakage, lipid peroxidation, and chromosomal aberrations (Renu et al., 2021; Sharma et al., 2014). Cd can also induce epigenetic changes, such as DNA hypermethylation at low levels of exposure (Renu et al., 2021).

1.1.4. Lead

Lead (Pb) is a naturally occurring bluish-grey metal present in ores with other metals (e.g., cerussite, anglesite, and galena). However, the highest environmental pollution concentrations are due to human activities, such as mining, smelting, fossil fuel burning, manufacturing, and recycling (Caito & Aschner, 2015; Tchounwou et al., 2012). Pb has many different industrial, agricultural, and domestic applications. It is currently used in producing lead-acid batteries, ceramics, ammunition, and devices to shield X-rays (Sharma et al., 2014; Tchounwou et al., 2012). Tetraethyllead (TEL) was once commonly used as an antiknock additive in automobiles' gasoline but has been banned in all countries. However, TEL and other organolead compounds are still approved for use in

aviation fuels (Caito & Aschner, 2015). Like other heavy metals, the use of Pb has been in decline due to its proven toxicity, and it is being replaced with safer options.

Human exposure can occur in occupational exposure, through inhalation and ingestion of Pb dust and vapours. The primary sources of Pb exposure in the general population are exposure to Pb dust and chips from deteriorating lead paint on older housing and exposure to Pb from aging water infrastructure. These sources of Pb exposure are of particular concern to children. Contamination of water and food is another source of Pb exposure, as well as traditional medicines and cosmetics (Tchounwou et al., 2012; Ufelle & Barchowsky, 2021).

Intentional poisoning cases involving Pb are uncommon. A more recent phenomenon observed in Pb poisoning cases is the adulteration of opium with Pb. Opium manufacturers may add Pb to opium to increase the weight of the substance, thereby increasing their profit margins. This results in Pb poisoning among drug users, with symptoms that are challenging to diagnose (Balali-Mood et al., 2015; Farnaghi et al., 2020).

Pb enters the organism mainly through gastrointestinal and respiratory tracts, but organic Pb compounds can be absorbed through the skin. Adults absorb 35 to 50% of Pb through ingestion, but absorption rates can be higher than 50% for children (de Souza et al., 2018; Tchounwou et al., 2012). Once in the bloodstream, more than 90% of Pb is associated with erythrocyte membranes and haemoglobin with a half-life of about 35 days. About 5% of Pb in the body forms an exchangeable pool, corresponding to plasmatic Pb, available to other tissues. Pb can remain stored as insoluble phosphates after achieving hard tissues such as bone and teeth, with a half-life of 20 to 30 years. Soft tissues, like the kidney, liver, lungs, and brain can also store Pb. Pb can also accumulate in the brain but only after inducing damages to the BBB that allows Pb to cross it (Baldwin & Marshall, 1999; de Souza et al., 2018). Renal excretion occurs through glomerular filtration with some renal tubular resorption. Fecal excretion accounts for only one-third of the total excretion of Pb (Ufelle & Barchowsky, 2021).

Pb toxicity is attributable to its ability to imitate other biologically significant metals, notably calcium, iron, and zinc, which function as cofactors in numerous enzymatic reactions. Pb can replace these metals, interfering with the enzyme's ability to catalyse normal reactions (Sharma et al., 2014). Pb can also bind to sulfhydryl and amide groups of enzymes, altering their configuration and diminishing their activities. Besides, it has

been demonstrated that Pb induces cellular damage mediated by the formation of ROS (Tchounwou et al., 2012).

The δ-aminolevulinic acid dehydratase (δ-ALAD) is one of the main targets of Pb, where it replaces the zinc in the enzyme metal binding site, inhibiting the δ-ALAD activity. This results in a decrease in heme biosynthesis and in the impairment of haemoglobin synthesis. Another pathway of heme interference by Pb is the inhibition of the enzyme ferrochelatase, which reduces the incorporation of iron into the heme group. Therefore, Pb-intoxicated individuals usually present anaemia (de Souza et al., 2018; Rehman et al., 2018).

Moreover, Pb causes a disturbance in the balance of GSH and glutathione disulfide (GSSG), due to its high binding affinity for sulfhydryl groups. The increased blood levels of δ-aminolevulinic acid (δ-ALA) and a depletion of GSH lead to an increase in ROS levels after Pb exposure (Rehman et al., 2018) (Figure 4). As a consequence, Pb-induced oxidative stress causes extensive DNA damage.

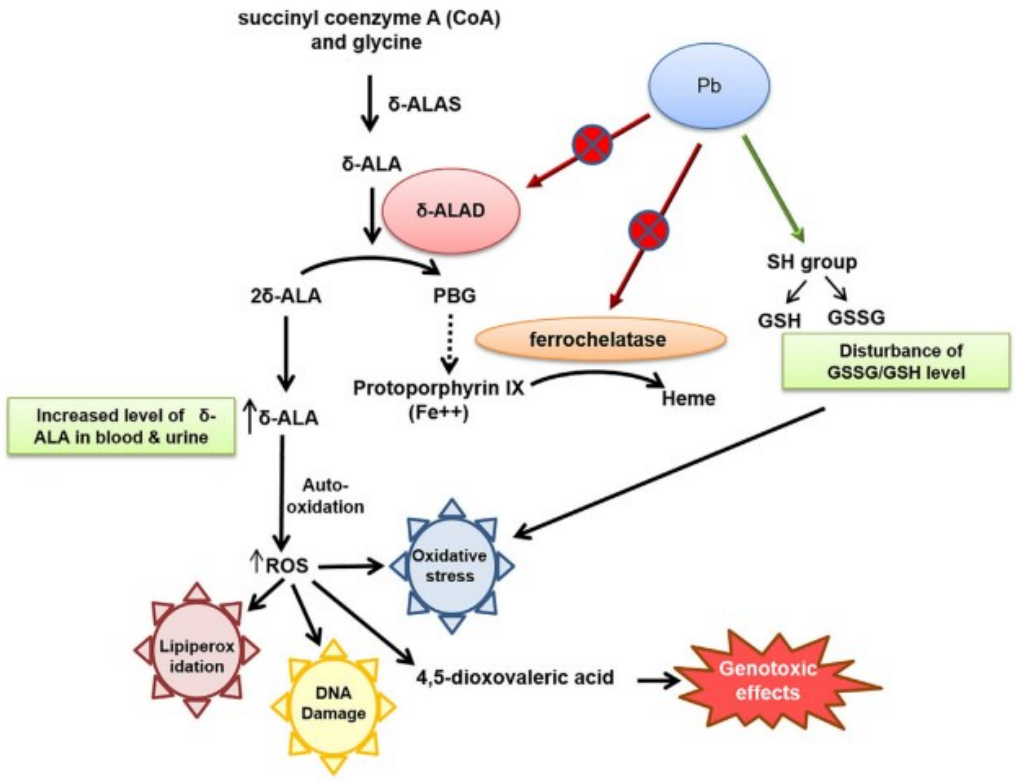

Figure 4: Lead toxicity mechanism. From Rehman et al. (2018).

In addition, Pb can potentially disrupt the functionality of DNA repair systems, leading to the introduction of critical DNA mutations and, subsequently, apoptosis. This evidence illustrates the potential for Pb to induce carcinogenesis (Ufelle & Barchowsky, 2021).

Pb is strongly associated with neurotoxicity. First, the stimulation of protein kinase C through calcium mimicry may alter the BBB permeability, allowing Pb to cross it (Ufelle & Barchowsky, 2021). Then, calmodulin-mediated pathways can be compromised due to calcium replacement. Calmodulin is a ubiquitous calcium-binding protein that affects and stimulates many metabolic functions such as inflammation, apoptosis, muscle contraction, intracellular movement, nerve growth, and immune response. Pb affinity to calmodulin causes inappropriate activation of several proteins involved in learning and cognitive functions. The inhibition of adenylate cyclase by Pb is another mechanism for its neurotoxic effects since adenylate cyclase plays a central role in axonal growth, in the interaction of astrocytes and neurons, and in neurotransmitter release (de Souza et al., 2018).

Pb has been described to bind to some members of the zinc finger family of transcription factors by competing with zinc ions. Zinc fingers are related to several functions such as DNA recognition, RNA packaging, transcriptional regulation, apoptosis, and protein packing (de Souza et al., 2018).

Pb exposure may result in elevated Pb levels in the bloodstream, which could potentially lead to Pb poisoning, also known as saturnism or plumbism. It is characterized by a broad range of physiological, biochemical, and behavioural dysfunctions, including those affecting the peripheral and central nervous systems, the haematopoietic system, the cardiovascular system, the kidneys, the liver, and the reproductive system. The nervous system is the most susceptible to the detrimental effects of Pb poisoning (Rehman et al., 2018; Sharma et al., 2014).

1.1.5. Methods for heavy metal analysis

According to Bhor’s atomic model, the atom consists of a nucleus surrounded by electrons that travel in discrete orbitals. Each electron orbital has an associated energy level, in which those further away from the nucleus have higher energies, and vice-versa.

An atom's stability is contingent upon its electrons' proximity to the nucleus. When electrons are closer to the nucleus, the atom is more stable, a state referred to as the ground state. However, when electromagnetic or thermal energy is introduced to the atom, it

absorbs the energy and becomes excited by moving an electron to a higher-energy orbital. However, this state is less stable and the atom will revert to a less excited state by losing energy through the emission of a particle of electromagnetic radiation, namely a photon. Each element has its own characteristic set of energy levels and, thus its unique set of absorption and emission wavelengths, allowing the use of light to its identification.

The most commonly used techniques for trace element analysis are the atomic spectroscopy techniques represented in Figure 5.

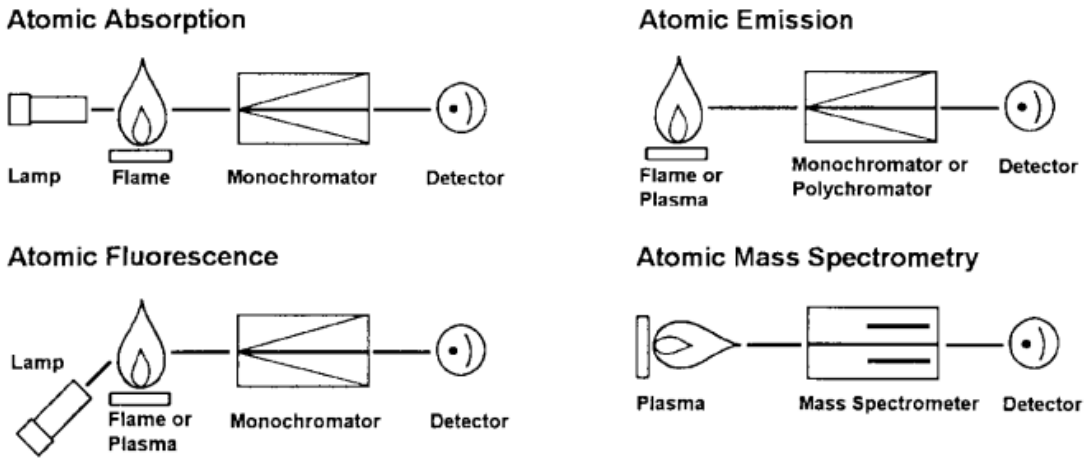

Figure 5: Atomic spectroscopy techniques. From Boss & Freedeen (2004).

In atomic absorption spectroscopy (AAS), light with a wavelength specific to the element of interest is shone at and absorbed by the atoms of that element. The intensity of light that is absorbed by these atoms is then measured and used to determine the concentration of that element in the sample.

In optical emission spectroscopy (OES), the sample is subjected to high temperatures that cause the dissociation and collisional excitation of the sample atoms. Once the atoms are excited, they can decay to lower energy states through the emission of radiation. In OES, the intensity of the light emitted at specific wavelengths is measured and used to determine the concentrations of the elements of interest.

In atomic fluorescence spectroscopy, a light source excites only the elements of interest through radiative absorption transitions. When these excited atoms decay to lower levels, their emission is measured.

In atomic mass spectrometry, a quadrupole mass spectrometer separates the ions of various elements according to their mass-to-charge ratio.

In these techniques, the sample is decomposed in intense heat to dissociate sample molecules into free atoms. Three types of thermal sources are usually used in analytical atomic spectroscopy: flames, furnaces, and electrical charges. In the case of OES, other types of discharges, namely plasmas, have been used as excitation sources (Boss & Fredeen, 2004).

Inductively Coupled Plasma Optical Emission Spectroscopy (ICP-OES) is a very commonly used technique for trace element analysis in different matrices. ICP-OES instrumentation is represented in Figure 6. In ICP-OES, the sample is transported into the instrument as a liquid stream. Once within the instrument, the liquid is converted into an aerosol through the process of nebulization, which is then transported to the plasma. A plasma can be defined as an ionized gas comprising positively charged ions and free electrons. To generate plasma, argon gas is supplied to the torch coil, and a high-frequency electric current is applied to the torch tube. Using the electromagnetic field created in the torch tube by the high-frequency current, argon gas is ionized, and plasma is generated. This plasma exhibits high electron density and temperature (10,000 K), which is employed in the excitation of the sample. The excited atoms and ions subsequently emit their characteristic photons, collected by a device that sorts the radiation by wavelength. Single-element measurements can be conducted with a simple monochromator/photomultiplier tube (PMT) combination, and simultaneous multielement determinations are achieved with the combination of a polychromator and an array detector (Ghosh et al., 2013; Wilschefski & Baxter, 2019).

ICP-OES usually uses Argon gas since most elements have a first ionisation potential much lower than argon and are efficiently ionised in the plasma, enabling the identification of almost all elements in the periodic table (Wilschefski & Baxter, 2019).

This technique presents many advantages, including multi-element analysis, large analytical range, high accuracy and precision, low background emission, low sample volume, and simple sample preparation. However, biological samples need to be thermally digested before analysis, leading to sample loss and inability to repeat analysis. Other disadvantages to ICP-OES include the equipment cost and laboratory set costs (Wilschefski & Baxter, 2019)

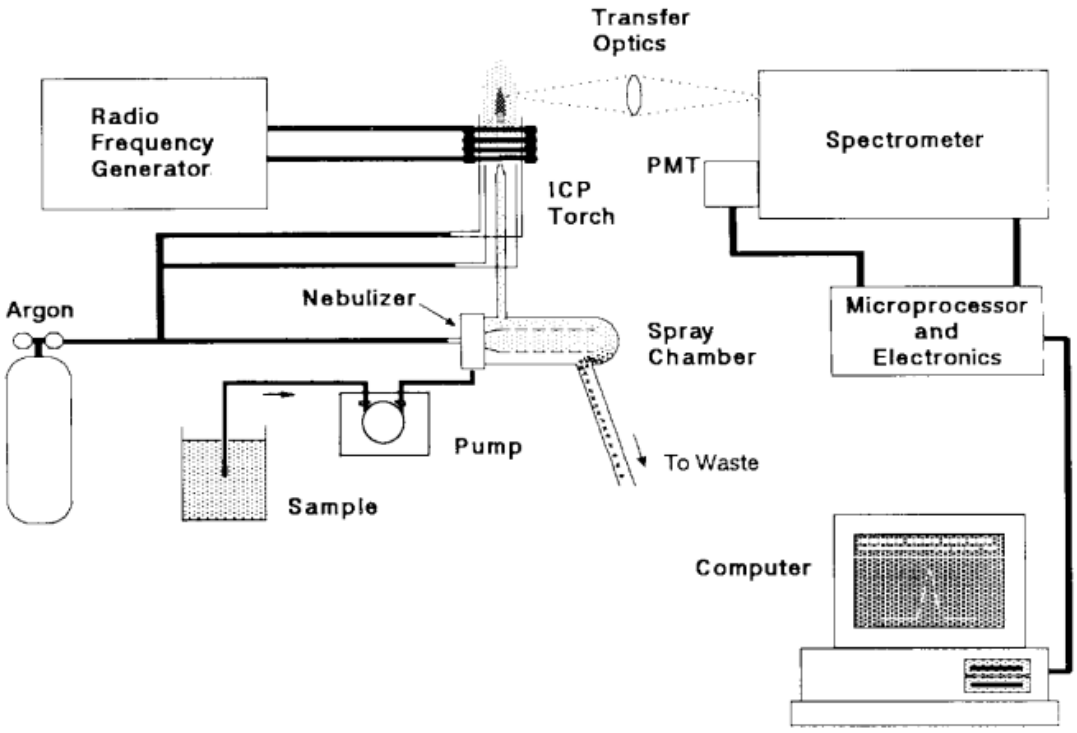

Figure 6: IPC-OES instrumentation. From Boss & Freedeen (2004).

The analysis of Hg in biological samples presents a significant challenge. Accordingly, a dedicated instrument for Hg analysis, the AMA-254, is available. This method is based on cold vapor atomic absorption spectrometry (CVAAS), which is the most commonly employed technique for determining Hg concentrations. In the context of CVAAS, Hg is reduced to its elemental form, producing Hg vapour. The Hg vapour is liberated from the sample by the passage of a gas, such as air, nitrogen, or argon, using a gas-liquid separator. Subsequently, the sample is introduced into the optical path of an atomic absorption spectrometer for measurement.

The AMA-254 apparatus comprises a nickel boat within a quartz combustion tube containing a catalyst. The solid sample is initially dried before combustion at 750°C in an oxygen atmosphere. Subsequently, Hg vapour is captured on the surface of a gold amalgamator. The amalgamator is heated to 900°C for a pre-specified time interval to release Hg. Then, Hg is transported to a heated cuvette (120°C) prior to analysis by AAS with a silicon diode detector at 253.6 nm (Figure 7) (Costley et al., 2000).

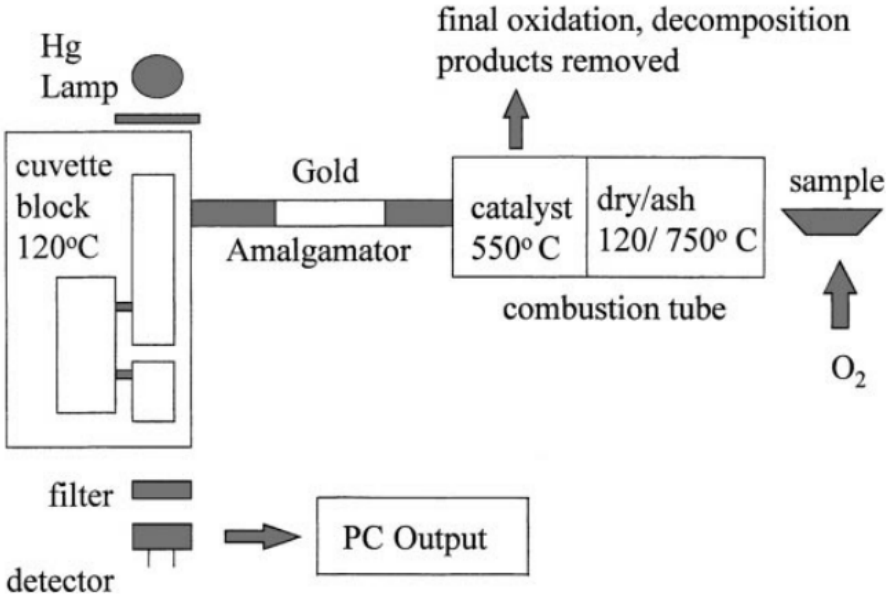

Figure 7: AMA-245 instrumentation. From Costley et al. (2000).

The principal benefit of this apparatus is the capacity to conduct direct analysis of solid samples without the necessity for preliminary treatment. Moreover, the analysis of samples is relatively rapid. However, a significant drawback of this instrument is the inability to perform background corrections, which could pose a challenge for samples with high organic content (Costley et al., 2000). In these cases, aluminium oxide is used to cover the sample to reduce the background noise. It also does not allow repetition of analysis, as the sample is destroyed.

X-Ray fluorescence (XRF) spectrometry represents an additional analytical technique for determining heavy metals based on the same fundamental principles as atomic spectroscopy. When a beam of X-rays interacts with a sample, it creates a vacancy in one of the shells of the atom. This phenomenon is known as the photoelectric effect, which results in the emission of characteristic X-rays. However, once a vacancy has been created in an inner shell, the atom can also emit Auger electrons to return to a stable state. For elements with a low atomic number, the emission of Auger electrons is the dominant process, whereas for elements with a high atomic number, the emission of characteristic X-rays is more prevalent.

The wavelength or energy of the emitted radiation is characteristic of each element, according to Moseley's law, which states that the square root of the frequency of the

emitted X-ray is proportional to the atomic number. Therefore, the elements of the analysed sample can be identified (Wobrauschek et al., 2010).

The sample can reflect a part of the irradiated X-rays instead of producing characteristic radiation. This process is called scattering and can be incoherent (Compton) and coherent (Rayleigh). Compton or incoherent scatter occurs when a photon loses a fraction of its energy, which is taken in by the electron. On the other hand, Rayleigh or coherent scatter happens when electrons stay in their shell, but begin to oscillate, emitting radiation at the same frequency as the incident radiation. The scattered X-rays are an important part of background radiation (Brouwer, 2003; Wobrauschek et al., 2010).

Wavelength-Dispersive X-ray Fluorescence (WDXRF) is an instrumentation of XRF spectrometry in which the wavelength of the characteristic photon is measured, allowing the determination of the elements of the sample. It is designed with several individual fixed spectrometer channels, each optimized for determining a designated element, allowing for a multi-element analysis (Potts, 2005). The configuration of the WDXRF instrument is presented in Figure 8.

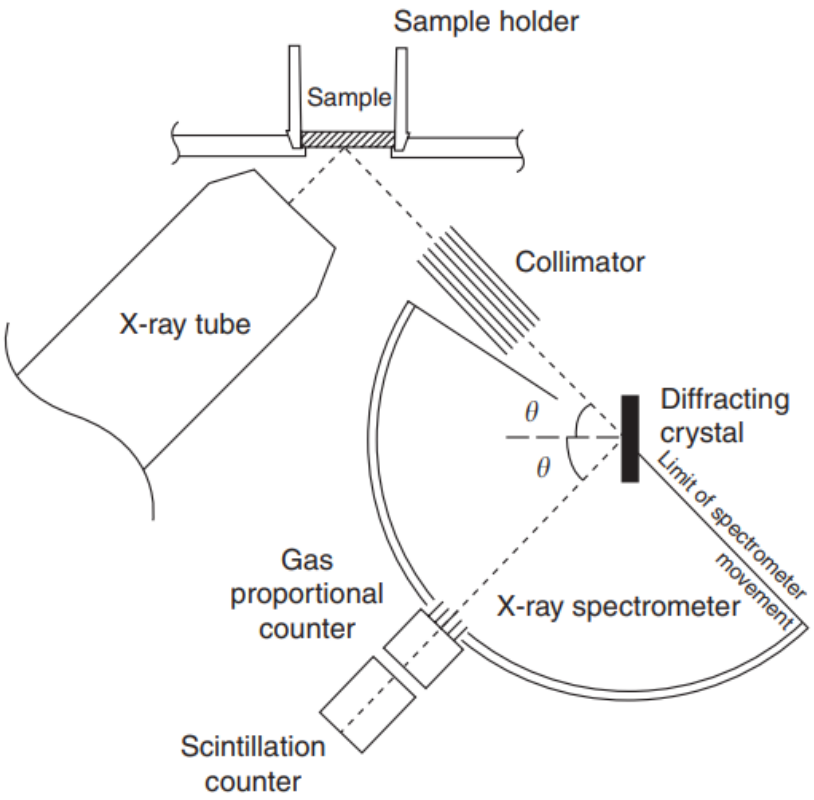

Figure 8: WDXRF instrumentation. From Potts (2005).

The X-ray tube irradiates the sample with high-energy X-ray photons, thereby exciting the elements present. The X-ray flux is generated when a beam of electrons, emitted from an incandescent filament, is accelerated through a large potential difference and directed at a metallic anode, resulting in the emission of characteristic fluorescence X-rays. The interaction of the electron beam with the atoms of the anode results in the emission of secondary X-ray radiation, a bremsstrahlung or continuous X-ray emission, directed at the sample. Rhodium (Rh) anode tube is usually used, since Rh K-lines efficiently excite the heavier elements, whereas Rh L-lines are more adequate to excite lighter elements (Potts, 2005).

The WDXRF spectrometer behaves as an X-ray monochromator, separating the radiation into a range of individual wavelengths. Selected crystalline materials are used to diffract X-ray photons and the intensity of the diffracted radiation is counted using a simple radiation counter. Besides, the X-ray spectrometer needs a collimator, to restrict the angular divergence of fluorescence X-rays accepted for diffraction and a goniometer mechanism to maintain the correct geometric relationship between these components. Finally, the radiation counter measures the intensity of the diffracted X-ray beam, allowing the determination of elements and their concentration in the sample, since the intensity is proportional to the concentration of the respective element (Potts, 2005; Wobrauschek et al., 2010).

The spectrometer chamber is usually operated under vacuum, but such conditions are incompatible with the analysis of liquids or loose powders, which require the use of helium gas at atmospheric pressure. Some samples, like loose powders, may be heterogeneous and contain grains of different sizes, affecting penetration depths for X-rays. Therefore, grinding into a fine powder may be necessary in these cases. During analysis, samples are normally rotated to minimize any variations caused by unevenness in the analysed surface (Potts, 2005; Wobrauschek et al., 2010).

The major advantage of WDXRF technique is that measurements are performed directly on the sample, without the need for pre-treatment, avoiding the lengthy and laborious process of preparation, and is non-destructive, allowing for repeated measurements without material loss. Also, this technique is relatively quick and has low detection limits. Besides, it is possible to perform a semi- and/or quantitative analysis (Fernandes et al., 2015).

1.2. Forensic entomology

Forensic entomology can be a valuable investigative tool in cases of heavy metal poisoning.

Forensic entomology is defined as the application of entomological evidence in criminal investigations. The objective of employing forensic entomology is to answer some key questions pertinent to the forensic investigation, particularly, at what time and where the victim died, and what's the cause of death.

The main application of forensic entomology is to estimate the time at which the death occurred, by estimating the *post-mortem* interval (PMI). The PMI is defined as the time between death and the discovery of the body and can be estimated through various ways.

A pathologist usually determines the PMI through the natural decomposition processes, such as *rigor mortis* or *livor mortis*. However, these methods are only used to roughly approximate how long the victim has been dead, as many factors affect human decomposition, some directly associated with the body (e.g. age, constitution, integrity of the corpse, cause of death) and others associated with the environment (e.g. temperature, humidity, access of the body to animals), and become inaccurate in application very quickly. In fact, they are only limited to the first 72 hours after death.

As such, insects can be a powerful tool for estimating the time since death, as necrophagous insects will quickly colonize the body within the first hours, depending on the accessibility of the body and environmental conditions. Therefore, calculating the age of the oldest developing insects on a body allows for the determination of the colonization time. This infers a minimum *post-mortem* interval (mPMI), i.e., the time of initial insect colonization of the body, rather than the specific time of death (Amendt et al., 2011). The estimation of mPMI using the oldest insects that have developed on the body is used during the earlier *post-mortem* periods. During the late *post-mortem* period, the estimate is based on the composition of the arthropod community in and around a corpse, as it changes in a predictable successional sequence as decomposition progresses (Amendt et al., 2007; Catts & Goff, 1992).

The first insects to arrive on a corpse are flies (Diptera), particularly blowflies (Calliphoridae), which can locate an odour source with great spatial precision, via antenna receptors (olfaction) and visual search, and deposit their eggs on a corpse within hours or even minutes after death. For this reason, blowflies are the most used for mPMI

estimations. Other families of forensic important flies are flesh flies (Sarcophagidae) and house flies (Muscidae) (Amendt et al., 2011; Byrd & Castner, 2009).

Among blowflies, *Calliphora vicina*, also known as the blue bottle fly, is of particular forensic importance. This species has a nearly worldwide distribution, with a high prevalence on human corpses in temperate regions of the United States and Europe. This species is particularly prevalent in shaded urban habitats, where it often represents the dominant species on human corpses (Byrd & Castner, 2009). In Portugal, *C. vicina* is the dominant species during winter but can be found throughout the year (Prado E Castro et al., 2012).

For an accurate mPMI estimation, several factors need to be considered. First, a proper identification of the species is imperative, as insect species differ in growth rate, arrival time, and order of succession. Secondly, it is important to consider that an insect's development rate is mainly governed by temperature. Generally, as temperature increases, the insect development is accelerated. However, there are temperature extremes that are lethal to the insect. As such, the local temperature and the maggot mass temperature need to be recorded, as the latter can generate a higher temperature than the ambient temperature. It is then necessary to reconstruct the crime scene temperatures and model the rate of development of the immature insects found (Amendt et al., 2011; Byrd & Castner, 2009). To model the rate of development of insects, the duration of development data is recorded at different temperatures, which are then summarized in developmental models, namely isomorphen diagrams, isomegalen diagrams, or thermal summation models. The developmental data typically employed encompass both size (in terms of both length and weight) and developmental events (such as the emergence of the first instar, the third instar, pupariation, and adult emergence) (Amendt et al., 2011). Additionally, certain toxic substances in or on the victim may have a variety of effects on carrion insects and insect growth can be accelerated or decelerated, depending on the substance and concentration. Factors affecting oviposition (such as meteorological conditions, covering the corpse, and the deposition of a body at night) also need to be considered (Byrd & Castner, 2009).

In cases of translocation of the body, forensic entomology can be useful to determine the original location of death. This is due to the fact that different species are associated with distinct biogeographical regions. Moreover, certain species are found in both urban and rural areas, whereas others are exclusive to a particular region. Consequently, identifying

specific species on a corpse may indicate a transfer of the body from one geographical area to another. Similarly, specific species are linked to either outdoor or indoor colonization (Byrd & Castner, 2009; Catts & Goff, 1992). Besides, detecting certain contaminants in the reared insects can indicate certain areas (Gagliano-Candela & Aventaggiato, 2001).

Forensic entomology can also aid the investigation of the cause of death. First, colonizers are attracted to exposed wounds due to the presence of blood. Thus, subsequent maggot mass formations and uneven distributions of insect activity can indicate *peri-mortem* trauma (Byrd & Castner, 2009). On the other hand, insects can be used as toxicological evidence for *ante-mortem* substances present in the body. This is part of a specialized field of forensic entomology, called entomotoxicology. The main objective of entomotoxicology is the use of necrophagous insects as alternative toxicological evidence for the determination of toxic substances, when traditional biological samples, such as blood, urine, or tissue, are not readily available, e.g., in the case of skeletonized remains. Also, in badly decomposed bodies, toxicological analysis can be facilitated by using insects, with less interference from matrix decomposition (Amendt et al., 2011; Gosselin et al., 2011). Besides, if the absorption rate exceeds a substance's excretion rate, insects will bioaccumulate it. In these cases, toxicant analysis might be easier in the insects than in traditional toxicological samples (da Silva et al., 2017).

Most substances involved in drug-related deaths (drugs, metals, and pesticides) are detectable on larvae, which are then processed similarly to traditional biological samples. Other organic materials of entomotoxicological interest are pupae, adult insects, puparial cases, exuviae (cast beetle skins), and beetle faecal material. The choice of technique for toxicological analysis depends on the physicochemical properties of the substance of interest and the required selectivity and sensitivity (Gagliano-Candela & Aventaggiato, 2001; Gosselin et al., 2011).

It is well established that forensic insects are useful as qualitative toxicological specimens, enabling the identification of certain toxic substances. However, they still have limited quantitative value due to contradictory information regarding the correlation between toxin concentrations in insects and the feeding tissues. This limitation may arise from factors such as drug pharmacokinetics, metabolism, and accumulation in different insect species. Additionally, differences between drug concentrations in larvae and tissues may be caused by the unpredictable movement of larvae on the corpse. If the larvae's

excretion rate of the substance exceeds the absorption rate or if the larvae do not accumulate the substance, then the concentrations in the larvae are expected to be lower than those in the substrate. Conversely, if the larvae have the capacity to bioaccumulate the substance, then the concentrations in the larvae will be higher than in the substrate. However, obtaining a consistent quantitative relationship remains challenging (Amendt et al., 2011; Chophi et al., 2019). Therefore, further studies are needed to better understand these dynamics, explore the potential of quantitative relationships, and improve the reliability of forensic entomotoxicology.

As previously mentioned, toxic substances can induce changes in necrophagous insects' development rate and behaviour, delaying or accelerating insect growth, and leading to significant errors in mPMI estimations. The effects on the development rate are dependent on the drug, drug concentration, the fly species, and the stage of development (Amendt et al., 2011).

Lastly, entomotoxicology can also be useful in identifying people by adding to profiling studies, e.g., by revealing chronic medication (da Silva et al., 2017).

Thus, in cases of heavy metal poisoning, forensic entomology can serve as a powerful tool, easing the detection of heavy metals in decaying corpses. However, it is necessary to consider the effects of these toxic substances on the development and survival of forensically important species, and their influence on mPMI estimations, since heavy metals might alter the insect's growth rates and life cycle, potentially leading to inaccurate mPMI calculations and restrict their use as toxicological markers.

1.2.1. Forensic entomology and heavy metals

The knowledge of the effects of heavy metals on forensically important insect species is still very shallow since only a few studies have been conducted in this area.

The accumulation of Cd has been studied in the flesh fly *Sarcophaga peregrina*, where it was found that larvae accumulate the metal mainly in the digestive tract, with the induction of Cd-binding proteins (Aoki et al., 1984). Furthermore, Cd content in adults decreased significantly, meaning that Cd was mainly excreted after adults' emergence (Aoki & Suzuki, 1984).

The accumulation and effects of Cd have also been studied in blowflies, namely *Lucilia sericata*. Cd has been detected in all development stages of *L. sericata* reared in Cd-contaminated food sources (Moe et al., 2001; Simkiss et al., 1993) and it was found a

linear relationship between Cd content on the substrate and Cd content on the specimens (Malejko et al., 2020). However, like *S. peregrina*, most Cd content is lost after adult emergence, with 80% left on the pupal case (Simkiss et al., 1993). Cd appears to cause an increase in the developmental time of *L. sericata* maggots and a decreased growth and weight, leading to smaller pupae and adult size (Kökdener et al., 2022; Moe et al., 2001; Simkiss et al., 1993). Simkiss et al. (1993) suggested that these results were probably due to a reduction in the intake of nutrients and extra demands on the metabolism for toxicant elimination. A higher mortality rate in all development stages is expected when Cd is introduced to the food supply (Kökdener et al., 2022; Moe et al., 2001).

Similar results were found on blowfly *Chrysomya megacephala,* where the prolonged development time caused by Cd exposure could lead to miscalculation of mPMI by up to 18-86 hours (Singh & Kaur Heer, 2017).

Shulman et al. (2017) also studied the effects of Cd on *C. vicina* to some extent. They verified decreased puparia mass, adult malformations, reduced motor activity, delayed development time, and a higher mortality rate.

Forensic entomology is utilized in gunshot residue (GSR) studies to investigate the potential use of insects in identifying gunshot wounds and detecting GSR chemically, providing a valuable tool for forensic investigations (Lagoo et al., 2010). Therefore, effects of Pb have been investigated through GSR studies since this element is its' main component. Besides Pb, barium (Ba) and antimony (Sb) are also characteristic elements of GSR (Lagoo et al., 2010), and several studies have explored larvae's capacity to accumulate these elements and, therefore, be used as forensic evidence.

Roeterdink et al. (2004) found high concentrations of Pb, Ba, and Sb in larvae and pupae of *Calliphora dubia* reared on pieces of beef that were shot and, therefore, contaminated with GSR. They verified that Sb and Pb concentrations decreased with time, probably because of increased larval activity or non-uniform distribution of GSR on the food source. However, Ba concentrations remained constant, possibly due to its physical-chemical similarities to calcium, leading to an inefficient elimination of this element. Furthermore, following the transfer of larvae from GSR-contaminated to uncontaminated food, Pb, Ba, and Sb concentrations decreased to control levels. Also, empty puparia did not show significant concentration differences from the control and thus were not helpful as toxicological evidence.

Similar studies have also obtained similar results with different species, namely *L. sericata* and *Chrysomya albiceps*, with all elements being detected and quantified on larvae (Lagoo et al., 2010; Motta et al., 2015; Rashid et al., 2012), even in real crime scenes (Costa et al., 2020).

Detection of these elements in these studies was performed using Inductively Coupled Plasma Mass Spectroscopy (ICP-MS) or ICP-OES techniques, finding Pb concentrations up to 156.8 mg/kg. However, these studies did not measure Pb concentrations on the rearing substrate, so no bioaccumulation determination was made. Still, Calliphoridae larvae seem adequate as toxicological evidence to detect GSR elements. Additionally, using the square wave anodic stripping voltammetry technique, Bessa et al. (2021) determined *Lucilia cuprina* larvae's Pb concentration was about 23.1% of that contained in the diet. As such, no bioaccumulation from Calliphoridae larvae was determined for Pb.

Besides detection, the effects of these elements on the development life-history parameters of blowflies have also been studied.

Rashid et al. (2012) observed a negative effect on the weight of *C. megacephala*'s larvae after 48 hours of exposure to GSR-contaminated food. The survival rate from larva to adult was also affected, with an increased mortality rate and prolonged duration of each development stage, causing a delay of about 12 hours, which could lead to inaccurate mPMI estimations. Similar results on *L. sericata* reared on GSR-contaminated food were observed, with decreased larvae and pupae length and weight, and reduced survival rate (Kökdener & Yllmaz, 2021). A study conducted on *Lucilia cuprina* larvae reared in a contaminated substrate with increasing concentrations of Pb showed its high toxicity, affecting larval survival at high concentrations. However, the results also show that low concentrations seem to accelerate the larval development of this species (Bessa et al., 2021).

On the other hand, Pb also negatively affected the developmental time of *C. vicina*, causing reduced motor activity at all developmental stages and malformations in adult flies. Higher mortality was also observed at the larval and pupal stages. However, it caused an increase in pupal mass (Shulman et al., 2017).

There is some evidence of the ability of blowflies to bioaccumulate Hg when reared on carcasses of animals with known Hg content. Nuorteva & Nuorteva (1982) detected Hg

concentrations on blowflies using AAS technique and determined a bioaccumulation factor from 1.5 up to 4.3 on blowflies reared in fish with methylated forms of Hg. However, when reared on seal liver containing mainly inorganic Hg, the bioaccumulation factor declined to 0.5. Therefore, blowfly larvae appear to have a greater capacity to excrete inorganic Hg than MeHg. Hg levels are also significantly reduced after adult emergence. No adverse effects were detected in either the adult flies or the larvae, with only some difficulties observed in pupariation. However, symptoms similar to those of Minamata disease were observed in adult tenebrionid beetles (*Tenebrio molitor*) fed with fly larvae containing Hg (Nuorteva & Nuorteva, 1982).

Kökdener et al. (2022) also investigated the effects of copper (Cu) and zinc (Zn). These heavy metals had the same effects as the other metals mentioned above, affecting the life history parameters of *L. sericata* - reduced larval weight and length, reduced pupal and adult weight, and increased mortality. In addition, elevated concentrations of Cu and Zn prolonged developmental time. Abajue & Ewuim (2020) detected zinc in maggots reared on pig cadavers contaminated with zinc phosphide. They also noted no delay in insects' colonization and oviposition on contaminated cadavers.

Malejko et al. (2020) also studied the effects of thallium (Tl) on *L. sericata*. Tl had the same effects as other heavy metals, described previously. Tl was detected in all development stages of *L. sericata*, and a saturable relationship between Tl content on the substrate and Tl content in *L. sericata* stages was verified. Tl content was higher in pupal cases than in larvae, suggesting that this might be *L. sericata*'s detoxification mechanism of Tl.

There are no published studies on the effects of As on forensically important insect species.

1.3. Objectives

This project aims to examine the impact of the most prevalent heavy metals responsible for human poisoning, namely As, Hg, Pb, and Cd, on *C. vicina* larvae. The objective is to determine the growth and survival rates of *C. vicina* for each heavy metal, establish the lethal dose 50 (LD50) for the larvae, and assess the potential for bioaccumulation. In conclusion, the objective is to determine whether *C. vicina* can serve as toxicological

evidence for these metals under certain conditions and evaluate the studied metals' impact on the *post-mortem* interval estimates.

2. Materials and Methods

2.1. Reagents

The following reagents were used for contaminating the rearing substrate: arsenic standard solution (1 g/L As in 2% nitric acid, prepared with high purity As_2O_3, HNO_3, NaOH and water, from Sigma-Aldrich, Lisbon, Portugal); cadmium acetate dihydrate (100 g, Thermo Fisher Scientific, Lisbon, Portugal); lead acetate (250 g, Carlo Erba Reagents, Emmendingen, Germany) and phenylmercuric acetate (25 g, Sigma-Aldrich, Lisbon, Portugal). Stock solutions were prepared with deionised water.

For sample digestion, concentrated nitric acid (65%, Pronalab, distributed by Jose M. Vaz Pereira Lda., Lisbon, Portugal) and hydrogen peroxide (30%, Normax Chem, Marinha Grande, Portugal) were used.

2.2. Model species

This experimental study began at the beginning of the winter season in Portugal. Due to this, *C. vicina* was used as a model as it is a standard organism in forensic entomology studies and is the dominant blowfly species during winter.

2.3. Experimental design

The adult specimens of *C. vicina* were collected using a Van Someren-Rydon trap baited with commercial dog food (paté with beef and liver, Elou Pet). Specimens were identified using entomological keys (Szpila, 2010b, 2010a). The specimens were maintained in a net cage with a diet of sugared water, fruit, and the same dog food used as bait, at temperatures between 20 and 22ºC. Some specimens were allowed to develop in order to maintain the colony fully. When eggs were required, 300 g of the dog food was provided for oviposition.

To prepare the substrates for each experiment, 50 g of dog food was weighed using a microbalance and transferred to 250 mL glass jars. 10 mL of solution was added and homogenized with a glass rod, making up the required concentrations of 0.5, 5, 30 and 60 mg/kg of each compound. The negative control was obtained by adding 10 mL of deionised water. The heavy metals subjected to analysis were As, Hg, Cd, and Pb. Various heavy metal compounds were utilized, including phenylmercury acetate, lead acetate, and cadmium acetate.

2.4. Survival and development rate

The eggs were collected, counted, and placed to hatch in substrate spiked with varying concentrations of each heavy metal compound (0, 0.5, 5, 30, and 60 mg/kg). The same number of eggs was allocated to each concentration.

After the larvae's emergence (about 24 hours after oviposition), unhatched eggs were counted for survival rate determination. At the end of each rearing period (6 days), the remaining larvae were washed with deionised water and stored at -80ºC until analysis.

To determine the larvae's development rate, their length was measured using a ruler under the observation of a stereomicroscope. Additionally, the larvae's weight was determined via microbalance.

To ascertain the survival rate, the number of surviving immatures was counted. Subsequently, an online platform (https://www.aatbio.com/tools/ld50-calculator) was employed to plot the survival rate and calculate the lethal dose 50 (LD50) for each metal.

The analysis of survival and development rate was performed in the Molecular Biology Laboratory of Egas Moniz School of Health & Science.

2.5. Sample preparation for metal analysis

Stored larvae samples were macerated using a mortar and pestle and stored at -20ºC for 24 hours. Samples were then lyophilised using the MODULYO D-230 Freeze Dryer (Thermo Electron Corporation, Asheville, NC) at -50ºC for 48 hours and macerated again. The same procedure was employed for prepared substrate samples. Both larvae and substrate samples were analysed for As, Cd, Hg, or Pb content using WDXRF, ICP-OES and AAS techniques.

2.5.1. WDXRF analysis

The concentration of each metal in the substrate samples and lyophilised larvae was determined using a WDXRF S4 Pioneer spectrometer (Bruker AXS, Karlsruhe).

The analytical procedure includes calibrating the equipment using standards prepared “in-house” with known concentrations of each metal, in which glycine was chosen to simulate the larvae matrix. For this, 3 g of glycine were weighed and spiked with each metal to obtain the required concentrations. The calibration standards were dried at 40ºC for 48 hours and then divided into 1 g replicates. The prepared glycine standards and samples weighed around 1 g and were directly analysed by the spectrometer.

As samples were loose powders, WDXRF analysis was performed in helium mode. WDXRF analysis was performed at Elementals Laboratory of Egas Moniz School of Health & Science. All heavy metals were analysed using this technique.

2.5.2. ICP-OES analysis

In order to conduct an ICP-OES analysis, acid digestion is necessary. A total of 200 mg of the sample's dry weight was placed in polypropylene vessels. Subsequently, 2 mL of 65% nitric acid and 1 mL of 30% hydrogen peroxide were added to the sample. Then, the vessels were left open overnight for pre-digestion at room temperature. Afterward, the vessels were partially sealed and placed in a water bath for 15 minutes at 80°C. Following cooling, the vessels were filtered using a 25 mm syringe filter with 0.2 µm cellulose acetate membrane, and the resulting solution was analysed for As, Cd, and Pb content.

ICP-OES analysis was conducted at NOVA School of Science and Technology's Analytical Laboratory.

2.5.3. AAS analysis

Mercury content was analysed using the AMA254 Mercury Analyzer (Leco 254 Advanced Mercury Analyzer). For this analysis, dried samples were analysed directly. Approximately 10 mg of each sample was analysed, except for the highest substrate concentration, where only 1 mg was analysed. This analysis was conducted at the Faculty of Pharmacy of the University of Lisbon's Toxicology, Biomarkers & Risk Assessment Laboratory.

2.5.4. Bioaccumulation

Following the determination of the results from the various techniques, the bioaccumulation factor (BAF) was calculated as the ratio of the heavy metal content in *C. vicina* samples to the metal content in the feeding substrate, as follows:

$$BAF = \frac{metal\ content\ in\ Calliphora\ vicina\ (ppm)}{metal\ content\ in\ feeding\ substrate\ (ppm)}$$

If the BAF value exceeds 1, it can be concluded that the organism is engaged in the process of bioaccumulation concerning the metal in question. Conversely, if BAF is less than one, no bioaccumulation is occurring.

2.6. Statistical analysis

Graphical analysis was conducted utilising the Jamovi software. The statistical analysis was conducted using the JASP software. A series of normality and homogeneity of

variances tests were conducted to evaluate the data structure to test if parametric or non-parametric methods should be used, with a significance level of $p < 0.05$. Subsequently, Kruskal-Wallis tests were conducted on the length and weight data, followed by Dunn's post hoc tests to compare the length and weight of larvae in different concentration groups with the control group.

3. Results

3.1. Arsenic

3.1.1. Survival rate

C. vicina larvae demonstrated resistance to lower concentrations of As, with no mortality observed at concentrations below 5 mg/kg. However, at higher concentrations (>30 mg/kg), a reduction in motor activity was observed and mortality began to occur on the surface of the substrate before the end of each experiment (Figure 9). Eventually, all specimens died at 60 mg/kg at the end of a six-day rearing period, with a mortality rate of 96% at 30 mg/kg. Lower concentrations (< 5 mg/kg) had minimal impact on larvae's survival, presenting a survival rate of 89.5% at 5 mg/kg.

The survival rate plot (Figure 10) indicates an LD50 of 10.3 mg/kg for As.

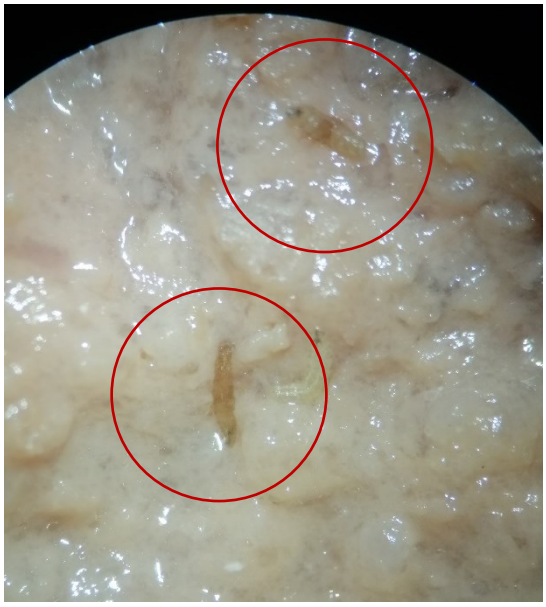

Figure 9: Dead larvae at the surface of the substrate after being exposed to Arsenic.

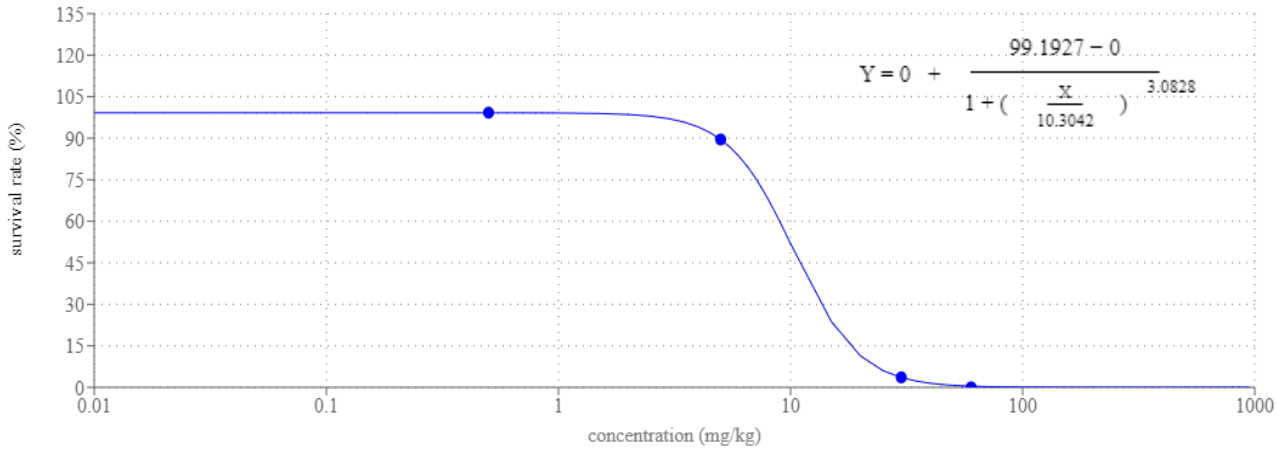

Figure 10: Survival rate plot for Arsenic. X stands for concentration (mg/kg); Y stands for survival rate (%).

3.1.2. Development rate

The mean length and weight of *C. vicina* larvae exposed to different As concentrations are presented in Table 1. In order to verify the statistical significance of the results, a Kruskal-Wallis test was applied after the statistical assumptions for an ANOVA analysis failed (see Table 1 and Attachment – Table A1). The Kruskal-Wallis test revealed significant differences between the groups (Table 2).

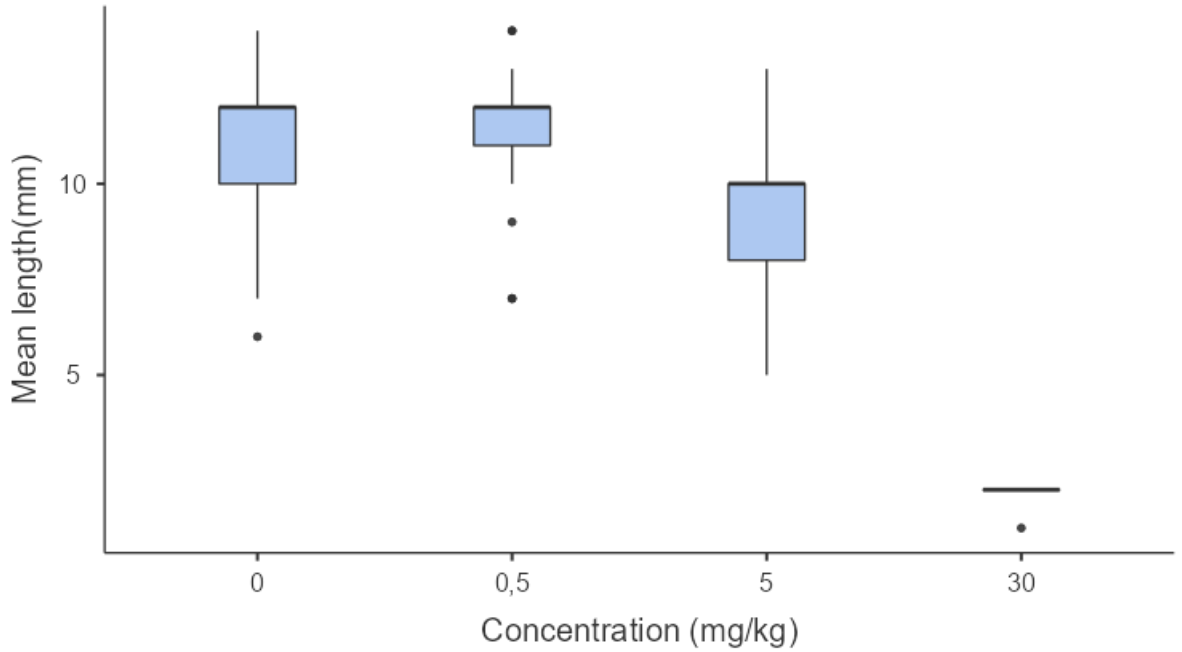

Figure 11: Box plot for the mean length of *C. vicina* larvae reared in increasing concentrations of Arsenic (respectively, n = 111; 110; 214; 5). Dots represent outlier values.

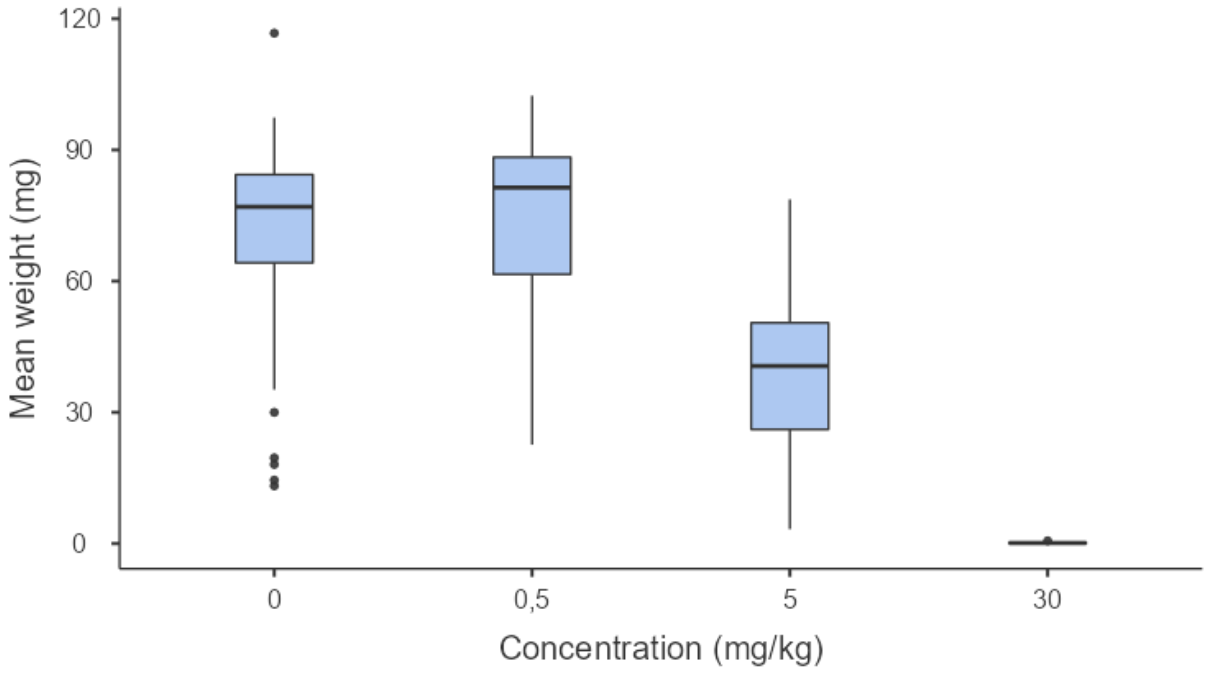

Figure 12: Box plot for the mean weight of *C. vicina* larvae reared in increasing concentrations of Arsenic (respectively, n = 111; 110; 214; 5). Dots represent outlier values.

The findings revealed that 0.5 mg/kg As concentrations had no significant impact on the larvae's developmental rate compared to the control group (Tables 3 and 4). Conversely, concentrations above 5 mg/kg deleteriously impacted the larvae's development rate (Tables 3 and 4), reducing mean length and weight (Figures 11 and 12). The differences were visually apparent in larvae reared at 30 mg/kg (Figure 13), exhibiting a size comparable to that of the first instar.

Table 1: Descriptive statistics for As exposure.

	Length (mm)				Weight (mg)			
Concentration (mg/kg)	0	0.5	5	30	0	0.5	5	30
Mean	11.27	11.53	9.34	1.80	72.89	75.73	38.86	0.22
Std. Deviation	1.41	1.19	1.69	0.45	17.55	17.35	17.85	0.23
Shapiro-Wilk	0.88	0.80	0.93	0.55	0.90	0.95	0.98	0.68
P-value of Shapiro-Wilk	**< 0.001**	**< 0.001**	**< 0.001**	**< 0.001**	**< 0.001**	**< 0.001**	**0.003**	**0.006**
Minimum	6.00	7.00	7.00	1.00	13.2	22.6	3.30	0.05
Maximum	14.00	14.00	14.00	2.00	116.7	102.4	78.7	0.62

Table 2: Kruskal-Wallis Test for As exposure.

	Mean length			Mean weight		
Factor	Test statistic	df	p	Test statistic	df	p
Concentration (mg/kg)	175.712	3	**< 0.001**	241.343	3	**< 0.001**

Note: Test statistic denotes the Kruskal-Wallis test value, reflecting the differences in ranks between groups; df denotes the degrees of freedom.

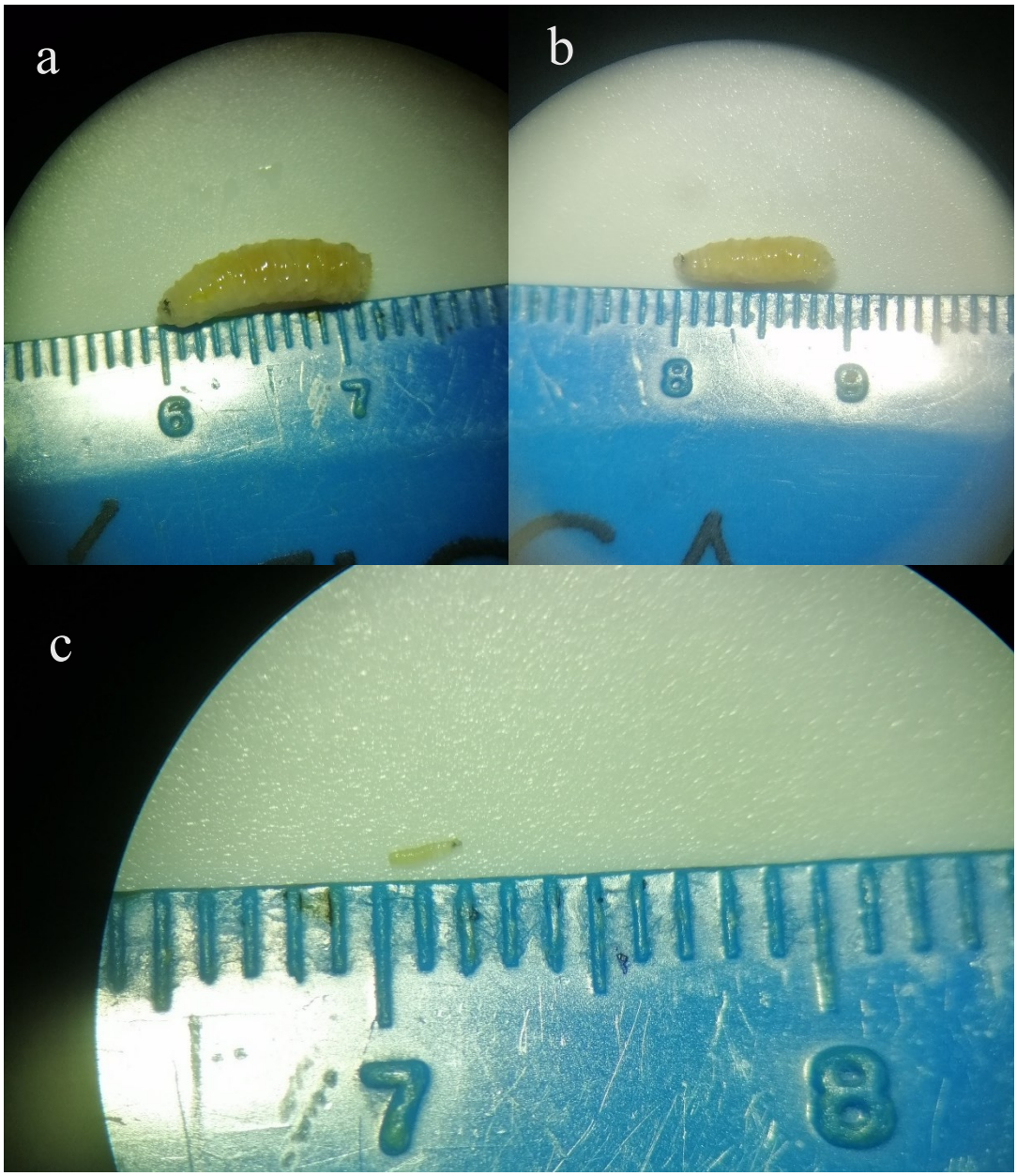

Figure 13: Images of the effects of As on the development of *C. vicina* larvae: (a) control larvae; (b) larvae exposed to 5 mg/kg; (c) larvae exposed to 30 mg/kg.

Table 3: Dunn's Post Hoc Comparisons for mean length after As exposure.

Comparison	z	p	p_{holm}
0 - 0.5	-1.12	0.26	0.26
0 - 5	9.70	< 0.001	**< 0.001**
0 - 30	4.99	< 0.001	**< 0.001**
0.5 - 5	10.96	< 0.001	**< 0.001**
0.5 - 30	5.32	< 0.001	**< 0.001**
5 - 30	2.54	0.011	**0.022**

Note: z is the test statistic for the Dunn's pairwise comparison; pholm is the p-value adjusted using the Holm method to account for multiple comparisons.

Table 4: Dunn's Post Hoc Comparisons for mean weight after As exposure.

Comparison	z	p	p_{holm}
0 - 0.5	-0.82	0.41	0.41
0 - 5	11.85	< 0.001	**< 0.001**
0 - 30	5.22	< 0.001	**< 0.001**
0.5 - 5	12.76	< 0.001	**< 0.001**
0.5 - 30	5.46	< 0.001	**< 0.001**
5 - 30	2.21	0.03	0.055

Note: z is the test statistic for the Dunn's pairwise comparison; pholm is the p-value adjusted using the Holm method to account for multiple comparisons.

3.1.3. Bioaccumulation

3.1.3.1. WDXRF

The As calibration curve was obtained using glycine standards prepared “in-house” with known As concentrations (0, 1, 2, 3, 5, 10, 15, 30, 60, 100 ppm). The quantitative model developed to determine elemental concentrations uses the normalization of the peak intensities for As by the Compton scattering peak intensities to control the matrix effects present in loose powder samples. The calibration curve for As was determined by linear regression (see Attachment – Figure A1), and a coefficient of determination (R^2) of 0.99 was obtained, demonstrating the method’s linearity.

Based on this quantitative model, the limit of detection (LD) of the analytical procedure was estimated using the standard error of the y-intercept ($\sigma = 3.1 \times 10^{-4}$) and the slope ($m = 4.57 \times 10^{-4}$) of the calibration curve, using the expression $LD = 3.3\sigma/m$. An LD = 2.21

ppm was obtained for As. It can be reasonably inferred that the estimated values below the LD indicate that the concentration of As is insufficient for the system to detect it with a high degree of reliability. In addition, such a result does not necessarily indicate the absence of the element in the sample. Alternatively, the element may be present at a low concentration in the sample.

Lyophilised spiked substrate and corresponding reared larvae samples were analysed directly with WDXRF and the results are presented in Table 5. As samples are lyophilised, a conversion is performed to correct the concentration for real wet weight.

Table 5: WDXRF measured As concentrations, associated standard error, and converted concentrations.

Sample	WDXRF Concentration (ppm)	Std. Error (%)	Converted Concentration (ppm)	Expected As concentration (ppm)
RAs0	2*	8.51	0.34*	0
RAs0.5	4	3.32	0.63	0.5
RAs5	32	0.289	5.41	5
LAs0	1*	NA	0.19*	NA
LAs0.5	2*	12.6	0.38*	NA
LAs5	20	0.456	2.8	NA

Note: (*) < LD; NA: Not applicable; Samples: RAs0: control dog food; RAs0.5: dog food doped at 0.5 mg/kg; RAs5: dog food doped at 5 mg/kg; LAs0: control larvae; LAs0.5: larvae reared at 0.5 mg/kg; LAs5: larvae reared at 5 mg/kg.

The calculated bioaccumulation factor for As in larvae is 0.61 and 0.52 for larvae reared at 0.5 and 5 mg/kg, respectively. Therefore, the findings suggest that the concentration identified in larvae is persistently inferior to that of the corresponding substrate, indicating an absence of evidence for As bioaccumulation in larvae.

Despite the majority of samples falling below the established LD, the use of WDXRF enabled the detection of elevated concentrations of As in *C. vicina* larvae. The accuracy of the method was evaluated through the percent recovery, which was determined by the matrix spike method and applied to the substrate samples. In order to achieve this, a known concentration (10 ppm) was added to the substrate samples and then measured again. The percent recovery was found to be 104.7%.

3.1.3.2. ICP-OES

In order to facilitate the IPC-OES analysis of the digested substrate and larvae samples, the calibration curve for As was provided (see Attachment – Figure A2). The resulting concentrations are presented in Table 6. The calculated LD was 0.2 ppm.

Table 6: IPC-OES measured As concentrations, associated relative standard deviation, and converted concentrations.

Sample	ICP-OES Concentration (mg/L)	RSD (%)	Converted Concentration (ppm)	Expected As concentration (ppm)
RAs0	0.87	0.08	2.216	0
RAs0.5	0.20	1.09	0.469	0.5
RAs5	1.39	0.4	3.520	5
LAs0	0.50	3.18	1.437	NA
LAs0.5	0.10*	0.21	0.295	NA
LAs5	0.94	0.14	1.967	NA

Note: (*) < LD; RSD: Relative Standard Deviation; NA: Not applicable; Samples: RAs0: control dog food; RAs0.5: dog food doped at 0.5 mg/kg; RAs5: dog food doped at 5 mg/kg; LAs0: control larvae; LAs0.5: larvae reared at 0.5 mg/kg; LAs5: larvae reared at 5 mg/kg.

The results obtained from ICP-OES were lower than those obtained from WDXRF. ICP-OES obtained concentrations for control larvae and substrate detected the presence of As. This was probably due to cross-contamination or a mismatch between control and 0.5 mg/kg samples. Therefore, these samples are not considered in the study. Notwithstanding, the concentrations of larvae are still lower than the substrate in these samples.

The calculated BAF for 5 mg/kg is analogous to that previously obtained, with a value of 0.56. Once more, there is no evidence of As bioaccumulation in *C. vicina* larvae.

3.2. Phenylmercury acetate

3.2.1. Survival rate

C. vicina larvae reared at concentrations between 0.5 and 30 mg/kg of phenylmercury acetate exhibited resistance to this compound. However, all larvae died at 60 mg/kg. Reduced motor activity was also observed at higher concentrations (>30 mg/kg).

The resulting plot for the survival rate of larvae exposed to phenylmercury acetate (Figure 14) indicates an LD50 of approximately 30 mg/kg for phenylmercury acetate.

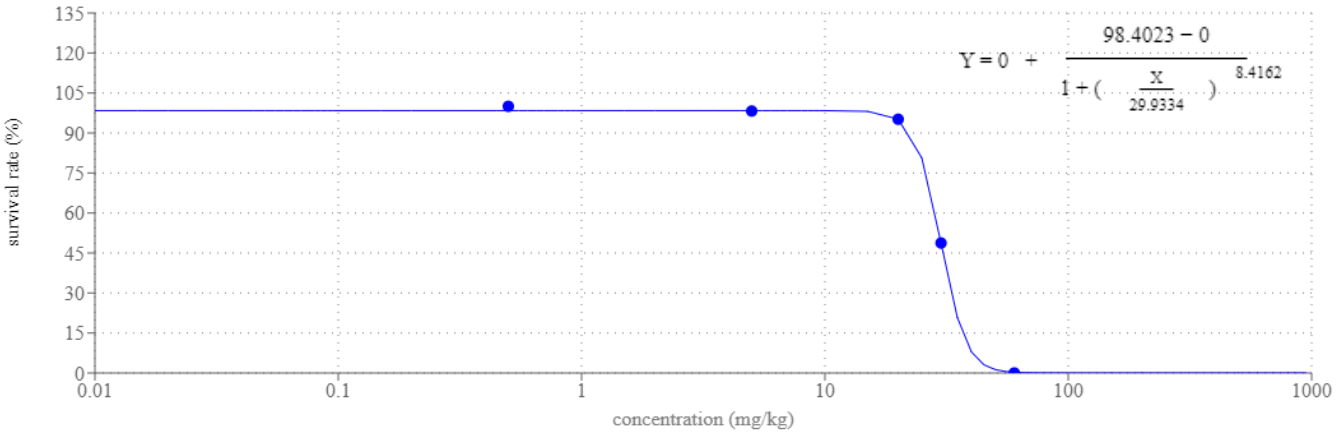

Figure 14: Survival rate plot for phenylmercury acetate. X stands for concentration (mg/kg); Y stands for survival rate (%).

3.2.2. Development rate

Descriptive data on the effects of phenylmercury acetate increased concentrations on *C. vicina* larvae's length and weight is presented in Table 7.

Once again, the statistical analysis of the results was performed. The Normality Test (Shapiro-Walk) and the Homogeneity of Variances Test (Levene's) yielded a significant p-value ($p < 0.01$), indicating that the assumptions underlying the ANOVA analysis were not met (see Table 7 and Attachment – Table A2). Subsequently, the Kruskal-Wallis test was conducted, which revealed statistically significant discrepancies in the mean length and weight among the various groups (Table 8).

A statistically significant discrepancy between the control and the 0.5 mg/kg concentration group was revealed (Tables 9 and 10), denoting a slight increase in both mean length and weight (Figures 15 and 16). The same is true for the 5 mg/kg dose with respect to length (Table 9), although no significant difference in weight was observed (Table 10).

Dunn's Post Hoc Comparisons denoted a significant result between the control and the 30 mg/kg group ($p < 0.01$) (Tables 9 and 10), confirming the negative effect of high phenylmercury acetate concentrations on the length and weight of *C. vicina* larvae (Figures 15 and 16). In this case, the differences were visually noticeable (Figure 17), where larvae sizes resembled those of first instars.

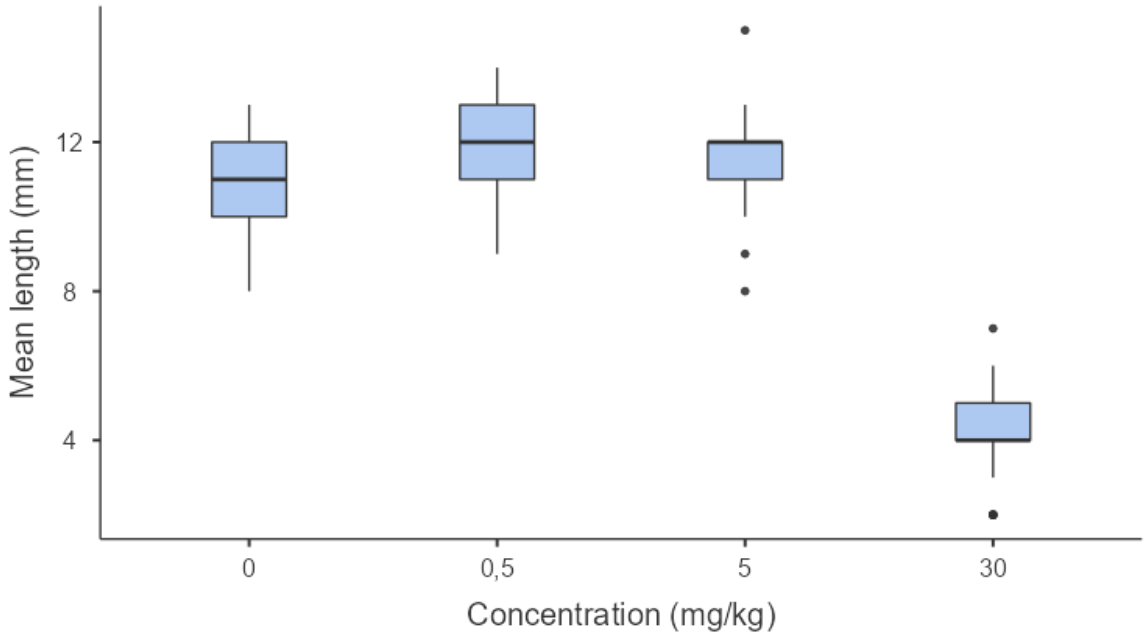

Figure 15: Box plot for the mean length of *C. vicina* larvae reared in increasing concentrations of phenylmercury acetate (respectively, n = 114; 71; 76; 109). Dots represent outlier values.

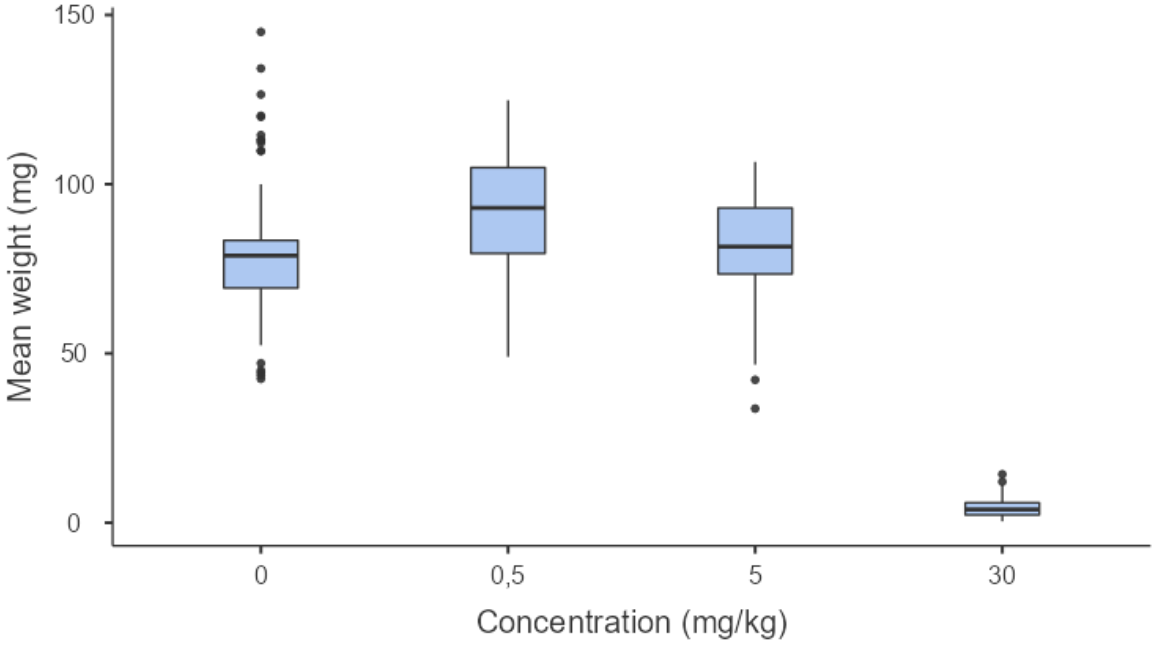

Figure 16: Box plot for the mean weight of *C. vicina* larvae reared in increasing concentrations of phenylmercury acetate (respectively, n = 114; 71; 76; 109). Dots represent outlier values.

Table 7: Descriptive statistics for phenylmercury acetate exposure.

	Length (mm)				Weight (mg)			
Concentration (mg/kg)	0	0.5	5	30	0	0.5	5	30
Mean	11.02	11.887	11.49	4.25	78.59	92.03	81.51	4.42
Std. Deviation	0.97	1.036	1.054	1.09	17.71	16.29	14.22	2.77
Shapiro-Wilk	0.89	0.916	0.912	0.92	0.91	0.99	0.97	0.93
P-value of Shapiro-Wilk	**< 0.001**	**< 0.001**	**< 0.001**	**< 0.001**	**< 0.001**	0.55	**0.007**	**< 0.001**
Minimum	8.00	9.00	8.00	2.00	42.50	49.00	33.70	0.40
Maximum	13.00	14.00	15.00	7.00	145.00	124.80	106.60	14.30

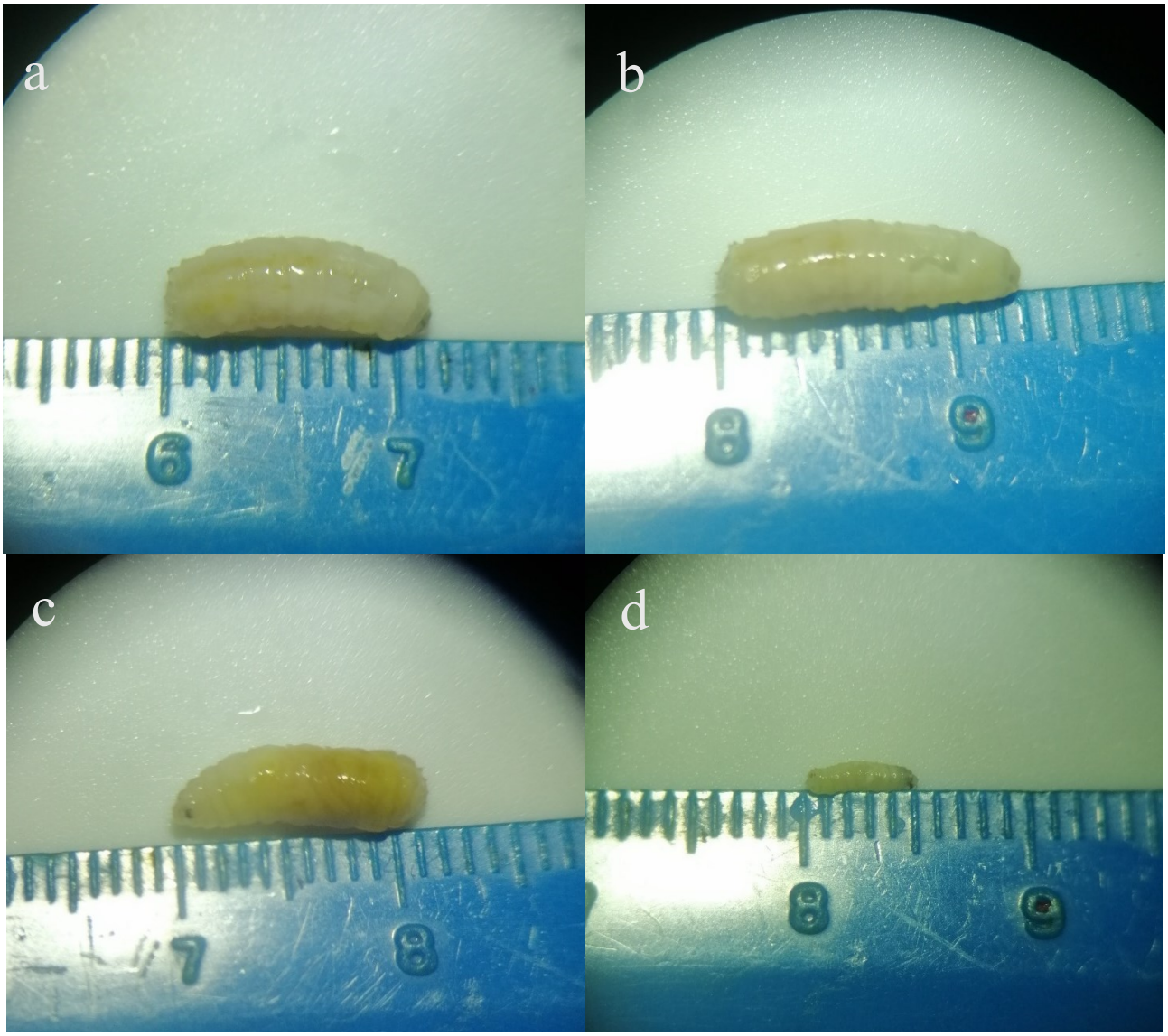

Figure 17: Effects of phenylmercury acetate on *C. vicina* larvae development: (a) control larvae; (b) larvae reared at 0.5 mg/kg; (c) larvae reared at 5 mg/kg; (d) larvae reared at 30 mg/kg.

Table 8: Kruskal-Wallis Test for phenylmercury acetate exposure.

	Mean length			Mean weight		
Factor	Test statistic	df	p	Test statistic	df	p
Concentration (mg/kg)	261.985	3	**< 0.001**	258.303	3	**< 0.001**

Note: Test statistic denotes the Kruskal-Wallis test value, reflecting the differences in ranks between groups; df denotes the degrees of freedom.

Table 9: Dunn's Post Hoc Comparisons for mean length after phenylmercury acetate exposure.

Comparison	z	p	p_{holm}
0 - 0.5	-3.909	< 0.001	**< 0.001**
0 - 5	-2.550	0.011	**0.022**
0 - 30	11.08	< 0.001	**< 0.001**
0.5 - 5	1.734	0.083	0.083
0.5 - 30	13.61	< 0.001	**< 0.001**
5 - 30	13.77	< 0.001	**< 0.001**

Note: z is the test statistic for the Dunn's pairwise comparison; pholm is the p-value adjusted using the Holm method to account for multiple comparisons.

Table 10: Dunn's Post Hoc Comparisons for mean weight after phenylmercury acetate exposure.

Comparison	z	p	p_{holm}
0 - 0.5	-4.19	< 0.001	**< 0.001**
0 - 5	-1.71	0.088	0.088
0 - 30	11.16	< 0.001	**< 0.001**
0.5 - 5	2.752	0.006	**0.012**
0.5 - 30	13.96	< 0.001	**< 0.001**
5 - 30	13.03	< 0.001	**< 0.001**

Note: z is the test statistic for the Dunn's pairwise comparison; pholm is the p-value adjusted using the Holm method to account for multiple comparisons.

3.2.3. Bioaccumulation

3.2.3.1. WDXRF

The calibration curve was developed using glycine standards prepared "in-house" with known Hg concentrations (0, 1, 3, 10, 15, 30 ppm) (see Attachment – Figure A3). The quantitative model developed to determine elemental concentrations uses peak intensities for Hg and the "variable alpha" method to correct the absorption effects present in loose powder samples. The calibration curve presents an R^2 of 0.99, demonstrating the method's linearity.

The calculated LD was 2.6 ppm. Once again, the estimated values below LD indicate that the concentration of Hg is insufficiently high to be reliably detected by the system.

Following the analysis of lyophilised larvae and substrate samples, the WDXRF and subsequently converted concentrations are presented in Table 11.

Table 11: WDXRF measured Hg concentrations, associated standard error, and converted concentrations.

Sample	WDXRF Concentration (ppm)	Std. Error (%)	Converted Concentration (ppm)	Expected Hg concentration (ppm)	Phenylmercury acetate concentration (ppm)
RHg0	0.6*	28.064	0.1*	0	0
RHg05	2.2*	3.959	0.36*	0.298	0.5
RHg5	23.9	0.393	4.30	2.98	5
LHg0	1.3*	7.116	0.22*	NA	NA
LHg05	1.7*	5.367	0.28*	NA	NA
LHg5	12.3	0.675	2.16	NA	NA

Note: (*) < LD; NA: Not applicable; Samples: RHg0: control dog food; RHg0.5: dog food doped at 0.5 mg/kg; RHg5: dog food doped at 5 mg/kg; LHg0: control larvae; LHg0.5: larvae reared at 0.5 mg/kg; LHg5: larvae reared at 5 mg/kg.

The BAF was calculated, and values of 0.78 and 0.50 were obtained for 0.5 and 5 mg/kg phenylmercury concentrations, respectively. The concentration of larvae is consistently below that of the substrate, indicating that no bioaccumulation for Hg is occurring. Notably, most of the measured samples exhibited concentrations below the calculated LD (2.6 ppm). Nevertheless, the presence of Hg in *C. vicina* larvae was successfully identified using WDXRF.

The method's accuracy was once more ascertained through the percent recovery, which yielded a value of 107.3%.

3.2.3.2. AAS

A second method, namely AAS, was employed for the analysis of Hg, as ICP-OES was not available for this purpose. In the analysis of Hg using the AMA 245 Mercury Analyser, the quantity of the sample subjected to analysis is contingent upon the presumed Hg concentration. In the case of dried samples, the analysis is conducted directly. Consequently, approximately 10 mg of each sample were subjected to analysis, with the exception of the lyophilised dog food sample spiked at 30 ppm of phenylmercury acetate, for which only 1 mg was analysed.

The AAS direct results and converted concentrations are presented in Table 12.

Table 12: AAS measured sample Hg concentrations and converted concentrations.

Sample	AAS Concentration (ppm)	Converted Concentration (ppm)	Expected Hg concentration (ppm)	Phenylmercury acetate concentration (ppm)
RHg0	0.004	0.001	0	0
RHg05	0.898	0.148	0.298	0.5
RHg5	14.606	2.629	2.98	5
RHg30	95.383	15.929	17.85	30
LHg0	0.004	0.001	NA	NA
LHg05	0.277	0.046	NA	NA
LHg5	8.719	1.532	NA	NA
LHg30	14.051	2.128	NA	NA

Note: NA: Not applicable; Samples: RHg0: control dog food; RHg0.5: dog food doped at 0.5 mg/kg; RHg5: dog food doped at 5 mg/kg; LHg0: control larvae; LHg0.5: larvae reared at 0.5 mg/kg; LHg5: larvae reared at 5 mg/kg.

The AAS results appear to be lower than those obtained by WDXRF. Nevertheless, the concentration of larvae remains lower than that of the substrate to which they are exposed, with BAF values of 0.31 and 0.58 for 0.5 and 5 mg/kg, respectively. It is noteworthy that the calculated BAF for 30 mg/kg was 0.134, indicating that larvae reared at this concentration exhibited a significantly lower concentration than that of the substrate in which they were reared. This observation suggests the existence of a limit for the accumulation of Hg.

3.3. Cadmium acetate

3.3.1. Survival rate

C. vicina larvae demonstrated resilience to all cadmium acetate concentrations. However, at higher concentrations (>30 mg/kg), the survival rate was somewhat affected, with about 67% of larvae surviving. A higher concentration of cadmium acetate was tested, and even so, larvae survived at 120 mg/kg, exhibiting a survival rate of 29%.

Although the desired outcome of 0% survival could not be achieved, the plotted survival rate is presented in Figure 18.

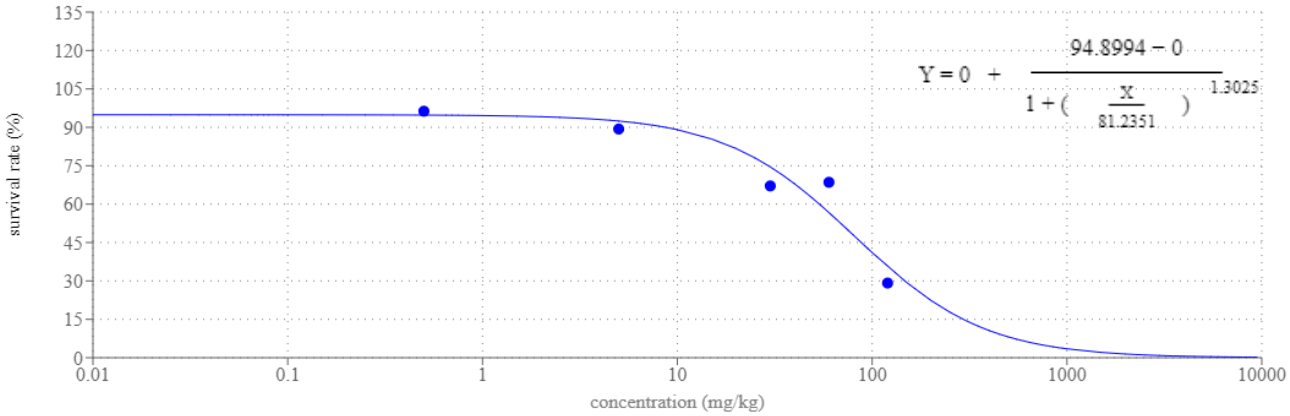

Figure 18: Survival rate plot for cadmium acetate. X stands for concentration (mg/kg); Y stands for survival rate (%).

The plotted survival rate indicates this compound's LD50 at 81.23 mg/kg.

3.3.2. Development rate

The mean larval weight and length sampled from different cadmium acetate concentrations are presented in Table 13.

To ascertain the statistical significance of the results, a Kruskal-Wallis test was conducted on mean length and weight data, which were identified as non-parametric (see Table 13 and Attachment – Table A3), and revealed a statistically significant result ($p < 0.001$) (Table 14).

Cadmium acetate affected *C. vicina* larvae development parameters at concentrations exceeding 30 mg/kg (Tables 14 and 15), exhibiting a visually notable reduction in length and weight compared to the control (Figures 19–21). However, no significant differences between the control and the 0.5 mg/kg treatment were verified (Tables 14 and 15). Nevertheless, a statistically significant difference was observed between the control and the 5 mg/kg group for mean weight ($p = 0.039$) (Table 16), with a slight reduction in this value, but no effect on the length was verified. Concluding that *C. vicina* larvae are

resistant to cadmium acetate, where only high concentrations have a significant impact on their development.

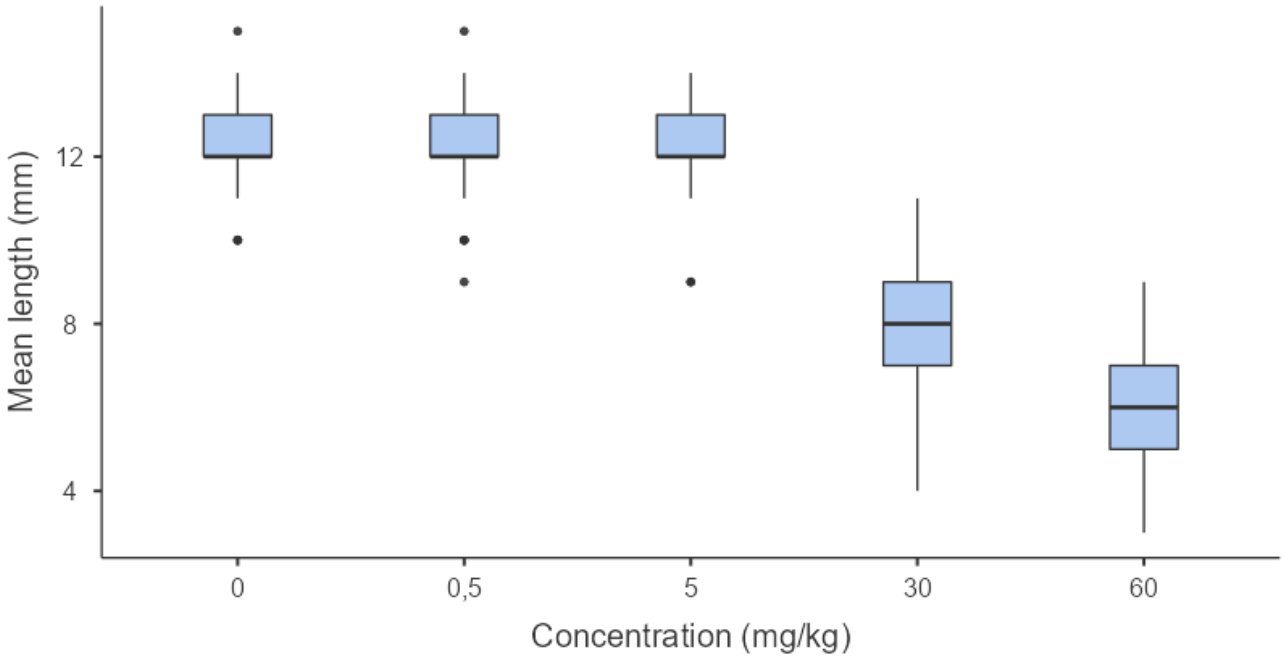

Figure 19: Box plot for the mean weight of *C. vicina* larvae reared in increasing concentrations of cadmium acetate (respectively, n = 77; 46; 61; 48; 60). Dots represent outlier values.

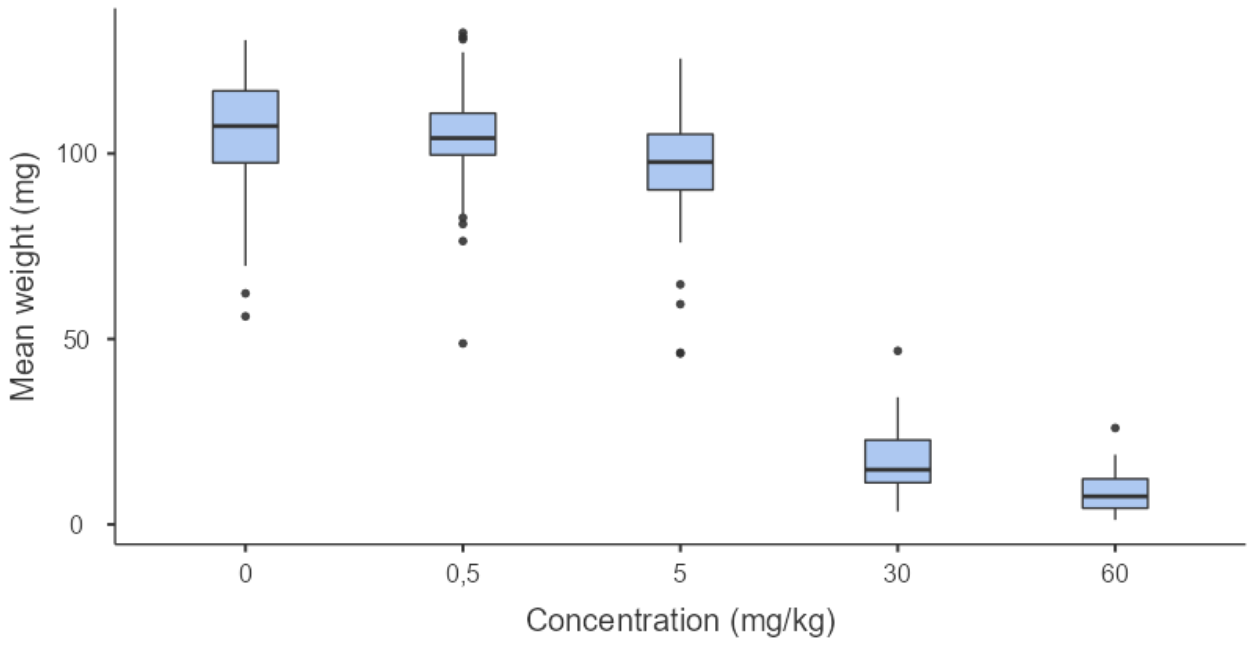

Figure 20: Box plot for the mean weight of *C. vicina* larvae reared in increasing concentrations of cadmium acetate (respectively, n = 77; 46; 61; 48; 60). Dots represent outlier values.

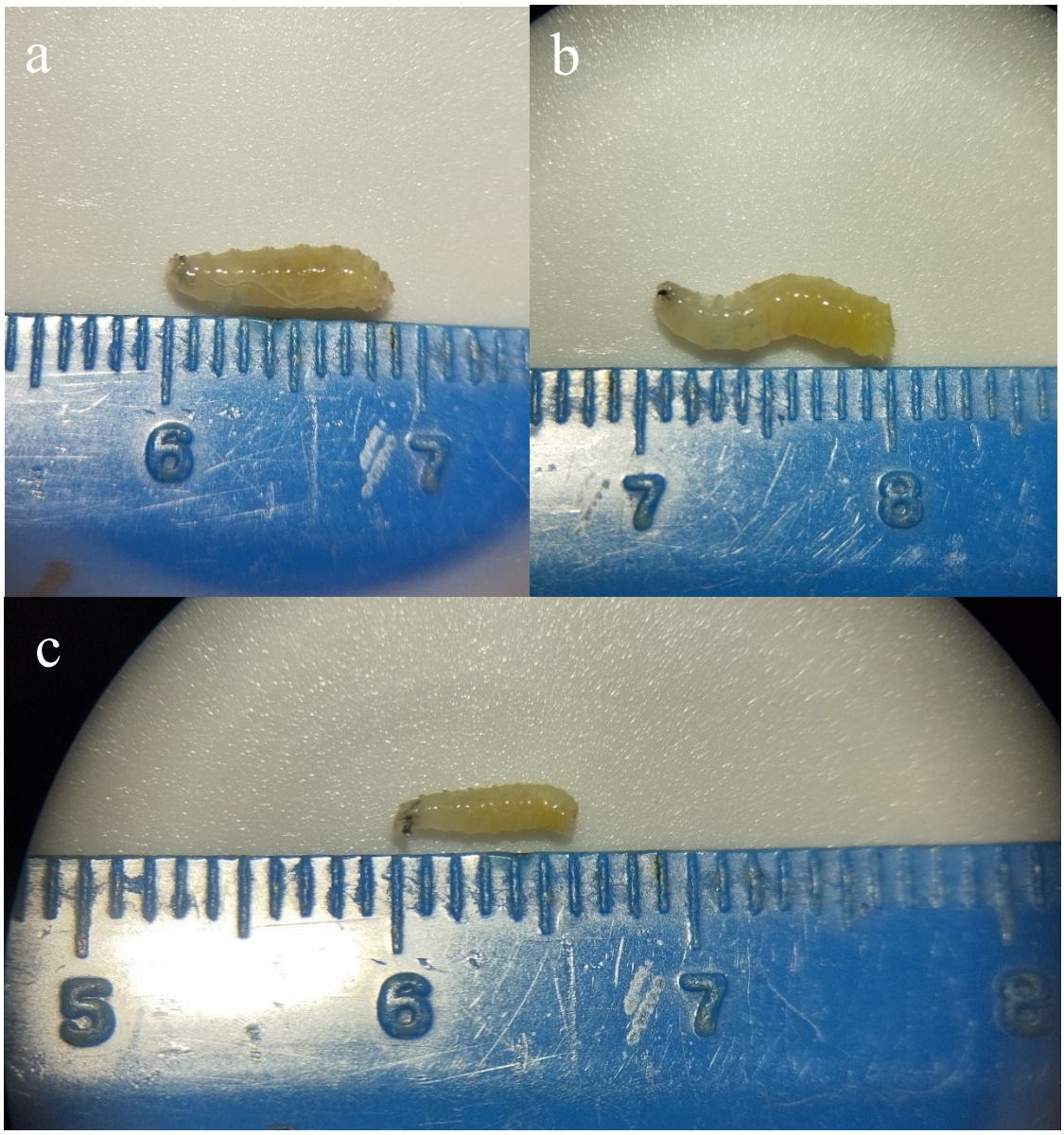

Figure 21: Images of the effects of cadmium acetate on the development of *C. vicina* larvae: (a) control larvae; (b) larvae reared at 5 mg/kg; (c) larvae reared at 30 mg/kg.

Table 13: Descriptive Statistics for cadmium acetate exposure.

	Length (mm)					Weight (mg)				
Concentration (mg/kg)	0	0.5	5	30	60	0	0.5	5	30	60
Mean	12.36	12.25	12.20	7.94	6.28	104.19	104.63	96.82	17.91	9.23
Std. Deviation	1.10	1.10	0.96	1.46	1.70	16.55	12.99	15.98	9.54	5.84
Shapiro-Wilk	0.92	0.93	0.84	0.95	0.92	0.93	0.93	0.92	0.92	0.92
P-value of Shapiro-Wilk	**< 0.001**	**< 0.001**	**< 0.001**	0.134	**0.016**	**< 0.001**	**< 0.001**	**0.001**	**0.022**	**0.012**
Minimum	10.00	9.00	9.00	4.00	3.00	56.10	48.80	46.10	3.50	1.20
Maximum	15.00	15.00	14.00	11.00	9.00	130.60	132.60	125.600	46.80	26.00

Table 14: Kruskal-Wallis Test for cadmium acetate exposure.

	Mean length			Mean weigth		
Factor	Statistic	df	p	Statistic	df	p
Concentration (mg/kg)	159.177	4	**< 0.001**	162.825	4	**< 0.001**

Note: Test statistic denotes the Kruskal-Wallis test value, reflecting the differences in ranks between groups; df denotes the degrees of freedom.

Table 15: Dunn's Post Hoc Comparisons for mean length after cadmium acetate exposure.

Comparison	z	p	p_{holm}
0 - 0.5	0.458	0.647	1.000
0 - 5	0.646	0.518	1.000
0 - 30	7.968	< 0.001	**< 0.001**
0 - 60	9.518	< 0.001	**< 0.001**
0.5 - 5	0.214	0.831	1.000
0.5 - 30	7.602	< 0.001	**< 0.001**
0.5 - 60	9.132	< 0.001	**< 0.001**
5 - 30	7.171	< 0.001	**< 0.001**
5 - 60	8.616	< 0.001	**< 0.001**
30 - 60	1.011	0.312	1.000

Note: z is the test statistic for the Dunn's pairwise comparison; pholm is the p-value adjusted using the Holm method to account for multiple comparisons

Table 16: Dunn's Post Hoc Comparisons for mean weight after cadmium acetate exposure.

Comparison	z	p	p_{holm}
0 - 0.5	0.371	0.711	0.711
0 - 5	2.583	0.010	**0.039**
0 - 30	8.287	< 0.001	**< 0.001**
0 - 60	9.877	< 0.001	**< 0.001**
0.5 - 5	2.227	0.026	0.078
0.5 - 30	7.987	< 0.001	**< 0.001**
0.5 - 60	9.560	< 0.001	**< 0.001**
5 - 30	5.957	< 0.001	**< 0.001**
5 - 60	7.382	< 0.001	**< 0.001**
30 - 60	1.034	0.301	0.602

Note: z is the test statistic for the Dunn's pairwise comparison; pholm is the p-value adjusted using the Holm method to account for multiple comparisons

3.3.3. Bioaccumulation

3.3.3.1. WDXRF

The calibration curve was determined using glycine standards prepared "in-house" with known Cd concentrations (0, 2, 3, 10, 15, 30, 100 ppm) (see Attachment – Figure A4). The quantitative model developed to determine elemental concentrations uses peak intensities for Cd and the "variable alpha" method to correct the absorption effects present in loose powder samples. An R^2 value of 0.99 was obtained for the Cd calibration curve, demonstrating the process' linearity. The estimated LD was determined to be 3.0 ppm.

WDXRF analysed dried substrate and larvae samples; the concentrations are presented in Table 17.

Table 17: WDXRF measured Cd concentrations, associated standard error, and converted concentrations.

Sample	WDXRF Concentration (ppm)	Std. Error (%)	Converted Concentration (ppm)	Expected Cd concentration (ppm)	Cadmium acetate concentration (ppm)
RCd0	*	NA	*	0	0
RCd05	*	NA	*	0.25	0.5
RCd5	13	2.93	2.16	2.5	5
LCd0	*	NA	*	NA	NA
LCd05	5	7.34	1.11	NA	NA
LCd5	30	1.40	6.15	NA	NA

Note: (*) < LD; NA: Not applicable; Samples: RCd0: control dog food; RCd0.5: dog food doped at 0.5 mg/kg; RCd5: dog food doped at 5 mg/kg; LCd0: control larvae; LCd0.5: larvae reared at 0.5 mg/kg; LCd5: larvae reared at 5 mg/kg.

The BAF was only calculated for a concentration of 5 mg/kg, with a resulting value of 2.84. This evidence indicates that the concentrations measured in larvae are superior to those of the substrate in which they were reared. Nevertheless, larvae reared at 0.5 mg/kg also exhibited a higher concentration than the rearing substrate, as substrate concentration was below the LD. In contrast to the findings for the other heavy metals under investigation, the results demonstrate that *C. vicina* larvae bioaccumulate Cd.

Once again, the accuracy of the method was determined by the recovery rate, with a calculated value of 104.2%.

3.3.3.2. ICP-OES

For ICP-OES analysis, the calibration curve was provided by the laboratory (see Attachment – Figure A5). Digested dog food and larvae samples were analysed, and the results are presented in Table 18. The calculated LD below 0.01 ppm.

Table 18: IPC-OES measured Cd concentrations, associated relative standard deviation, and converted concentrations.

Sample	ICP-OES Concentration (mg/L)	RSD %	Converted Concentration (ppm)	Expected Cd concentration (ppm)	Cadmium acetate concentration (ppm)
RCd0	0.00	0.94	0.000	0	0
RCd0.5	0.040	0.11	0.108	0.25	0.5
RCd5	0.525	0.14	1.310	2.5	5
RCd30	2.574	1.31	6.642	15	30
RCd60	5.928	2.46	14.123	30	60
LCd0	0.00	1.34	0.000	NA	NA
LCd0.5	0.149	1.33	0.497	NA	NA
LCd5	1.200	1.59	3.691	NA	NA

Note: RSD: Relative Standard Deviation; NA: Not applicable; Samples: RCd0: control dog food; RCd0.5: dog food doped at 0.5 mg/kg; RCd5: dog food doped at 5 mg/kg; RCd30: dog food doped at 30 mg/kg; RCd60: dog food doped at 60 mg/kg; LCd0: control larvae; LCd0.5: larvae reared at 0.5 mg/kg; LCd5: larvae reared at 5 mg/kg; LCd30: larvae reared at 30 mg/kg; LCd60: larvae reared at 60 mg/kg.

Although ICP-OES results are lower than WDXRF, they confirm that Cd bioaccumulation occurs in *C. vicina* larvae, as larvae concentrations are consistently higher than the substrate they are reared in. BAF was 4.60 for 0.5 mg/kg and 2.82 for 5 mg/kg, a similar value to the previously determined with WDXRF.

3.4. Lead acetate

3.4.1. Survival rate

C. vicina larvae exhibited resilience to lead acetate. The survival of the larvae was not affected by concentrations up to 5 mg/kg. The survival rate of larvae reared at 30 mg/kg was 70%, while at 60 mg/kg it was approximately 65%. A higher concentration (120 mg/kg) was also tested, and a survival rate of 37.5% was observed.

Although attaining a zero percent survival rate for this compound was not feasible, the plotted survival rate is illustrated in Figure 22.

From the survival rate plot, an LD50 of 83.5 mg/kg for lead acetate was determined.

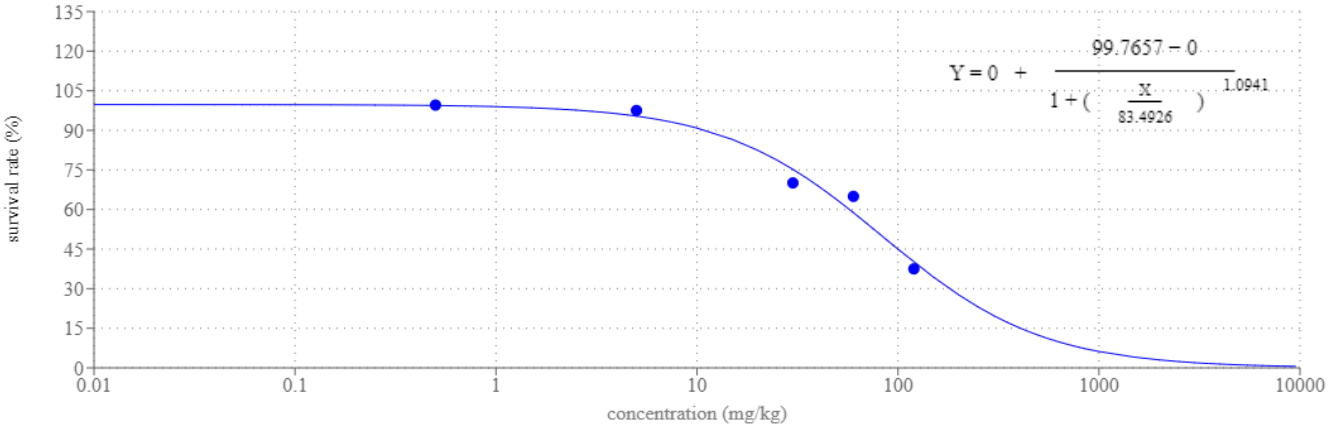

Figure 22: Survival rate plot for lead acetate. X stands for concentration (mg/kg); Y stands for survival rate (%).

However, while exhibiting resistance, a distinct behavioural pattern was observed in larvae reared at concentrations above 30 mg/kg – the larvae remained stationary on the substrate surface with minimal movement (Figure 23).

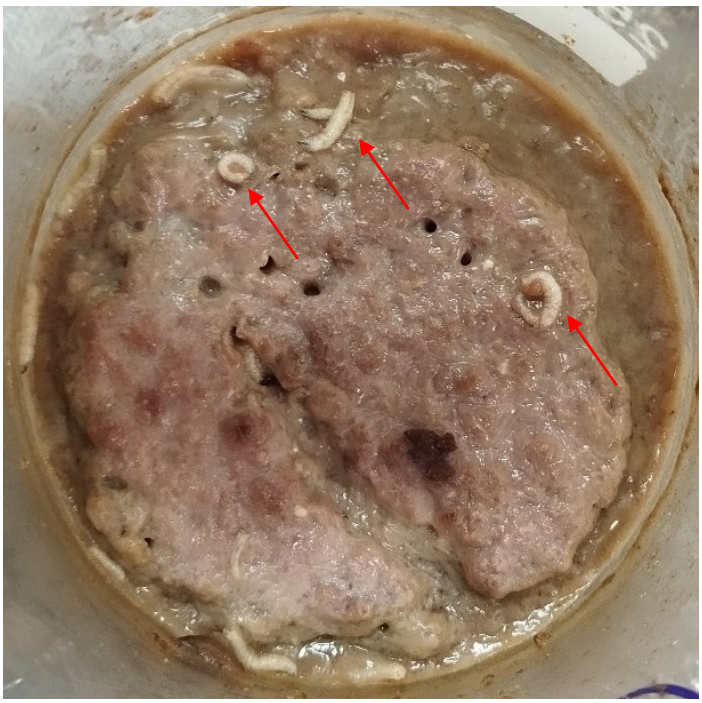

Figure 23: Stationary larvae at the surface of the substrate spiked at 60 mg/kg of lead acetate.

3.4.2. Development rate

The mean weight and length of *C. vicina* larvae exposed to increasing lead acetate concentrations are presented in Table 19.

As was the case previously, Shapiro-Wilk and Levene's tests yielded significant results (see Table 19 and Attachment – Table A4). Accordingly, a Kruskal-Wallis test was

conducted, which revealed statistically significant differences between the treatment groups (Table 20).

No statistical differences were observed between the control group and the 0.5 and 5 mg/kg groups with regard to the development parameters (Tables 21 and 22). Statistical differences were only identified between the control and the higher concentrations (>30 mg/kg) (Tables 21 and 22), in which the larvae were observed to be smaller and lighter than the control group (Figures 24 and 25).

The results exhibited considerable variability at the higher concentrations, with a broad range of values being recorded. For instance, the length of larvae reared at 60 mg/kg exhibited a range of 2 to 12 mm, while their weight demonstrated a range of 1.5 to 59.9 mg (Table 19).

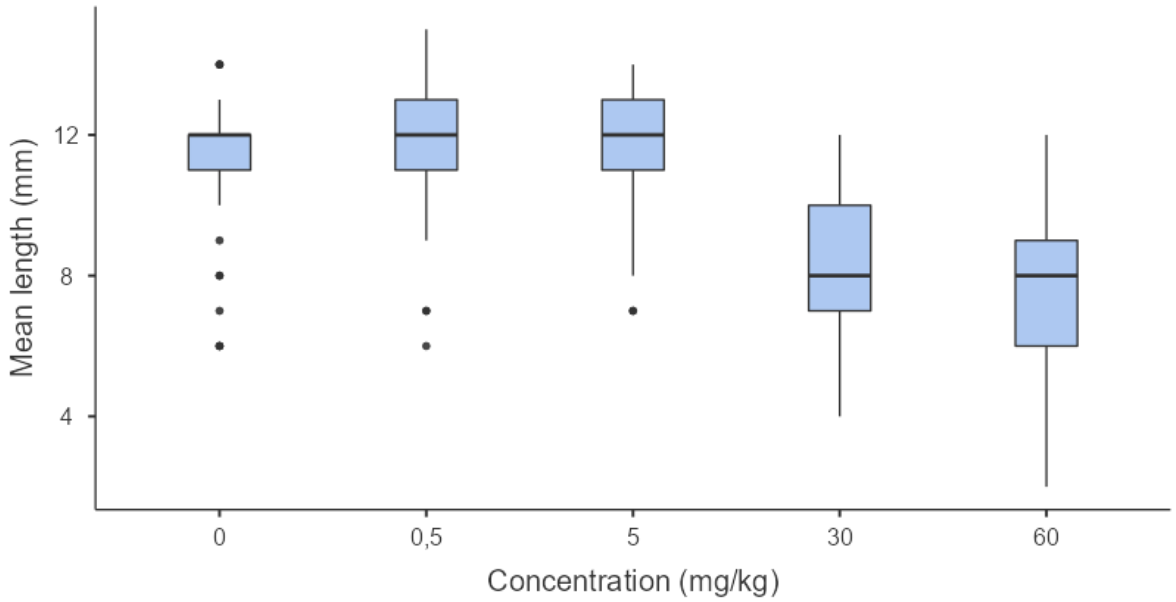

Figure 24: Box plot for the mean length of *C. vicina* larvae reared in increasing concentrations of lead acetate (respectively, n = 103; 117; 105; 54; 36). Dots represent outlier values.

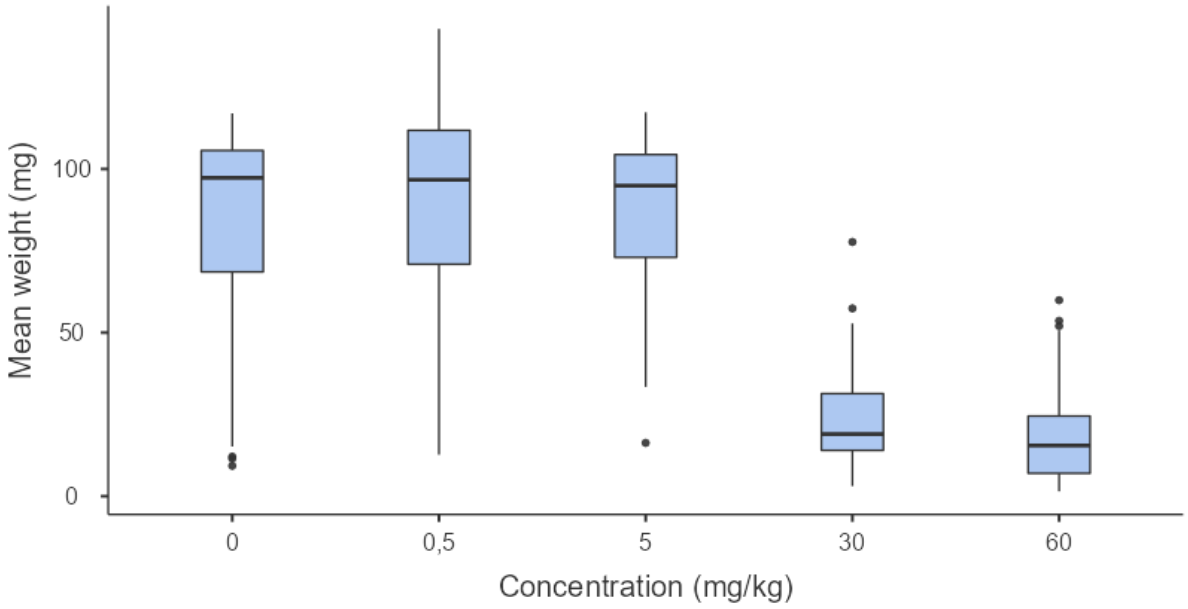

Figure 25: Box plot for the mean weight of *C. vicina* larvae reared in increasing concentrations of lead acetate (respectively, n = 103; 117; 105; 54; 36). Dots represent outlier values.

Table 19: Descriptive statistics for lead acetate exposure.

	Length (mm)					Weight (mg)				
Concentration (mg/kg)	0	0.5	5	30	60	0	0.5	5	30	60
Mean	11.50	11.90	11.83	8.33	7.59	86.19	89.85	87.57	23.31	18.37
Std. Deviation	1.55	1.42	1.59	2.02	2.49	26.52	27.33	21.43	14.91	14.20
Shapiro-Wilk	0.83	0.88	0.91	0.96	0.96	0.86	0.94	0.91	0.91	0.89
P-value of Shapiro-Wilk	**< 0.001**	**< 0.001**	**< 0.001**	0.058	**0.047**	**< 0.001**	**< 0.001**	**<0 .001**	**< 0.001**	**< 0.001**
Minimum	6.00	6.00	7.00	4.00	2.00	9.30	12.70	16.30	3.10	1.50
Maximum	14.00	15.00	14.00	12.00	12.00	117.00	142.80	117.30	77.70	59.90

Table 20: Kruskal-Wallis Test for lead acetate exposure.

	Mean length			Mean weight		
Factor	Statistic	df	p	Statistic	df	p
Concentration (mg/kg)	191.304	4	**< 0.001**	229.977	4	**< 0.001**

Note: Test statistic denotes the Kruskal-Wallis test value, reflecting the differences in ranks between groups; df denotes the degrees of freedom.

Table 21: Dunn's Post Hoc Comparisons for mean length after lead acetate exposure.

Comparison	z	p	p_{holm}
0 - 0.5	-1.615	0.106	0.425
0 - 5	-1.382	0.167	0.501
0 - 30	7.673	< 0.001	**< 0.001**
0 - 60	8.655	< 0.001	**< 0.001**
0.5 - 5	0.197	0.843	1.000
0.5 - 30	9.162	< 0.001	**< 0.001**
0.5 - 60	10.24	< 0.001	**< 0.001**
5 - 30	8.843	< 0.001	**< 0.001**
5 - 60	9.876	< 0.001	**< 0.001**
30 - 60	0.584	0.559	1.000

Note: z is the test statistic for the Dunn's pairwise comparison; pholm is the p-value adjusted using the Holm method to account for multiple comparisons

Table 22: Dunn's Post Hoc Comparisons for mean weight after lead acetate exposure.

Comparison	z	p	p_{holm}
0 - 0.5	-1.089	0.276	1.000
0 - 5	-0.060	0.952	1.000
0 - 30	9.016	< 0.001	**< 0.001**
0 - 60	10.17	< 0.001	**< 0.001**
0.5 - 5	1.032	0.302	1.000
0.5 - 30	10.10	< 0.001	**< 0.001**
0.5 - 60	11.33	< 0.001	**< 0.001**
5 - 30	9.096	< 0.001	**< 0.001**
5 - 60	10.26	< 0.001	**< 0.001**
30 - 60	0.684	0.494	1.000

Note: z is the test statistic for the Dunn's pairwise comparison; pholm is the p-value adjusted using the Holm method to account for multiple comparisons

Larvae reared at any Pb concentration exhibited the development of orange stains on the body (Figure 26). Additionally, alterations in their morphology were observed at higher concentrations, with a deformed appearance (Figure 27).

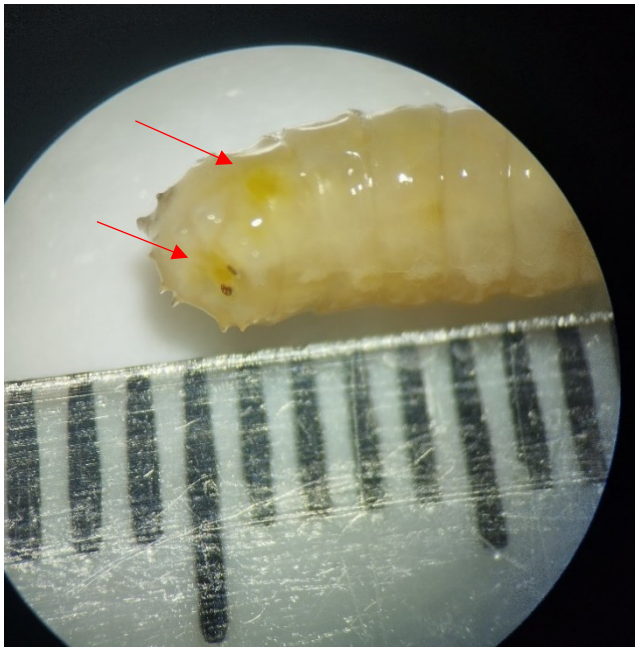

Figure 26: Orange stains close to the anal region of larvae reared in lead acetate.

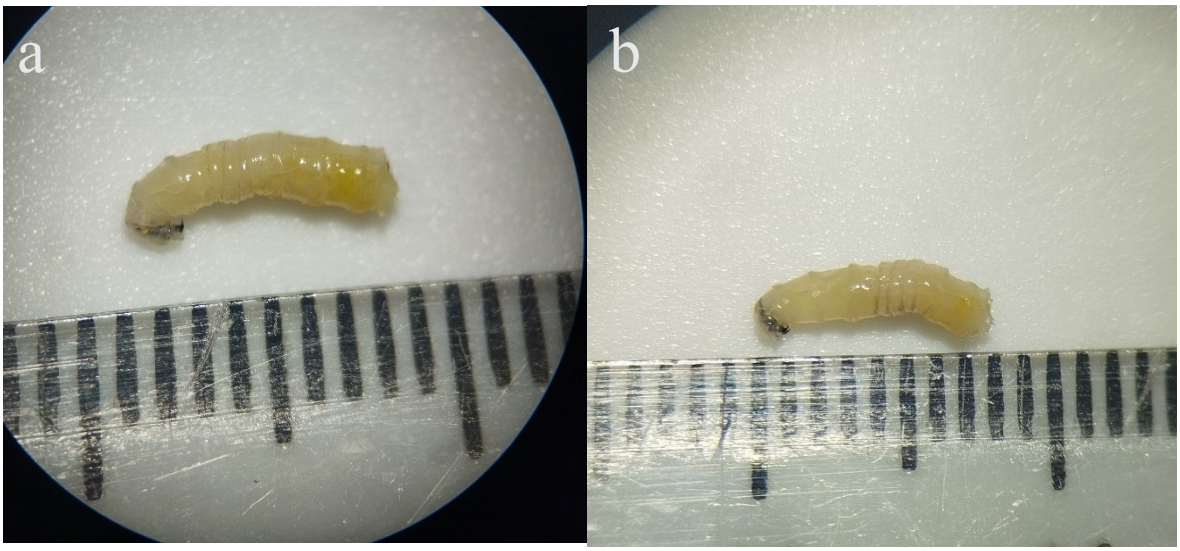

Figure 27: Larvae reared at (a) 30 mg/kg and (b) 60 mg/kg, with deformed appearance.

3.4.3. Bioaccumulation

3.4.3.1. WDXRF

The Pb calibration curve was obtained using glycine standards prepared “in-house” with known Pb concentrations (0, 1, 2, 5, 15, 30, 60, 100 ppm) (see Attachment – Figure A6).

The quantitative model developed to determine elemental concentrations uses peak intensities for Pb and the "variable alpha" method to correct the absorption effects. The calculated R^2 was 0.996, demonstrating the process' linearity. The calculated LD was 2.0 ppm.

Once the calibration curve had been established, the samples were subjected to analysis. The results for WDXRF-determined concentrations and converted concentrations are presented in Table 23.

Table 23: WDXRF measured Pb concentrations, associated standard error, and converted concentrations.

Sample	WDXRF Concentration (ppm)	Std. Error (%)	Converted Concentration (ppm)	Expected Pb concentration (ppm)	$Pb(C_2H_3O_2)_2$ concentration (ppm)
RPb0	*	NA	*	0	0
RPb05	*	NA	*	0.32	0.5
RPb5	19.7	2.0	3.21	3.2	5
LPb0	*	NA	*	NA	NA
LPb05	*	NA	*	NA	NA
LPb5	4.0	16.1	0.78	NA	NA

Note: (*) < LD; NA: Not applicable; Samples: RPb0: control dog food; RPb0.5: dog food doped at 0.5 mg/kg; RPb5: dog food doped at 5 mg/kg; LPb0: control larvae; LPb0.5: larvae reared at 0.5 mg/kg; LPb5: larvae reared at 5 mg/kg.

Regrettably, most values fall below the calculated LD (2.0 ppm), which can be attributed to the probable low concentration of the samples, which in turn made quantification challenging. Furthermore, even the quantified concentration of larvae reared at 5 mg/kg showed a high standard error (16.1%). Nevertheless, the calculated BAF for 5 mg/kg of lead acetate was 0.24. Therefore, bioaccumulation of Pb cannot be established, as the concentration of larvae is below that of the substrate.

The method's accuracy was evaluated through percent recovery, resulting in a value of 94.3%.

3.4.3.2. ICP-OES

The laboratory provided an ICP-OES calibration curve for Pb (see Attachment – Figure A7). The digested samples of the spiked substrate and larvae were subjected to analysis by ICP-OES, and the results are presented in Table 24. An LD of 0.01 ppm was determined.

Table 24: IPC-OES measured Pb concentrations, associated relative standard deviation, and converted concentrations.

Sample	ICP-OES Concentration (mg/L)	RSD %	Converted Concentration (ppm)	Expected Pb concentration (ppm)	$Pb(C_2H_3O_2)_2$ concentration (ppm)
RPb0.5	0.05	1.71	0.125	0.32	0.5
RPb5	0.53	1.08	1.296	3.2	5
RPb30	3.31	0.56	8.267	19	30
RPb60	7.64	1.29	19.111	38	60
LPb0	0.00*	1.79	0.009	NA	NA
LPb0.5	0.02	1.89	0.072	NA	NA
LPb5	0.10	1.90	0.297	NA	NA

Note: (*) < LD; RSD: Relative Standard Deviation; NA: Not applicable; Samples: RPb0: control dog food; RPb0.5: dog food doped at 0.5 mg/kg; RPb5: dog food doped at 5 mg/kg; RPb30: dog food doped at 30 mg/kg; RPb60: dog food doped at 60 mg/kg; LPb0: control larvae; LPb0.5: larvae reared at 0.5 mg/kg; LPb5: larvae reared at 5 mg/kg; LPb30: larvae reared at 30 mg/kg; LPb60: larvae reared at 60 mg/kg.

Once again, the results obtained by IPC-OES are lower than those obtained by WDXRF. Nonetheless, the calculated BAF for 5 mg/kg was 0.23, a value close to the one obtained with WDXRF. For a concentration of 0.5 mg/kg, the BAF was found to be 0.58. It can, therefore, be concluded that no bioaccumulation of Pb is occurring in *C. vicina* larvae.

4. Discussion

C. vicina is frequently one of the first colonizers of cadavers, especially during winter in Portugal. Therefore, it is an eligible species to be used for mPMI estimations, as well as for toxicological analysis. In cases of heavy metal poisoning, entomological species might ease their detection, but the effects on insects' survival and development need to be considered. This project is a complete study of the effects of four important toxic metals (As, Hg, Cd, and Pb) on *C. vicina* larvae and of their capacity to bioaccumulate them.

High concentrations of each heavy metal caused an increase in the mortality rate of *C. vicina* larvae, in a dose-dependent manner. Of all the heavy metals studied, As had the greater impact on the survival of *C. vicina* larvae, with very high mortality rates when reared above 30 mg/kg. The calculated LD50 for As (10 mg/kg) is much lower than the other heavy metals studied, and development is affected by only 5 mg/kg, with a significant reduction in length and weight. However, resistance was verified to a lower concentration (0.5 mg/kg) of this metal, presenting no differences compared to the control. High As concentrations (30 mg/kg) limited *C. vicina* larvae's growth, with sizes similar to the first instar, and caused a reduction in motor activity.

The LD50 for phenylmercury acetate for *C. vicina* larvae was about 30 mg/kg, corresponding to 17.85 mg/kg of Hg. As such, from all the metals studied, Hg is the second most toxic for *C. vicina* larvae, and exposure to high levels of Hg causes reduced motor activity. However, it was verified that low concentrations of phenylmercury acetate (< 5 mg/kg) led to a slight but significant increase in larvae's mean length and weight. On the other hand, as expected, higher concentrations (>30 mg/kg) had a negative effect on developmental parameters. Hence, low concentrations of Hg might contribute to an acceleration of the development rate of *C. vicina* larvae, but higher concentrations have the opposite effect, debilitating larvae's development. These results contrast with the findings of Nuorteva & Nuorteva (1982), who did not report any adverse effects on the development of calliphorid specimens after Hg exposure. However, they studied different forms of Hg, namely MeHg, which leads to the conclusion that Calliphoridae species may be more resistant to methylated forms of Hg than phenylmercury.

Both Cd and Pb had similar effects on *C. vicina* larvae. They showed to be resilient to cadmium acetate and lead acetate, even at high concentrations (>30 mg/kg), with the

LD50 for both these compounds around 80 mg/kg, corresponding to about 40 and 50 mg/kg for Cd and Pb, respectively. It was found that only high concentrations (>30 mg/kg) of each metal had a significantly negative impact on the development of the larvae, resulting in a reduction in length and weight.

In the present study, the larvae reared at higher concentrations (>30 mg/kg) of Pb exhibited a considerable range of developmental measurements. This could indicate that *C. vicina* larvae possess intrinsic differences in their resistance to Pb. Additionally, in this experiment, high concentrations (>30 mg/kg) of lead acetate induced deformation to larvae and led them to a stationary state at the surface of the substrate. Similarly, Shulman et al. (2017) also documented malformations in *C. vicina* adults and a reduction in motor activity following Pb exposure, although their study did not encompass the effects on larvae. Therefore, Pb has a detrimental effect on the survival and development of *C. vicina*, causing a reduction in motor activity and malformations in both adult and immature stages. In addition, previous studies (Kökdener & Yllmaz, 2021; Rashid et al., 2012) confirm the adverse effects of Pb in other Calliphoridae larvae species, demonstrating an increase in mortality and a reduction in the length and weight of larvae when exposed to this metal.

During the experimental assays, yellow stains were visible on reared larvae after exposure to any Pb concentration. These yellow stains could be attributed to the oxidation of Pb, creating lead oxide, a yellowish compound. They could also be the consequence of necrosis, and the dead tissue accumulating creates these yellow structures. Another hypothesis would be the association of Pb to proteins or lipids, leading to yellowish Pb compounds. However, these findings have not been reported in previous studies, highlighting the need for a more in-depth investigation to explore these hypotheses further.

In the present study, the survival rate of *C. vicina* was affected only at a concentration of 30 mg/kg of cadmium acetate, equivalent to approximately 15 mg/kg of Cd. No adverse effects on survival were observed below this threshold. Previous studies have reported similar findings regarding the impact of Cd on Calliphoridae larvae. For instance, Simkiss et al. (1993) and Kökdener et al. (2022) observed increased mortality and prolonged developmental time in *L. sericata* larvae exposed to rising concentrations of Cd. However, there were notable differences between these two reports. Simkiss et al. (1993) reported increased mortality at 25 mg/kg, while Kökdener et al. (2022) observed the same

effects at much lower concentrations (2 mg/kg). Additionally, these same studies and Malejko et al. (2020) also reported reductions in larval weight and length of *L. sericata* after Cd exposure, similar to the findings here discussed. Shulman et al. (2017) also documented decreased motor activity in adult *C. vicina* flies exposed to Cd. However, this effect was not observed in the current study with larvae of the same species.

In summary, high concentrations of all heavy metals caused harmful effects on the development of *C. vicina* larvae, with a decrease in weight and length documented. These results are expected as these heavy metals lead to the generation of ROS, cause DNA damage, and impair the normal function of essential proteins by binding to thiol groups and displacing vital nutrients (Balali-Mood et al., 2021). All this can result in the restriction of larvae's growth and affect their survival. These results severely impact mPMI estimations based on entomological evidence, as the size of these larvae was similar to those of the first or second instar.

The intrinsic variation between specimens regarding their developmental parameters gave rise to substantial differences between the experiments conducted under identical conditions. To illustrate, the size of the control larvae in two consecutive experiments on occasion yielded markedly different results (see Attachment – Figures A8 to A15). This resulted in a highly dispersed data set. One potential explanation for this discrepancy is the inability to maintain consistent humidity and temperature levels within the laboratory, which fluctuated between 20 and 22ºC. Additionally, the precise timing of larval death could not be determined with certainty.

It was not feasible to conduct additional experimental assays due to seasonal alterations and the unavailability of *C. vicina* flies. Furthermore, the rearing and maintenance of *C. vicina* adult specimens in laboratory conditions proved to be a significant challenge. This is likely due to the species' sensitivity to temperature fluctuations, which can impact its survival and development.

The results reported here show that *C. vicina* larvae do not bioaccumulate As, Hg, or Pb, as larvae concentrations were consistently lower than the rearing substrate. However, when present in the food source, the metals are detectable in the larvae using elemental analysis techniques, such as the ones used in this experiment.

A mean BAF of 0.6 was determined for *C. vicina* reared in increasing As concentrations. It was observed that the As concentrations in the substrate increased linearly in

conjunction with the increase in As concentrations in the substrate. However, it is important to note that most samples were below the calculated LD in WDXRF analysis, and contamination was verified in ICP-OES analysis. Also, larvae reared at 30 mg/kg were not subjected to analysis, as they were too small and fragile to be manipulated. Therefore, although no bioaccumulation was verified for As, a more in-depth study is needed for a correct BAF determination.

No previous studies of bioaccumulation of As were made on insects of forensic importance. However, Mogren et al. (2013), who studied As in *Chironomus riparius*, an aquatic insect, discovered that larvae bioaccumulated approximately 51.7 times the As in which they were reared. Therefore, bioaccumulation of As might be a species-dependent process.

For Hg, larvae concentrations also increased with increased concentrations in the substrate. However, there appears to be a limit to the accumulation of Hg in the larvae. Those reared in higher concentrations (30 mg/kg) showed significantly lower Hg levels than the substrate in which they were reared, resulting in a BAF much lower than that observed at previous concentrations. These findings are again in contrast to Nuorteva & Nuorteva (1982). They verified the bioaccumulation of organic Hg on Calliphoridae species, with BAF values from 1.5 to 4.3. However, when Hg was in its inorganic form, a BAF of 0.5 was determined, a similar value to those determined in the present study. Therefore, as phenylmercury and inorganic Hg have similar pharmacokinetics, bioaccumulation processes in *C. vicina* larvae might be similar.

C. vicina larvae seem to excrete Pb more efficiently since a lower concentration on larvae reared at 5 mg/kg of lead acetate is verified (BAF = 0.2) compared to the other heavy metal compounds at the same concentration. This may be the reason for enhanced resistance to Pb, as corroborated by an LD50 of 50 mg/kg. A similar BAF was indicated by Bessa et al. (2021), as they found 23.1% of Pb on *Lucilia cuprina* larvae compared to the substrate when reared at 50 µg/g. Therefore, Calliphoridae species might have a better excretion system for Pb than other heavy metals, allowing for a stronger resistance to this metal.

Bioaccumulation was verified on *C. vicina* larvae only for Cd, where larvae accumulated about 3 to 4 times the substrate concentration. As such, the determination of Cd is easier in *C. vicina* larvae than in the rearing substrate. However, Malejko et al. (2020) did not

report bioaccumulation of Cd in *L. sericata* larvae, obtaining a mean BAF of 0.2. Therefore, heavy metal bioaccumulation processes might differ depending on the species.

The analysis of larvae reared at 30 and 60 mg/kg of lead acetate and cadmium acetate was not performed using WDXRF due to the absence of a minimum weight threshold. The samples were dispatched for analysis by ICP-OES, but unfortunately, the results were not received on time. This prevented the determination of the BAF for these concentrations.

In summary, *C. vicina* larvae are adequate as toxicological evidence for heavy metals, as all the metals studied were successfully detected. However, bioaccumulation was verified only for Cd, allowing for better metal detection using *C. vicina* in this case. Nevertheless, bioaccumulation seems to be a species-dependent process. Consequently, the accurate identification of species is of paramount importance, which may prove challenging in immature stages.

Both AAS and IPC-OES results differed from WDXRF, probably due to the heterogeneity of samples and the fact that the sample quantity measured for these methods (from 1 to 200 mg) is much lower than the one used for WDXRF (1 g). Besides, some larvae might accumulate the toxicant more than others, or they might accumulate in certain areas of their bodies; thus, a small sample of larvae might not represent the overall accumulation process occurring.

Nevertheless, the WDXRF method was found to be an effective means of analysing metal concentration in larvae and food, with consistent and dependable outcomes. To ensure the reliability of the method, the accuracy, linearity, and sensitivity were evaluated, and satisfactory outcomes were obtained. The method's accuracy was determined by percent recovery, which was approximately 100% for all analysed metals. Furthermore, the linearity of the method was evaluated using coefficients of determination, which yielded values of approximately 0.99. The limits of detection for the heavy metals under investigation were relatively low, ranging from 2 to 3 ppm. However, this method also exhibited several limitations in the context of this analysis, the most significant of which was the minimum required weight of 1 g of lyophilised material. It was demonstrated that obtaining 1 g of lyophilised larvae is exceedingly challenging, particularly for larvae reared at higher concentrations, due to their limited growth. As a result, the planned metal concentration analysis of the samples mentioned above using WDXRF was not feasible due to the unavailability of a minimum weight. Moreover, the calibration process and sample analysis were found to be a time-consuming procedure, particularly in the case of

the Cd calibration. Despite the relatively low detection limits for each metal, most larvae samples exhibited concentrations below the determined value, making the analysis of these samples unreliable. Nevertheless, the WDXRF results were closer to the expected concentrations of each metal, except for Hg, than those of atomic spectroscopy. Therefore, this method is reliable for analysing concentrations in biological samples, with the main advantage being that it allows for the repetition of analysis without the loss of material.

Forensic entomotoxicology is a rising discipline that offers significant advantages to forensic investigation. The qualitative analysis of toxic substances on insects has been demonstrated to constitute valuable evidence. However, as previously mentioned, some scientists remain sceptical about the interpretation of quantitative results, especially when attempting to establish correlations. The argument is made that the movement of larvae on a cadaver is highly unpredictable, which results in differences in concentration and thus presents a challenge to interpreting the results. As larvae wander and feed from different areas, it is impossible to determine their exact feeding location, making it impossible to directly link drug levels in the larvae to a specific site on the body. Additionally, drug pharmacokinetics and metabolism in insects are not yet completely understood, and these processes are dependent on species, the developmental stage, and their feeding activity (Chophi et al., 2019; Gosselin et al., 2011). How the person ingests a toxicant affects its metabolism and distribution in the body. Besides, variations in drug distribution are based on their physicochemical properties and factors like blood flow, ionization, protein binding, and tissue affinity influence how drugs spread through tissues. Metabolic processes further modify these substances. Also, *post-mortem* changes occur due to rupturing of cell membranes, which changes the concentrations of the toxicant due to diffusion through different tissues (da Silva et al., 2017; Gosselin et al., 2011).

In most studies, like the present one, larvae are reared in substrate spiked with certain drug concentrations. As such, these drugs are not metabolized nor distributed by a living system. The results of these studies may differ from real poisoning cases, as drugs undergo natural metabolic processes and drug availability would differ (Chophi et al., 2019; Gosselin et al., 2011). However, the only means of overcoming this obstacle is to utilise living animal models for these experiments, which gives rise to ethical considerations and makes interpreting results more complex.

Although there is a lack of consensus regarding the quantitative analysis of maggots, it may be beneficial for forensic entomologists to elucidate the alterations in blowfly development and their implications for *post-mortem* interval estimation (Gosselin et al., 2011), as demonstrated in the present study.

5. Conclusion

The present study sought to elucidate the effects of As, Hg, Pb, and Cd on *C. vicina* larvae. It was established that each heavy metal increased mortality rates in a dose-dependent manner, with As being the most toxic for this species, followed by Hg. *C. vicina* larvae exhibited greater resistance to Pb and Cd, with high survival rates observed even at elevated concentrations.

The presence of high concentrations of heavy metals resulted in harmful effects on the development of *C. vicina* larvae, impeding their growth and leading to a reduction in size comparable to that observed in the first and second instars. In practical applications, this can result in significant inaccuracies in mPMI estimations based on entomological evidence.

The bioaccumulation of each metal was determined using WDXRF, ICP-OES, and AAS techniques. Although all metals were successfully detected on larvae and rearing substrate, there was no evidence to suggest bioaccumulation of As, Hg, or Pb from *C. vicina* larvae, with bioaccumulation factor values consistently lower than 1.0. Bioaccumulation was verified only for Cd, with larvae concentrations 3 to 4 times higher than the substrate. However, it would appear that the process of bioaccumulation is species-dependent, as other blowfly species have yielded different results. It is also possible that the methylation of certain elements may influence the bioaccumulation process.

The WDXRF method was found to be a reliable technique for analysing metals in biological samples, offering high accuracy, low detection limits, and the ability to repeat analyses without material loss. Additionally, no pre-sample treatments are required. Nevertheless, the detection limits remained higher than optimal for analysed samples, and the requisite minimum weight may present a challenge in these analyses.

In conclusion, the results demonstrate that *C. vicina* larvae can be employed as a toxicological indicator, enabling the detection of toxic metals within the body. However, the presence of these substances has been demonstrated to exert a considerable influence on the survival and development of the larvae species in question, thereby introducing a degree of bias into the estimation of mPMI.

6. References

Abajue, M. C., & Ewuim, S. C. (2020). Evaluation of activities of dipteran maggots on a poisoned pig cadaver at Nnamdi Azikiwe University Awka, Nigeria. *Egyptian Journal of Forensic Sciences*, *10*(1). https://doi.org/10.1186/s41935-020-00208-0

Amendt, J., Campobasso, C. P., Gaudry, E., Reiter, C., LeBlanc, H. N., & J. R. Hall, M. (2007). Best practice in forensic entomology - Standards and guidelines. *International Journal of Legal Medicine*, *121*(2), 90–104. https://doi.org/10.1007/s00414-006-0086-x

Amendt, J., Richards, C. S., Campobasso, C. P., Zehner, R., & Hall, M. J. R. (2011). Forensic entomology: Applications and limitations. *Forensic Science, Medicine, and Pathology*, *7*(4), 379–392. https://doi.org/10.1007/s12024-010-9209-2

Aoki, Y., & Suzuki, K. T. (1984). Excretion of Cadmium and change in the relative ration of iso-cadmium-binding proteins during metamorphosis of fleshfly (Sarcophaga peregrina). In *Biochem. Physiol* (Vol. 78, Issue 2).

Aoki, Y., Suzuki, K. T., & Kubota, K. (1984). Accumulation of Cadmium and Induction of its binding protein in the digestive tract of fleshfly (Sarcophaga peregrina) larvae. In *Biochem. Physiol: Vol. IX* (Issue 2).

Balali-Mood, M., Kianoush, S., Sadeghi, M., & Balali-Mood, M. (2015). Recent Advances in the Clinical Management of Lead Poisoning. *Acta Med Iran*, *53*(6), 327–336.

Balali-Mood, M., Naseri, K., Tahergorabi, Z., Khazdair, M. R., & Sadeghi, M. (2021). Toxic Mechanisms of Five Heavy Metals: Mercury, Lead, Chromium, Cadmium, and Arsenic. *Frontiers in Pharmacology*, *12*(643972), 1–19. https://doi.org/10.3389/fphar.2021.643972

Baldwin, D. R., & Marshall, W. J. (1999). Heavy metal poisoning and its laboratory investigation. *Annals of Clinical Biochemistry*, *36*, 267–300.

Bernhoft, R. A. (2012). Mercury toxicity and treatment: A review of the literature. *Journal of Environmental and Public Health*, *2012*, 1–10. https://doi.org/10.1155/2012/460508

Bessa, B. G. de O. , Silva-Neto, H. de A. , Coltro, W. K. T. , Rocha, T. L. , & Lopes, W. R. (2021). Lead toxicity in Lucilia cuprina and electrochemical analysis: a simple and low-cost alternative for forensic investigation. *Analytical and Bioanalytical Chemistry*, *413*(12), 3201–3208. https://doi.org/https://doi.org/10.1007/s00216-021-03257-z

Boss, C. B., & Fredeen, K. J. (2004). *Concepts, Instrumentation and Techniques in Inductively Coupled Plasma Optical Emission Spectrometry*. www.perkinelmer.com

Brouwer, Peter. (2003). *Theory of XRF : getting acquainted with the principles*. PANalytical BV.

Byrd, J. H., & Castner, J. L. (2009). *Forensic Entomology: The Utility of Arthropods in Legal Investigations* (CRC Press, Ed.; 2nd ed.).

Caito, S., & Aschner, M. (2015). Neurotoxicity of metals. In *Handbook of Clinical Neurology* (Vol. 131, pp. 169–189). Elsevier B.V. https://doi.org/10.1016/B978-0-444-62627-1.00011-1

Campbell, B. G. (1999). Broadsheet number 48: Mercury, cadmium and arsenic: Toxicology and laboratory investigation. *Pathology*, *31*(1), 17–22. https://doi.org/10.1080/003130299105467

Catts, E. P., & Goff, M. L. (1992). Forensic Entomology in Criminal Investigations. *Annual Review of Entomology*, *37*, 253–272. https://doi.org/10.1146/annurev.en.37.010192.001345

Chophi, R., Sharma, S., Sharma, S., & Singh, R. (2019). Forensic entomotoxicology: Current concepts, trends and challenges. *Journal of Forensic and Legal Medicine*, *67*, 28–36. https://doi.org/10.1016/j.jflm.2019.07.010

Costa, R. A., dos Santos, N. A., Corrêa, T. S. M., Wyatt, N. L. P., Chamoun, C. A., Carneiro, M. T. W. D., & Romão, W. (2020). Detection of Pb, Ba, and Sb in Cadaveric Maggots and Pupae by ICP-MS*. *Journal of Forensic Sciences*, *65*(6), 2188–2193. https://doi.org/10.1111/1556-4029.14526

Costley, C. T., Mossop, K. F., Dean, J. R., Garden, L. M., Marshall, J., & Carroll, J. (2000). Determination of mercury in environmental and biological samples using pyrolysis atomic absorption spectrometry with gold amalgamation. *Analytica Chimica Acta*, *405*, 179–183. https://doi.org/10.1016/S0003-2670(99)00742-4

Crespo-López, M. E., Macêdo, G. L., Pereira, S. I. D., Arrifano, G. P. F., Picanço-Diniz, D. L. W., Nascimento, J. L. M. do, & Herculano, A. M. (2009). Mercury and human genotoxicity: Critical considerations and possible molecular mechanisms. *Pharmacological Research*, *60*(4), 212–220. https://doi.org/10.1016/j.phrs.2009.02.011

Da Broi, U., Moreschi, C., Colatutto, A., Marcon, B., & Zago, S. (2017). Medico legal aspects of self-injection of metallic mercury in cases of suicide or self-harming. *Journal of Forensic and Legal Medicine*, *50*, 12–19. https://doi.org/10.1016/j.jflm.2017.06.002

da Silva, E. I. T., Wilhelmi, B., & Villet, M. H. (2017). Forensic entomotoxicology revisited—towards professional standardisation of study designs. *International Journal of Legal Medicine*, *131*(5), 1399–1412. https://doi.org/10.1007/s00414-017-1603-9

de Souza, I. D., de Andrade, A. S., & Dalmolin, R. J. S. (2018). Lead-interacting proteins and their implication in lead poisoning. *Critical Reviews in Toxicology*, *48*(5), 375–386. https://doi.org/10.1080/10408444.2018.1429387

Dias, D., Bessa, J., Guimarães, S., Soares, M. E., Bastos, M. de L., & Teixeira, H. M. (2016). Inorganic mercury intoxication: A case report. *Forensic Science International*, *259*, 1–18. https://doi.org/10.1016/j.forsciint.2015.12.021

Duncan, A., Taylor, A., Leese, E., Allen, S., Morton, J., & McAdam, J. (2015). Homicidal arsenic poisoning. *Annals of Clinical Biochemistry*, *52*(4), 510–515. https://doi.org/10.1177/0004563214559222

Farnaghi, F., Chouhdari, A., Hassanian-Moghaddam, H., Zamani, N., Sabeti, S., & Shahrabi Farahani, H. (2020). Blood Lead Levels in Opium-Poisoned Children: One Cross-Sectional Study in Iran. *Addict Health, Summer*, *12*(3), 1–8. https://doi.org/10.22122/ahj.v12i3.268

Fernandes, T. A. P., Brito, J. A. A., & Gonçalves, L. M. L. (2015). Analysis of Micronutrients and Heavy Metals in Portuguese Infant Milk Powders by Wavelength Dispersive X-ray Fluorescence Spectrometry (WDXRF). *Food Analytical Methods*, *8*(1), 52–57. https://doi.org/10.1007/s12161-014-9866-y

Flora, S. J. S. (2009). Metal Poisoning: Threat and Management. *Al Ameen Journal of Medical Sciences*, *2*(2), 4–26.

Gagliano-Candela, R., & Aventaggiato, L. (2001). The detection of toxic substances in entomological specimens. *International Journal of Legal Medicine*, *114*(4–5), 197–203. https://doi.org/10.1007/s004140000181

Ghosh, S., Banji, D., Laxmi Prasanna, V., Sowjanya, B., Srivani, P., & Alagaraja, M. (2013). Inductively coupled plasma-Optical emission spectroscopy: A review. *Asian J. Pharm. Ana*, *3*(1), 24–33. https://www.researchgate.net/publication/288811956

Gosselin, M., Wille, S. M. R., Fernandez, M. del M. R., Di Fazio, V., Samyn, N., De Boeck, G., & Bourel, B. (2011). Entomotoxicology, experimental set-up and interpretation for forensic toxicologists. *Forensic Science International*, *208*(1–3), 1–9. https://doi.org/10.1016/j.forsciint.2010.12.015

Graeme, K. A., & Pollack, C. V. (1998). Selected Topics: Toxicology Heavy Metal Toxicity, Part I: Arsenic and Mercury. *The Journal of Emergency Medicine*, *16*(1), 45–56.

Harada, M. (1995). Minamata Disease: Methylmercury Poisoning in Japan Caused by Environmental Pollution. *Critical Reviews in Toxicology*, *25*(1), 1–24.

Hardin, J., Seltzer, J., Suhandynata, R., Spiegel, B., Silver, R., Thomas, D., Galust, H., Friedman, N., Clark, R., & Momper, J. (2023). Severe arsenic poisoning due to Ayurvedic supplements. *Clinical Case Reports*, *11*(7), 1–7. https://doi.org/10.1002/ccr3.7733

Hung, Y. M., & Chung, H. M. (2004). Acute self-poisoning by ingestion of cadmium and barium. *Nephrology Dialysis Transplantation*, *19*(5), 1308–1309. https://doi.org/10.1093/ndt/gfh169

Jomova, K., Jenisova, Z., Feszterova, M., Baros, S., Liska, J., Hudecova, D., Rhodes, C. J., & Valko, M. (2011). Arsenic: Toxicity, oxidative stress and human disease. *Journal of Applied Toxicology*, *31*(2), 95–107. https://doi.org/10.1002/jat.1649

Kökdener, M., Gündüz, N. E. A., Zeybekoğlu, Ü., Aykut, U., & Yllmaz, A. F. (2022). The Effect of Different Heavy Metals on the Development of Lucilia sericata (Diptera:

Calliphoridae). *Journal of Medical Entomology*, *59*(6), 1928–1935. https://doi.org/10.1093/jme/tjac134

Kökdener, M., & Yllmaz, A. F. (2021). The effects of gunshot residue components (pb, ba, and sb) on the life history traits of lucilia sericata (diptera: Calliphoridae). *Journal of Medical Entomology*, *58*(6), 2130–2137. https://doi.org/10.1093/jme/tjab123

Lagoo, L., Schaeffer, L. S., Szymanski, D. W., & Smith, R. W. (2010). Detection of gunshot residue in blowfly larvae and decomposing porcine tissue using inductively coupled plasma mass spectrometry (ICP-MS). *Journal of Forensic Sciences*, *55*(3), 624–632. https://doi.org/10.1111/j.1556-4029.2010.01327.x

Li, Y., Jiang, Y., & Yan, X. P. (2006). Probing mercury species-DNA interactions by capillary electrophoresis with on-line electrothermal atomic absorption spectrometric detection. *Analytical Chemistry*, *78*(17), 6115–6120. https://doi.org/10.1021/ac060644a

Lu, Q., Liu, Z., & Chen, X. (2017). Mercury poisoning through intravenous administration: Two case reports with literature review. *Medicine*, *96*(46), 1–5. https://doi.org/10.1097/MD.0000000000008643

Malejko, J., Deoniziak, K., Tomczuk, M., Długokencka, J., & Godlewska-Żyłkiewicz, B. (2020). Puparial Cases as Toxicological Indicators: Bioaccumulation of Cadmium and Thallium in the Forensically Important Blowfly Lucilia sericata. *Frontiers in Chemistry*, *8*(586067). https://doi.org/10.3389/fchem.2020.586067

Michielan, A., Schicchi, A., Cappuccio, R., Lonati, D., Lamboglia, F., Vitalba, A., Caroli, A., Crevani, M., Locatelli, C. A., & Betetto, G. (2018). Intentional ingestion of elemental mercury requiring multi-step decontamination and prophylactic appendectomy: a case report and treatment proposal. *Clinical Toxicology*, *56*(1), 69–73. https://doi.org/10.1080/15563650.2017.1338346

Mills, D. A., Tomassoni, A. J., Tallon, L. A., Kade, K. A., & Savoia, E. S. (2013). Mass arsenic poisoning and the public health response in Maine. *Disaster Medicine and Public Health Preparedness*, *7*(3), 319–326. https://doi.org/10.1001/dmp.2011.1

Mochizuki, H. (2019). Arsenic neurotoxicity in humans. *International Journal of Molecular Sciences*, *20*(14), 1–11. https://doi.org/10.3390/ijms20143418

Moe, S. J., Stenseth, N. C., & Smith, R. H. (2001). Effects of a toxicant on population growth rates: Sublethal and delayed responses in blowfly populations. *Functional Ecology*, *15*(6), 712–721. https://doi.org/10.1046/j.0269-8463.2001.00575.x

Mogren, C. L., Webb, S. M., Walton, W. E., & Trumble, J. T. (2013). Micro x-ray absorption spectroscopic analysis of arsenic localization and biotransformation in Chironomus riparius Meigen (Diptera: Chironomidae) and Culex tarsalis Coquillett (Culicidae). *Environmental Pollution*, *180*, 78–83. https://doi.org/10.1016/j.envpol.2013.05.021

Motta, L. C., Vanini, G., Chamoun, C. A., Costa, R. A., Vaz, B. G., Costa, H. B., Bassane, J. F. P., Carneiro, M. T. W. D., & Romão, W. (2015). Detection of Pb, Ba, and Sb in

Blowfly Larvae of Porcine Tissue Contaminated with Gunshot Residue by ICP OES. *Journal of Chemistry*, *2015*. https://doi.org/10.1155/2015/737913

Munday, S. W., & Ford, M. D. (2011). Arsenic. In The McGraw-Hill Companies (Ed.), *Goldfrank's Toxicologic Emergencies* (9th ed., pp. 1214–1228). http://url-s.gq/paypal

Nishijo, M., Nakagawa, H., Suwazono, Y., Nogawa, K., & Kido, T. (2017). Causes of death in patients with Itai-itai disease suffering from severe chronic cadmium poisoning: A nested case-control analysis of a follow-up study in Japan. *BMJ Open*, *7*(e015694), 1–7. https://doi.org/10.1136/bmjopen-2016-015694

Nuorteva, P., & Nuorteva, S.-L. (1982). The Fate of Mercury In Sarcosaprophagous Flies and In Insects Eating Them Report. *Ambio*, *11*, 34–37.

Nurchi, V. M., Djordjevic, A. B., Crisponi, G., Alexander, J., Bjørklund, G., & Aaseth, J. (2020). Arsenic toxicity: Molecular targets and therapeutic agents. *Biomolecules*, *10*(2), 1–15. https://doi.org/10.3390/biom10020235

Podgorski, J., & Berg, M. (2020). Global threat of arsenic in groundwater. *Science*, *368*(6493), 845–850. https://doi.org/doi.org/10.1126/science.aba1510

Potts, P. J. (2005). Wavelength Dispersive X-Ray Fluorescence. *Encyclopedia of Analytical Science*, 419–429. https://doi.org/10.1016/B0-12-369397-7/00674-9

Prado E Castro, C., Serrano, A., Martins Da Silva, P., & García, M. D. (2012). Carrion flies of forensic interest: A study of seasonal community composition and succession in Lisbon, Portugal. *Medical and Veterinary Entomology*, *26*(4), 417–431. https://doi.org/10.1111/j.1365-2915.2012.01031.x

Rashid, R. A., Arifuddin, N. 'Atiqah, & Ahmad, N. W. (2012). Blowfly, Chrysomya megacephala as An Alternative Specimen in Determination of Gunshot Residue. *IEEE Symposium on Business, Engineering and Industrial Applications*, 542–547.

Rehman, K., Fatima, F., Waheed, I., & Akash, M. S. H. (2018). Prevalence of exposure of heavy metals and their impact on health consequences. *Journal of Cellular Biochemistry*, *119*(1), 157–184. https://doi.org/10.1002/jcb.26234

Renu, K., Chakraborty, R., Myakala, H., Koti, R., Famurewa, A. C., Madhyastha, H., Vellingiri, B., George, A., & Valsala Gopalakrishnan, A. (2021). Molecular mechanism of heavy metals (Lead, Chromium, Arsenic, Mercury, Nickel and Cadmium) - induced hepatotoxicity – A review. *Chemosphere*, *271*(129735), 1–23. https://doi.org/10.1016/j.chemosphere.2021.129735

Roeterdink, E. M., Dadour, I. R., & Watling, R. J. (2004). Extraction of gunshot residues from the larvae of the forensically important blowfly Calliphora dubia (Macquart) (Diptera: Calliphoridae). *International Journal of Legal Medicine*, *118*(2), 63–70. https://doi.org/10.1007/s00414-003-0408-1

Sharma, B., Singh, S., & Siddiqi, N. J. (2014). Biomedical implications of heavy metals induced imbalances in redox systems. *BioMed Research International*, *2014*, 1–26. https://doi.org/10.1155/2014/640754

Shulman, M. V., Pakhomov, O. Y., & Brygadyrenko, V. V. (2017). Effect of lead and cadmium ions upon the pupariation and morphological changes in Calliphora vicina (Diptera, Calliphoridae). *Folia Oecologica*, *44*(1), 28–37. https://doi.org/10.1515/foecol-2017-0004

Sikary, A. K. (2019). Homicidal poisoning in India: A short review. *Journal of Forensic and Legal Medicine*, *61*, 13–16. https://doi.org/10.1016/j.jflm.2018.10.003

Simkiss, K., Daniels, S., & Smith, R. H. (1993). Effects of population density and cadmium toxicity on growth and survival of blowflies. *Environmental Pollution*, *81*(1), 41–45. https://doi.org/10.1016/0269-7491(93)90026-K

Singh, D., & Kaur Heer, B. (2017). Effect of Cadmium Chloride on the Development of Chrysomya Megacephala (Diptera:Calliphoridae) and its Importance to Postmortem Interval Estimate. *Journal of Forensic Sciences & Criminal Investigation*, *3*(5), 1–6. https://doi.org/10.19080/jfsci.2017.03.555622

Sukheeja, D., Kumar, P., Singhal, M., & Subramanian, A. (2014). Subcutaneous Mercury Injection by a Child: A Histopathology Case Report. *Journal of Laboratory Physicians*, *6*(01), 055–057. https://doi.org/10.4103/0974-2727.129095

Szpila, K. (2010a). *Key for identification of European and Mediterranean blowflies (Diptera, Calliphoridae) of forensic importance Adult flies*.

Szpila, K. (2010b). Key for the Identification of Third Instars of European Blowflies (Diptera: Calliphoridae) of Forensic Importance. In *Current Concepts in Forensic Entomology* (pp. 43–56). Springer Netherlands. https://doi.org/10.1007/978-1-4020-9684-6_3

Tchounwou, P. B., Yedjou, C. G., Patlolla, A. K., & Sutton, D. J. (2012). Heavy metal toxicity and the environment. *Molecular, Clinical and Environmental Toxicology*, *101*, 133–164. https://doi.org/10.1007/978-3-7643-8340-4_6

Tournel, G., Houssaye, C., Humbert, L., Dhorne, C., Gnemmi, V., Bécart-Robert, A., Nisse, P., Hédouin, V., Gosset, D., & Lhermitte, M. (2011). Acute Arsenic Poisoning: Clinical, Toxicological, Histopathological, and Forensic Features. *Journal of Forensic Sciences*, *56*(SUPPL. 1), 1–5. https://doi.org/10.1111/j.1556-4029.2010.01581.x

Ufelle, A. C., & Barchowsky, A. (2021). Toxic Effects of Metals. In McGraw Hill (Ed.), *Casarett & Doull's Essentials of Toxicology* (4th ed., pp. 757–789).

Vantroyen, B., Heilier, J. F., Meulemans, A., Michels, A., Buchet, J. P., Vanderschueren, S., Haufroid, V., & Sabbe, M. (2004). Survival after a lethal dose of arsenic trioxide. *Journal of Toxicology - Clinical Toxicology*, *42*(6), 889–895. https://doi.org/10.1081/CLT-200035344

Wang, E. E., Mahajan, N., Wills, B., & Leikin, J. (2007). Successful Treatment of Potentially Fatal Heavy Metal Poisonings. *Journal of Emergency Medicine*, *32*(3), 289–294. https://doi.org/10.1016/j.jemermed.2006.12.013

Wilschefski, S. C., & Baxter, M. R. (2019). Inductively Coupled Plasma Mass Spectrometry: Introduction to Analytical Aspects. *Clinical Biochemist Reviews*, *40*(3), 115–133. https://doi.org/10.33176/AACB-19-00024

Wobrauschek, P., Streli, C., & Lindgren, E. S. (2010). Energy Dispersive, X-ray Fluorescence Analysis. *Encyclopedia of Analytical Chemistry*, 1–17. https://doi.org/10.1002/9780470027318.a6806.pub2

Yan, P., Huang, G., Li, D., & Li, L. (2012). Homicide due to intravenous metallic mercury injection followed by sodium cyanide injection. *American Journal of Forensic Medicine and Pathology*, *33*(3), 273–275. https://doi.org/10.1097/PAF.0b013e318221b693

Yilmaz, Y., Armagan, E., Olmez, O. F., Esen, M., Alkis, N., & Dolar, E. (2009). Acute arsenic self-poisoning for suicidal purpose in a dentist: A case report. *Human and Experimental Toxicology*, *28*(1), 63–65. https://doi.org/10.1177/0960327108097432

Yudelowitz, G. (2017). Intentional intravenous mercury injection. *South African Medical Journal*, *107*(2), 112–114. https://doi.org/10.7196/SAMJ.2017.v107i2.12046

Attachment

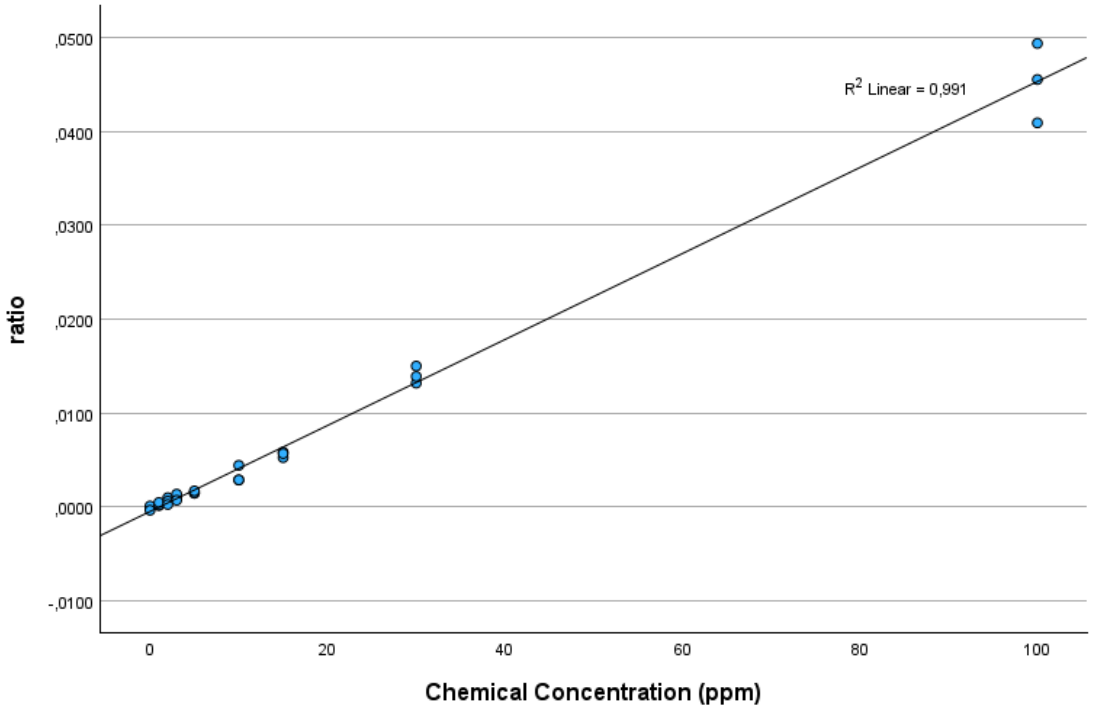

Figure A1: Arsenic calibration curve obtained for WDXRF analysis.

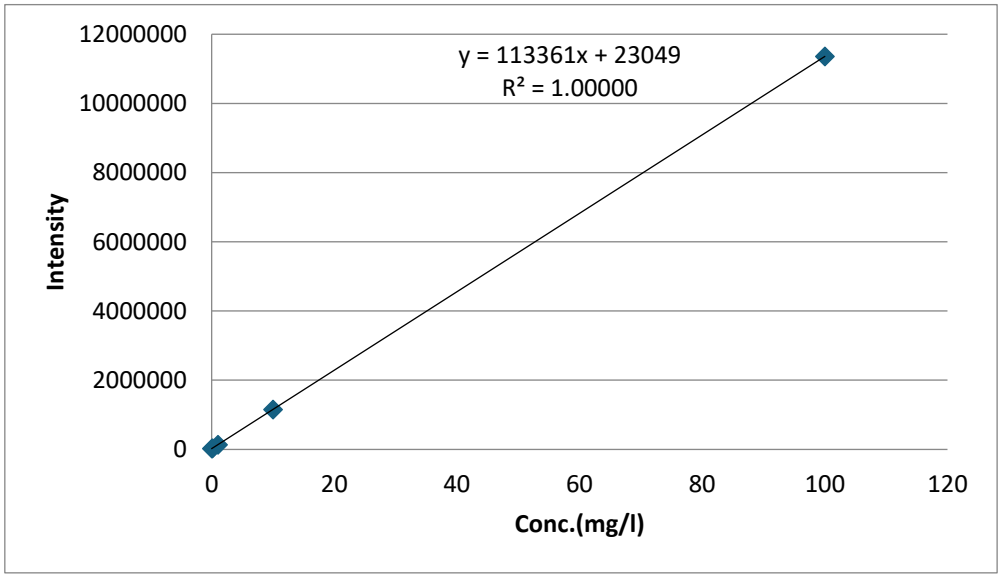

Figure A2: Arsenic calibration curve for ICP-OES analysis.

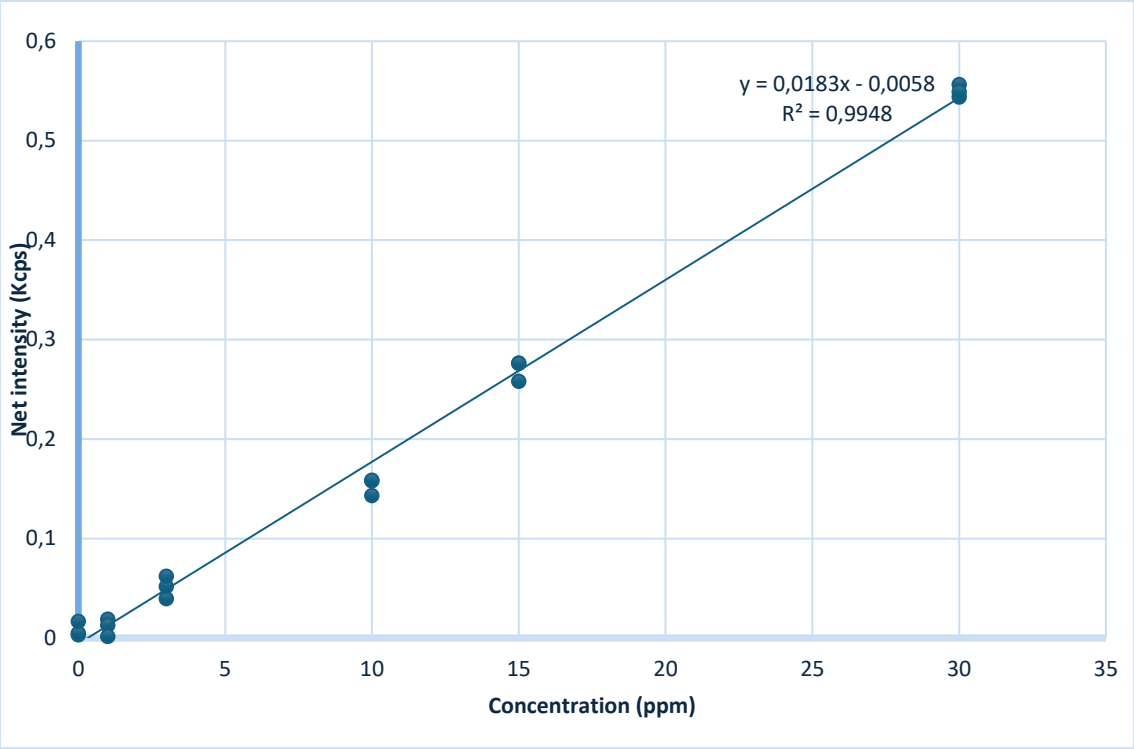

Figure A3: Mercury calibration curve obtained for WDXRF analysis.

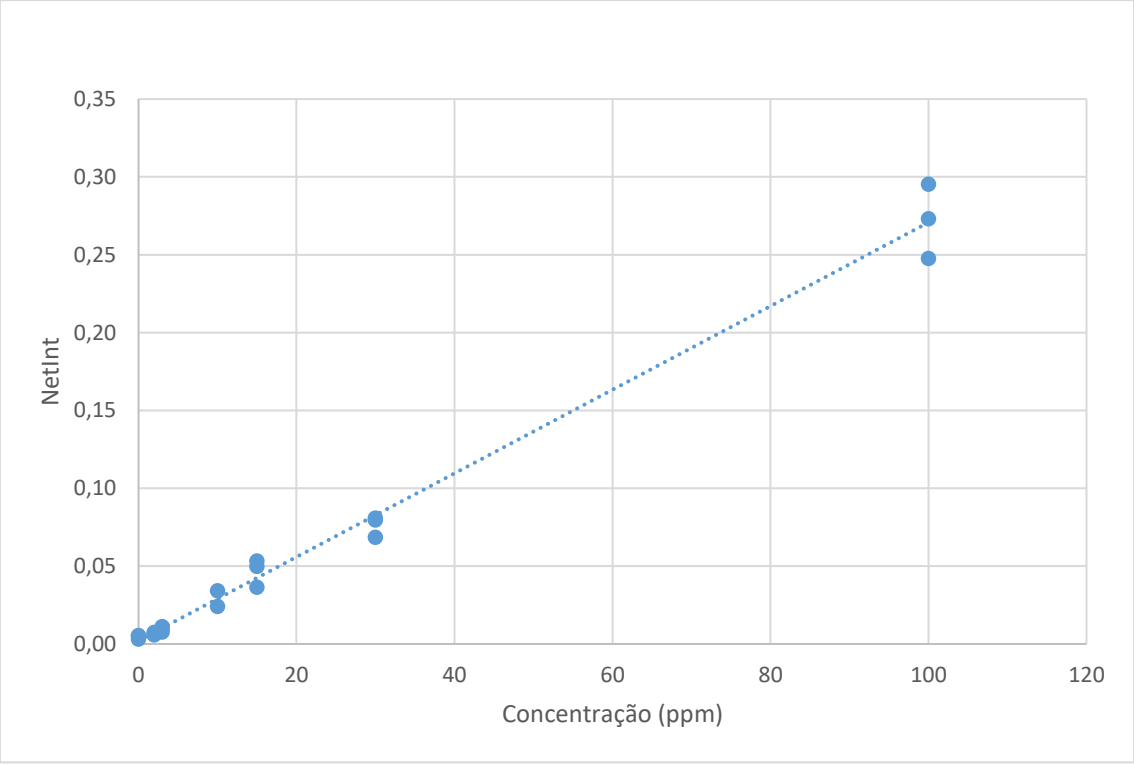

Figure A4: Cadmium calibration curve for WDXRF analysis.

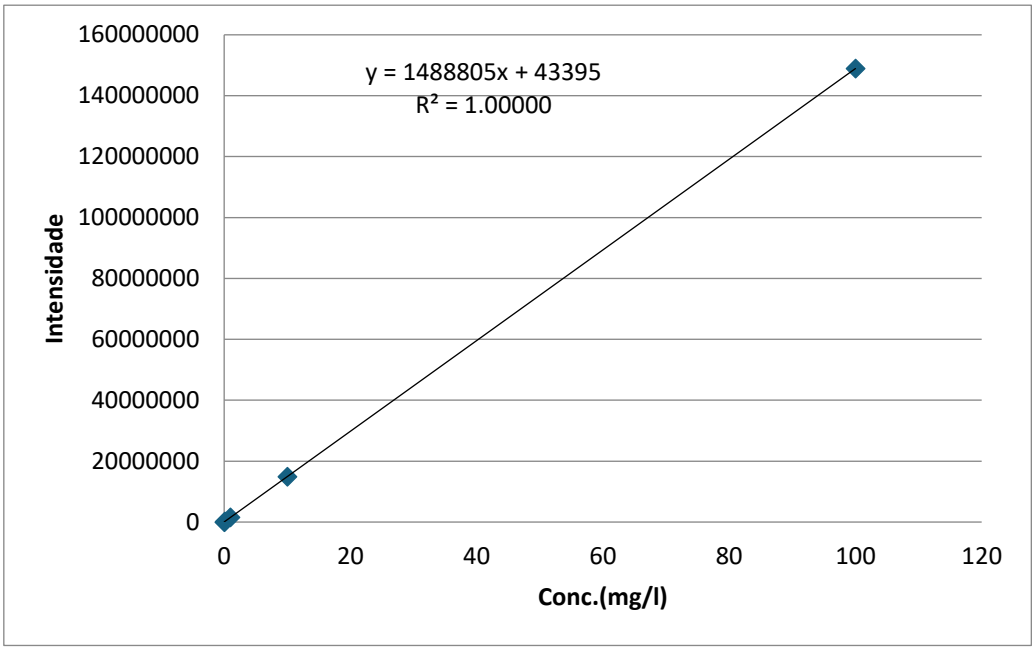

Figure A5: Cadmium calibration curve for ICP-OES analysis.

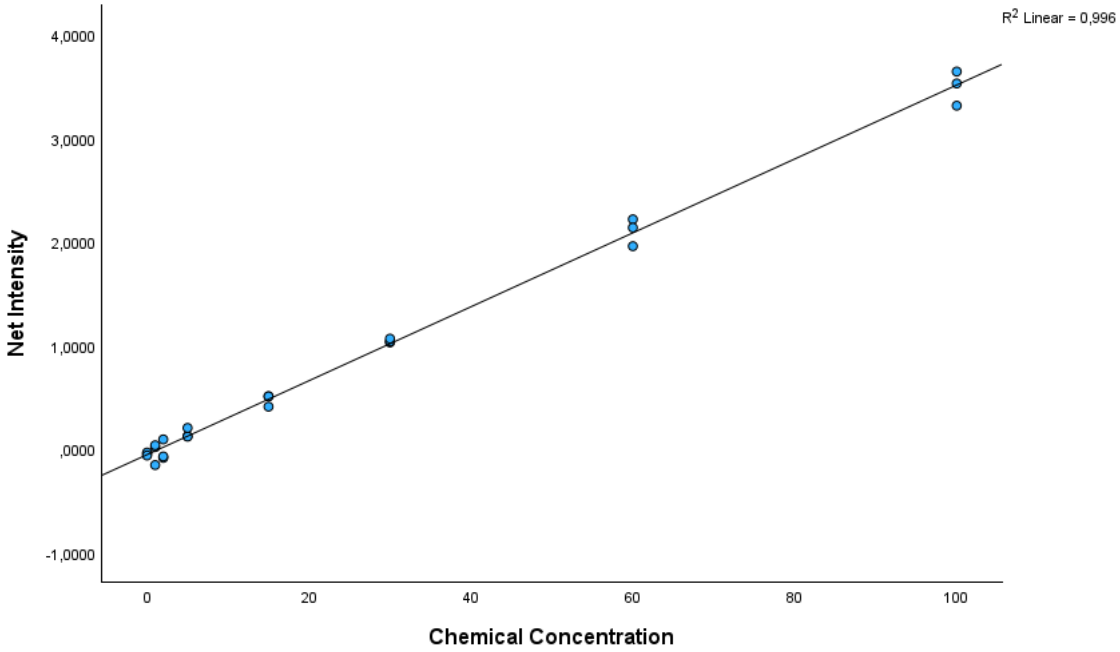

Figure A6: Lead calibration curve for WDXRF analysis.

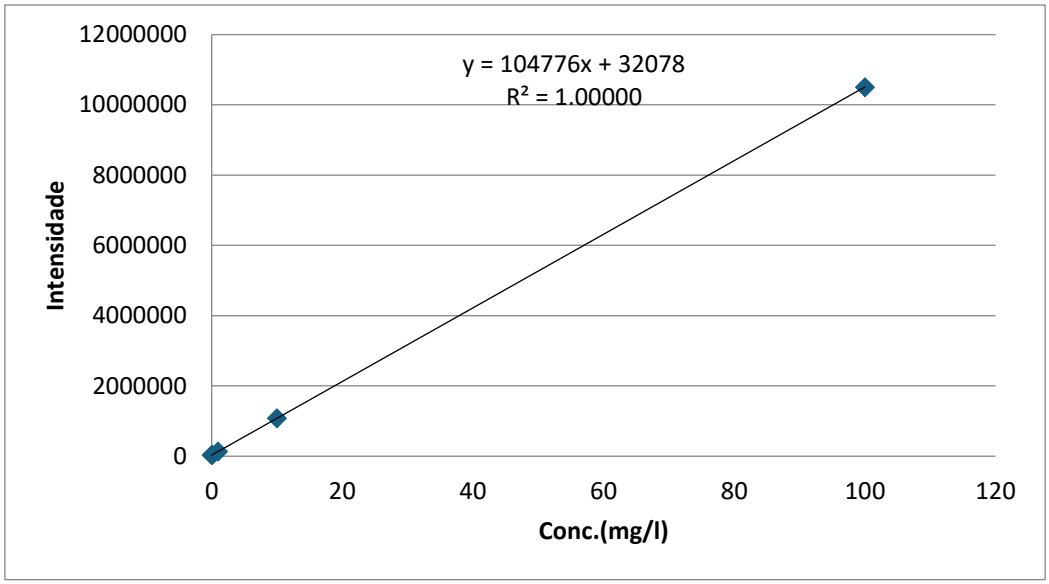

Figure A7: Lead calibration curve for ICP-OES analysis.

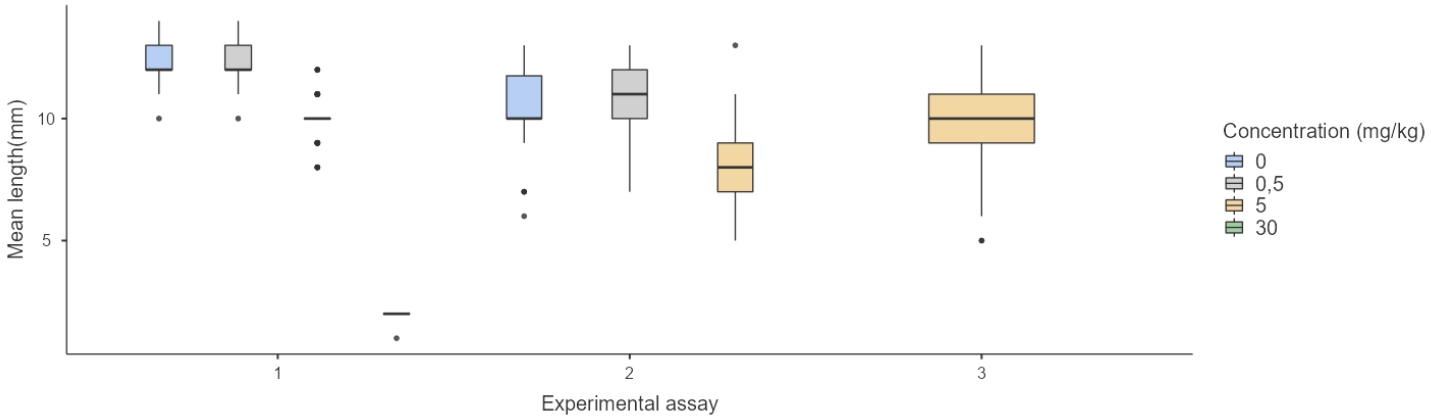

Figure A8: Box plot for the mean length of *C. vicina* larvae reared in increasing concentrations of arsenic, divided by experimental assays (respectively, *n* = 111; 110; 214; 5). Dots represent outlier values.

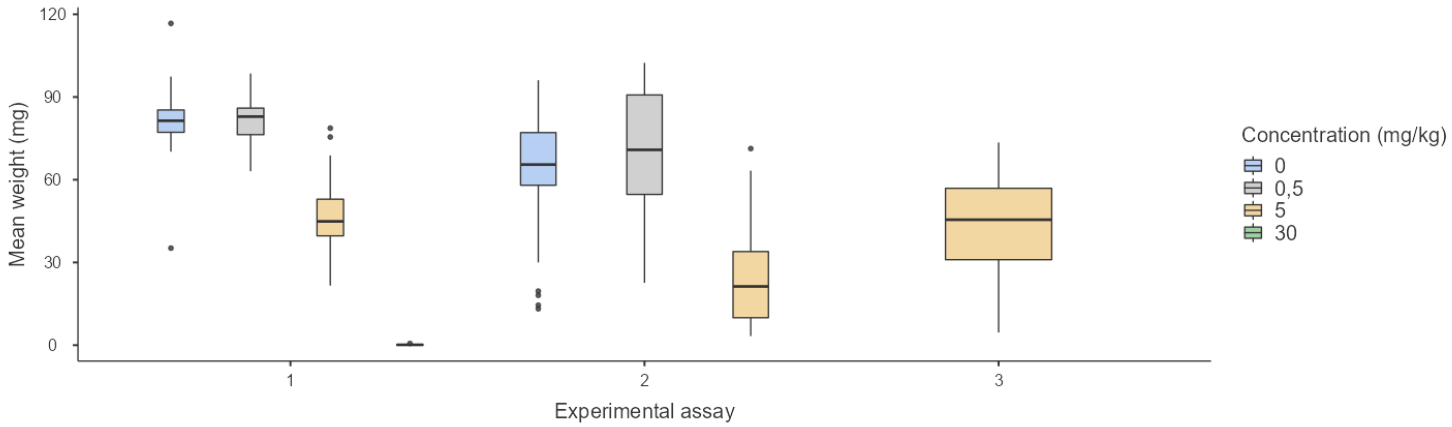

Figure A9: Box plot for the mean weight of *C. vicina* larvae reared in increasing concentrations of arsenic, divided by experimental assays (respectively, *n* = 111; 110; 214; 5). Dots represent outlier values.

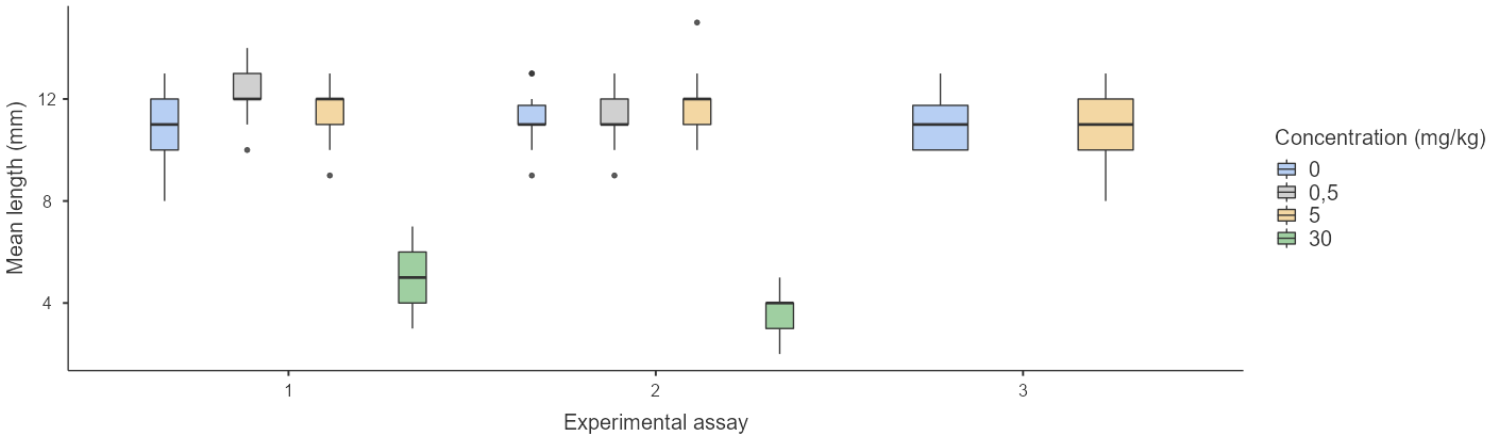

Figure A10: Box plot for the mean length of *C. vicina* larvae reared in increasing concentrations of phenylmercury acetate, divided by experimental assays (respectively, *n* = 114; 71; 76; 109). Dots represent outlier values.

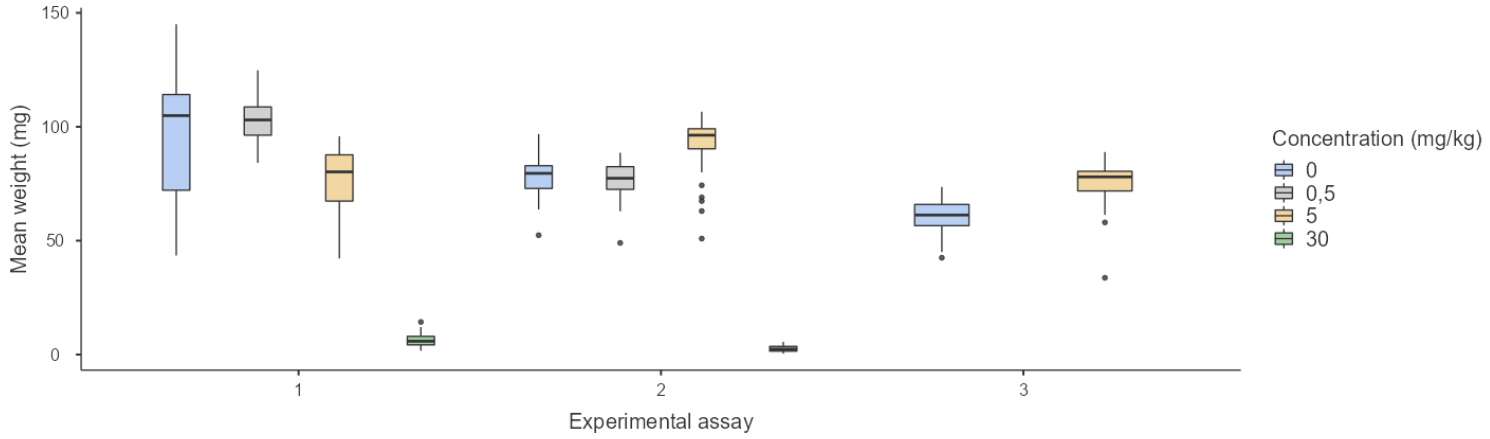

Figure A11: Box plot for the mean weight of *C. vicina* larvae reared in increasing concentrations of phenylmercury acetate, divided by experimental assays (respectively, *n* = 114; 71; 76; 109). Dots represent outlier values.

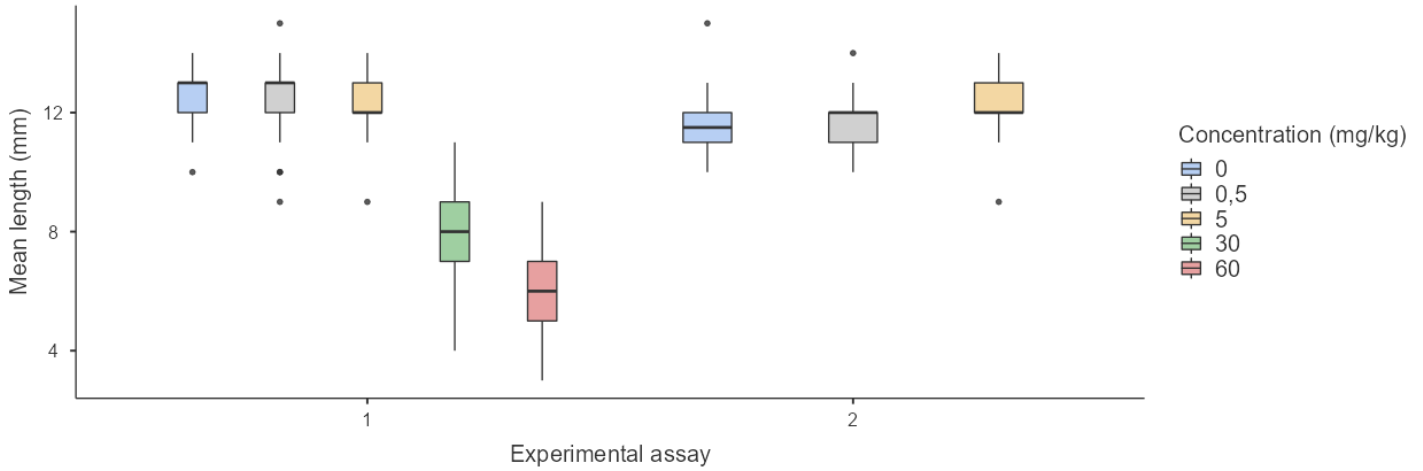

Figure A12: Box plot for the mean length of *C. vicina* larvae reared in increasing concentrations of cadmium acetate, divided by experimental assays (respectively, *n* = 77; 46; 61; 48; 60). Dots represent outlier values.

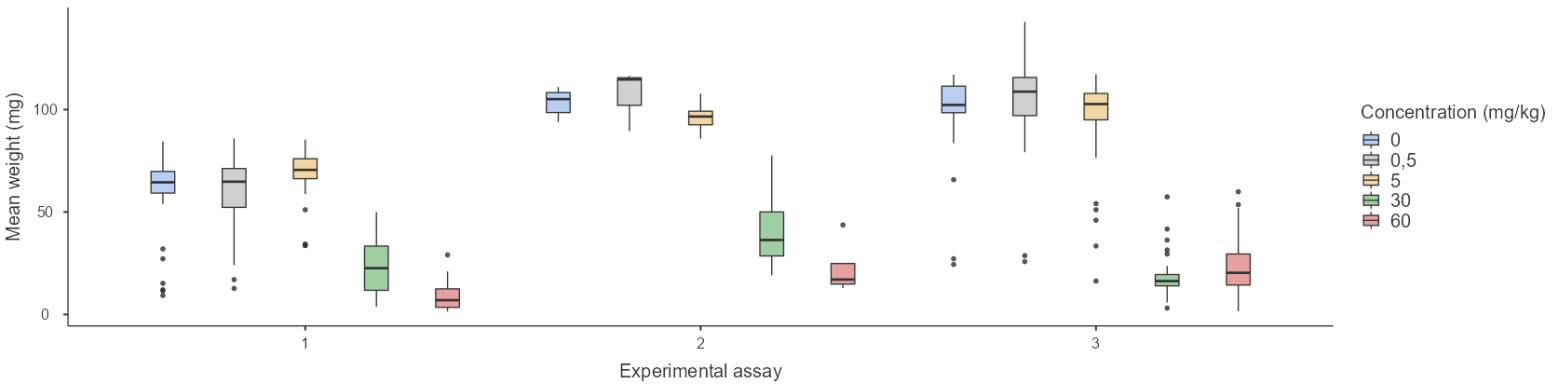

Figure A13: Box plot for the mean weight of *C. vicina* larvae reared in increasing concentrations of cadmium acetate, divided by experimental assays (respectively, n = 77; 46; 61; 48; 60). Dots represent outlier values.

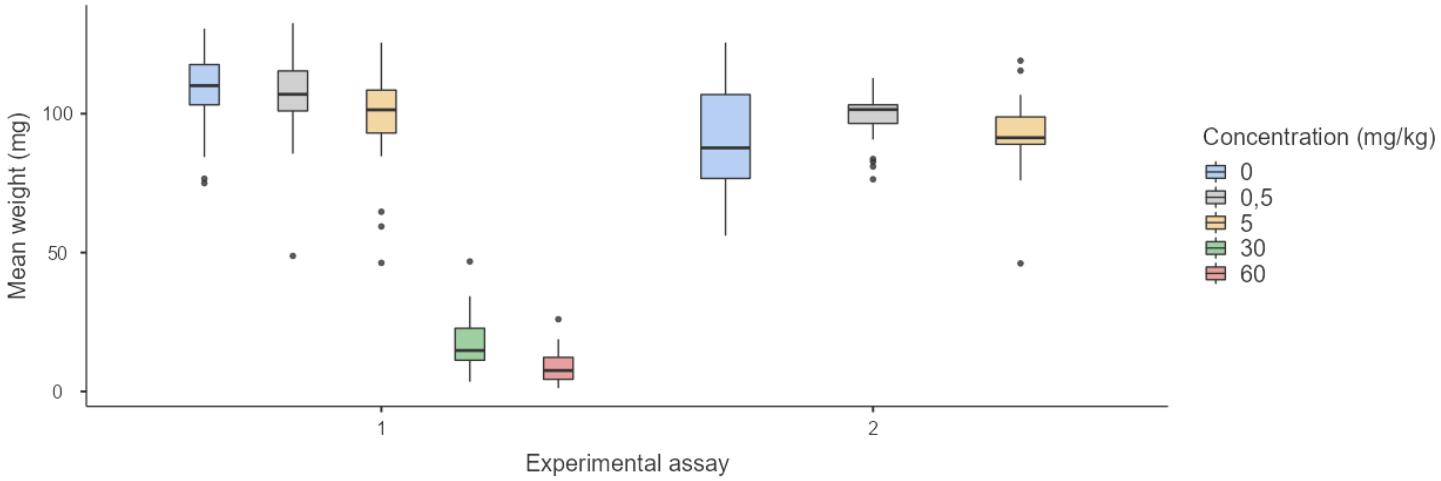

Figure A14: Box plot for the mean length of *C. vicina* larvae reared in increasing concentrations of lead acetate, divided by experimental assays (respectively, n = 103; 117; 105; 54; 36). Dots represent outlier values.

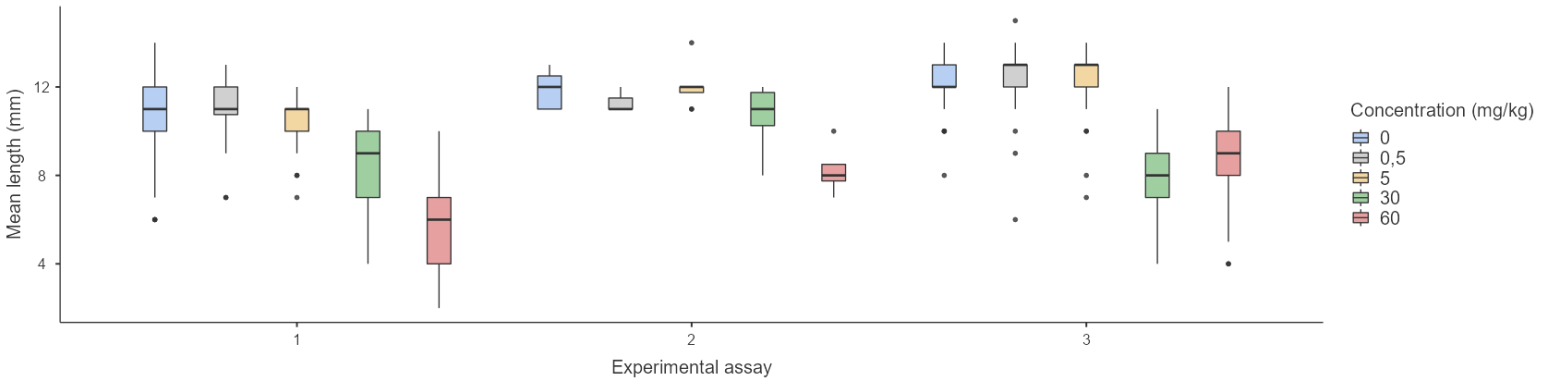

Figure A15: Box plot for the mean weight of *C. vicina* larvae reared in increasing concentrations of lead acetate, divided by experimental assays (respectively, n = 103; 117; 105; 54; 36). Dots represent outlier values.

Table A1: Levene's Test for Equality of Variances for arsenic exposure.

Mean length				Mean weight			
F	df1	df2	p	F	df1	df2	p
5.955	3.000	436.000	**< 0.001**	3.661	3.000	436.000	**0.013**

Note: F is the test statistic; df1 refers to the degrees of freedom between the groups; df2 refers to the degrees of freedom within the groups.

Table A2: Levene's Test for Equality of Variances for phenylmercury acetate exposure.

Mean length				Mean weigth			
F	df1	df2	p	F	df1	df2	p
2.589	3.000	410.000	0.053	34.221	3.000	412.000	**< 0.001**

Note: F is the test statistic; df1 refers to the degrees of freedom between the groups; df2 refers to the degrees of freedom within the groups.

Table A3: Levene's Test for Equality of Variances for cadmium acetate exposure.

Mean length				Mean weight			
F	df1	df2	p	F	df1	df2	p
6.583	4.000	277.000	**< 0.001**	6.367	4.000	277.000	**< 0.001**

Note: F is the test statistic; df1 refers to the degrees of freedom between the groups; df2 refers to the degrees of freedom within the groups.

Table A4: Levene's Test for Equality of Variances for lead acetate exposure.

Mean length				Mean weight			
F	df1	df2	p	F	df1	df2	p
11.688	4.000	435.000	**< 0.001**	14.724	4.000	435.000	**< 0.001**

Note: F is the test statistic; df1 refers to the degrees of freedom between the groups; df2 refers to the degrees of freedom within the groups.